

UNIVERSITY OF JORDAN
FACULTY OF GRADUATE STUDIES

PERFORMANCE OF SALINITY SOLAR POND IN JORDAN

Handwritten signature or initials in the left margin.

BY
ALA'A RATEB EL-BAZ

M.Sc THESIS
Under the supervision of
Dr. Bassam Ali Jubran

Handwritten signature and stamp in the right margin, including Arabic text: "عميد كلية الدراسات العليا".

Submitted in partial fulfillment of the
requirements for the degree of master
of science in Mechanical Engineering
Faculty of Graduate Studies
University of Jordan

December , 1993

This thesis was defended successfully on18/12/1993.....

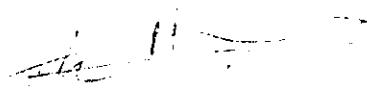
COMMITTEE MEMBERS

SIGNATURE

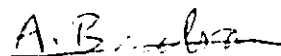
1. Dr. Bassam A. Jubran



2. Dr. Mohammad A. Hamdan



3. Dr. Ali Badran



ACKNOWLEDGMENTS

I wish gratefully to thank Dr. Bassam Jubran for his sincere guidance and encouragement through this work.

I would like to acknowledge the management and the staff of the Industrial Development Bank and the Higher Council for Science and Technology for their cooperation and financial support of the project. Also, I would like to thank the support received from Arab Potash company.

Thanks are also extended to Mr. Aref Shahin for his serious assisting in the experiments.

Finally, I would like to dedicate this dissertation to my parents, brothers, sisters and my aunt Hayat for their encouragement and support.

TABLE OF CONTENTS

COMMITTEE DECISION	ii
DEDICATION	iii
ACKNOWLEDGEMENT	iv
TABLE OF CONTENTS	v
LIST OF TABLES	viii
LIST OF FIGURES	xiv
ABSTRACT	xiii
1. INTRODUCTION	1
1.1 Introduction	1
1.2 Present work contribution	2
1.3 Importance of the work	3
1.4 Organization of the thesis	3
2. THEORITICAL AND PRACTICAL ASPECTS OF SOLAR PONDS	4
2.1 History	4
2.2 Salinity-gradient solar pond	5
2.3 Thermal performance of salt-gradient solar pond	8
2.4 Stability analysis for salt-gradient solar pond	11
2.5 General design considerations	14
2.5.1 Site requirements	14
2.5.2 Pond sizing and construction	15
2.5.3 Filling the pond	16
2.5.4 Heat extraction	18
2.6 Problems encountered during operation of solar pond	20

2.7 Applications	23
2.7.1 Heating and cooling	23
2.7.2 Agricultural systems applications	24
2.7.3 Electrical power generation	25
2.7.4 Desalination	25
2.7.5 Salt production	26
2.8 Costs	27
3. LITERATURE SURVEY	28
3.1 Introduction	28
3.2 Theoretical studies	28
3.3 Experimental studies	30
3.3.1 Introduction	30
3.3.2 Stability experiments	31
3.3.3 Wind effects experiments	34
3.3.4 Leakage experiments	38
4. EXPERIMENTAL SET-UPS AND PROCEDURES	41
4.1 Introduction	41
4.2 Liner experimental set-up and procedure	41
4.3 Solar ponds experimental set-up and procedure	44
4.4 Salt quantities	46
4.5 Meteorological data	47
4.6 Measurements	47
4.6.1 Temperature profile	47
4.6.2 Salinity profile	48
4.7 Accuracy of measurements	49
4.7.1 Introduction	49
4.7.2 Reproducibility of measurements	49

5. RESULTS AND DISCUSSION	50
5.1 Introduction	50
5.2 Lining material experiments	50
5.2.1 Liquid limit	51
5.2.2 Plastic limit	51
5.2.3 Plastic index	51
5.2.4 Optimum moisture content	55
5.2.5 Permeability	57
5.3 Results of liner test rig	63
5.3.1 Results of the scheme without LDPE film	63
5.3.2 Results of the scheme with LDPE film	64
5.3.3 Results of the scheme with a punctured LDPE film	65
5.4 Results of prototype solar ponds	68
5.4.1 Introduction	68
5.4.2 Results of SGSPs behaviour after filling	68
5.4.3 Results of SGSPs behaviour after introducing rings	76
5.4.4 Effect of rainfall on solar ponds	107
6. CONCLUSIONS AND RECOMMENDATIONS	108
6.1 Introduction	108
6.2 Conclusions	108
6.3 Recommendations and future works	109
NOMENCLATURE	112
ABBREVIATIONS	114
REFERENCES	115
APPENDICES	
Appendix A: Error analysis	121
ABSTRACT (In Arabic)	122

LIST OF TABLES

Table 5.1: Clay Classification in Jordan	55
Table 5.2: Summary of clays scanning results	61
Table 5.3: Summary of permeability results of different schemes	66

LIST OF FIGURES

Fig. 2.1: Schematic diagram of the SGSP	7
Fig. 3.1: Plasticity chart for clay classification	40
Fig. 4.1: Laboratory apparatus for testing permeability	53
Fig. 4.2: Prototype solar pond tank	45
Fig. 4.3: Solar pond diffuser	45
Fig. 5.1: Liquid limit for Amman clay	52
Fig. 5.2: Liquid limit for Irbid clay	52
Fig. 5.3: Liquid limit for Dead Sea clay	53
Fig. 5.4: Liquid limit for Karak clay	53
Fig. 5.5: Liquid limit for Tafilah clay	54
Fig. 5.6: Plasticity chart for clay classification in Jordan	56
Fig. 5.7: Optimum moisture for Amman clay	58
Fig. 5.8: Optimum moisture for Irbid clay	58
Fig. 5.9: Optimum moisture for Dead Sea clay	59
Fig. 5.10: Optimum moisture for Karak clay	59
Fig. 5.11: Optimum moisture for Tafilah clay	60
Fig. 5.12: Temperature profiles on 29/9/1993 at 9:30	70
Fig. 5.13: Temperature profiles on 29/9/1993 at 11:30	70
Fig. 5.14: Temperature profiles on 29/9/1993 at 13:00	71
Fig. 5.15: Temperature profiles on 29/9/1993 at 15:00	71
Fig. 5.16: Temperature profiles on 4/10/1993 at 11:00	72
Fig. 5.17: Temperature profiles on 4/10/1993 at 15:00	72
Fig. 5.18: Salinity profiles on 2/10/1993	73
Fig. 5.19: Maximum storage zone temperature on 29/9/93	74
Fig. 5.20: Meteorological data for Amman on 29/9/1993	74

Fig. 5.21: Maximum storage zone temperature on 4/10/93	75
Fig. 5.22: Meteorological data for Amman on 4/10/1993	75
Fig. 5.23: Temperature profiles on 9/10/1993 at 11:00 when 30 cm rings are introduced into pond A	78
Fig. 5.24: Temperature profiles on 9/10/1993 at 15:30 when 30 cm rings are introduced into pond A	78
Fig. 5.25: Temperature profiles on 13/10/1993 at 11:00 when 30 cm rings are introduced into pond A	79
Fig. 5.26: Temperature profiles on 13/10/1993 at 15:30 when 30 cm rings are introduced into pond A	79
Fig. 5.27: Salinity profiles on 9/10/1993 when 30 cm rings are introduced into pond A	80
Fig. 5.28: Maximum storage zone temperature on 9/10/93	81
Fig. 5.29: Meteorological data for Amman on 9/10/1993	81
Fig. 5.30: Maximum storage zone temperature on 13/10/93	82
Fig. 5.31: Meteorological data for Amman on 13/10/1993	82
Fig. 5.32: Temperature profiles on 16/10/1993 at 11:00 when 40 cm rings are introduced into pond A	85
Fig. 5.33: Temperature profiles on 16/10/1993 at 15:00 when 40 cm rings are introduced into pond A	85
Fig. 5.34: Temperature profiles on 20/10/1993 at 11:00 when 40 cm rings are introduced into pond A	86
Fig. 5.35: Temperature profiles on 20/10/1993 at 15:00 when 40 cm rings are introduced into pond A	86
Fig. 5.36: Salinity profiles on 16/10/1993 when 40 cm rings are introduced into pond A	87
Fig. 5.37: Maximum storage zone temperature on 16/10/93	88
Fig. 5.38: Meteorological data for Amman on 16/10/1993	88
Fig. 5.39: Maximum storage zone temperature on 20/10/93	89

ABSTRACT

" Performance of Salinity Solar Pond in Jordan "

Prepared by: Ala'a Rateb El-Baz

Supervisor: Dr. Bassam Jubran

The study contains a review of the theory, the description and the development of the salt gradient solar ponds together with a revision of the world wide activities in this field. It also covers two experimental set-ups that were built and investigated in Jordanian climate conditions.

The aim of this research is partly to acquire some of the know how needed to design, construct and test a large scale salt gradient solar pond for Jordan. The first experimental part of the research concentrates on experimental investigations of the local clays for their potential use as lining and base material for solar ponds. It investigates their characteristics; their liquid limit, plastic limit, plasticity index, optimum water content and permeability. The work describes and evaluates an optimum scheme consisting of combinations of compacted local clay and low density polyethylene film by means of a solar pond liner test rig. The results indicate that this scheme can be used effectively for lining solar ponds.

The other experimental part of this research consists of building up two prototype solar ponds. The temperature and salinity profiles of these ponds are described. The effect of plastic rings with different

sizes that were introduced to the solar ponds at different periods of time are investigated. Results show that these rings can work as wind suppressors and can improve the performance of the salt gradient solar ponds considerably.

CHAPTER 1

INTRODUCTION

1.1 Introduction

The solar energy reaching Earth's surface is sufficient to meet current world energy requirement. If appropriately harnessed, it could provide a long-lasting energy source that would contribute directly to improving the quality of life in this planet.

One of the properties of solar energy is that it is a diffuse source. Therefore a large area is required to collect a substantial quantity of energy. One option that could be used to utilize solar energy is the solar pond, which presents a low-cost large-area solar collector.

Solar ponds have great potential as an inexpensive low-temperature heat source. Seasonal energy storage capability and economic feasibility are attractive features of solar ponds.

The term "solar ponds" describes several different concepts, in all of which water is heated by the absorption of solar radiation, and serve as a thermal storage medium for the collected energy. Most common, convection is suppressed at or near the top of the solar pond so as to reduce heat losses by a means that is partially transparent to solar radiation.

Serious researches with solar ponds began in 1960. Sharp escalation

of energy costs during 1970's brought more interest in solar ponds on a global basis. It is considered as an alternative source of energy, which has many applications, i.e. generating electricity, heating source for green houses, and a variety of low temperature thermal applications.

A salt gradient solar pond (SGSP) is one type of solar ponds that is a body of saline water which performs both as a collector of solar energy and as a long-term thermal storage system. It usually consists of three distinct zones; the upper convective zone (UCZ) of uniform relatively low salinity and temperature at the surface of the pond, the non-convective zone (NCZ) in the middle of the pond where the salinity and temperature increases with the depth and the lower convective zone (LCZ) of uniform high salinity and temperature at the bottom of the pond.

Thermal performance of the solar pond is influenced by number of parameters such as the thickness of each of the three zones, salinity, depth, size of the pond, insolation, bottom temperature, wind speed and surrounding medium.

1.2 Present Work Contribution

The present research investigates the potential of various local clays as lining materials for solar ponds in Jordan, as well as looking at some of the factors affecting the performance and stability of solar ponds.

The experimental work includes the construction of a lining scheme experimental set-up to test various local clays. Furthermore, two

identical solar ponds have been constructed, with one is used to introduce the factors to be investigated, while the other one is used as a reference solar pond. Wind suppressors have been introduced to one of them and a comparison between the behaviour of the two ponds was carried out in order to study the effect of these suppressors on the solar pond stability.

1.3 Importance of the Work

Jordan has the potentials to establish a solar pond specially in the area of the Dead Sea, because of many attractive characteristics such as the availability of free salt, the high incident solar radiation and relatively low wind speed. Therefore it is important to look at the problems that could occur during the construction and operation of such a solar pond. This research offers an alternative local lining material that would reduce the capital cost of the construction of solar pond in Jordan. This work also introduces some technique in order to maintain the stability and maximum efficiency of a solar pond.

1.4 Organization of the Thesis

The thesis is divided into six chapters, the first one is this introduction. Theoretical and Practical aspects of solar ponds are presented in chapter (2). Literature review is discussed in chapter (3). In chapter (4) the experimental setups and procedure of the work is described. The results obtained and the discussion of these results are presented in chapter (5). Finally in chapter (6) concluding remarks and recommendations for future work are presented.

CHAPTER 2

THEORITICAL AND PRACTICAL ASPECTS OF SOLAR PONDS

2.1 History

The concept of the solar pond was first appeared in the scientific literature by the beginning of the 20th century as an explanation for the temperature phenomena observed in several naturally occurring lakes in a salt region of Transylvania, then in Hungary. This phenomena was described in the Medve Lagoon, Transylvania, where the temperature in excess of 70°C had been measured in the lake [1].

Similar conditions have been found in other few places in the world. Solar pond behaviour was discovered in Lake Vanda in Antarctica, where the surface of the lake is covered by ice and the temperature at 60 m depth approaches 25°C. It was also found in Panama Canal, Lake Mahega in Uganda and in the Los Roques Islands in Venezuela [1,2].

Serious investigation and studies of the solar ponds as solar collectors were initiated in the Occupied Palestine in 1958 Bloch carried out by a group led by Tabor [3] and Martz [4], which resulted in very important reports of operating experience from several ponds and several theoretical papers including a hydraulic theory of heat extraction and a theory of stability and energy balance.

The work stopped in 1966 due to the competitive energy from

available and cheap oil. But the solar pond research and development program restarted in 1973 in the United States and Occupied Palestine.

Solar pond activities in the U.S.A began with the work of Rabl and Nielsen at the Ohio State University [1]. while many feasibility and some engineering design studies have been conducted for the use of solar ponds to generate electricity. The majority of solar ponds experimental work has been devoted to process heat applications. There are several ponds in the United States in operation, e.g. Argonne National Laboratory Pond (1,080 m²), Great Salt Lake in Utah (2 x 36000 m²), University of Illinois (2,000 m²), Nevada Power Co. Pond (2 x 160,000 m²), etc.

Theoretical and experimental research on solar ponds have been widely conducted in other countries in the world such as Mexico, India, Ausralia, Egypt [1].

2.2 Salinity-Gradient Solar Pond

The salinity-gradient solar pond as the name suggests is a solar pond in which a salinity gradient is established. More specifically, over some range in depth the concentration of salt dissolved in water (salinity) increases with depth. As shown in figure 2.1, a salinity-gradient solar pond is a body of water that typically has three distinct regions, which are:

1- The Upper Convective Zone (UCZ):

The upper convective zone or the surface zone is a homogeneous layer of low-salinity brine or fresh water. Vertical convection takes place due to the effect of both wind and evaporation action, thus it has a temperature equilibrium with ambient air. These surface influences act of the transition region to move it downward which is unfavorable, and there are limited studies of different possible practical procedures for minimizing these effects of wind and evaporation action and other surface influences.

2- The Non-Convective Zone (NCZ):

The non-convective zone which lie below the upper convective zone constitutes a thermally insulating layer that contains a salinity gradient such that water closer to the surface is always less salty than the water below it.

This zone serves both as a "window" through which incident solar radiation passes into the storage zone and as a "cover" that insulates storage zone from the cooler environment. A relatively thin gradient zone functions more effectively as a window while a relatively thick gradient zone functions more effectively as an insulation cover. Therefore there exists an optimum thickness for which the rate of energy collected in the storage zone is maximized.

3- The Lower Convective Zone (LCZ):

The lower convective zone is a homogenous, concentrated salt solution that either can be convecting or temperature stratified.

This zone acts as a thermal storage layer, of almost constant, relatively high salinity and temperature.

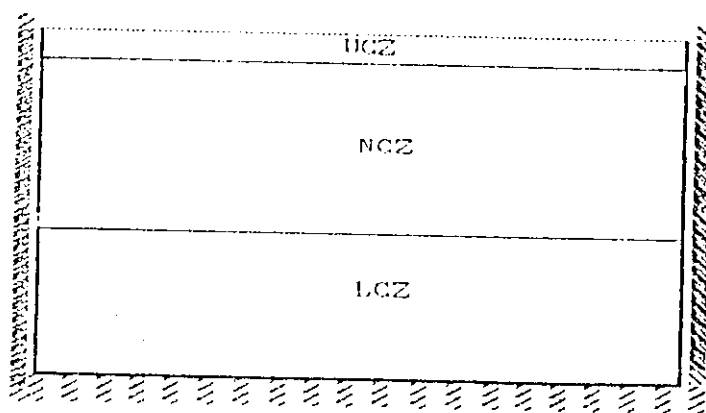


Fig. 2.1: Schematic diagram of the SGSP

2.3 Thermal Performance of Salt-Gradient Solar Pond

The utility of solar pond depends on the amount of thermal energy that it can deliver and the cost of constructing and maintaining it. The thermal performance of a solar pond depends on many factors such as the intensity of solar radiation, the transmissivity of the water, the heat losses, and others.

Calculations of steady-state or mean-value solar pond performance were made by Weinberger [5], Rabl and Nielsen [6] and Kooi [7]. Weinberger developed an analytical solution of the partial differential equation for the transient temperature distribution by superimposing the effects of radiation absorption at the surface, in the body of water and the bottom and he considered each effect separately. Rabl and Nielsen, and Kooi used similar approach to solve for the general one-dimensional equation for temperature T in a conducting nonconvecting medium that is transmitting and absorbing radiation which is [1]:

$$k \frac{\partial^2 T}{\partial z^2} - I \frac{\partial \chi(z)}{\partial z} = C \frac{\partial T}{\partial t} \quad (2.1)$$

Where:

k : The thermal conductivity of the medium.

I : The irradiance on the top surface.

$\chi(z)$: The fraction of the incident radiation transmitted to depth Z .

Z : The depth that measured as positive downward.

C : The heat capacity per unit volume.

t : time.

The derivative $\partial \bar{\tau} / \partial z$ is negative, so that the term $-I_0 \partial \bar{\tau} / \partial z$ represents energy flux into the medium from radiation absorption.

The heat balance equations that Beniwal and Singh [8] used for SGSP was specified for each zone as the following:

* The Upper Convective Zone:

$$\Delta H = q_o + q_e + q_1 \quad (2.2)$$

* The Non-Convective Zone:

The one-dimensional equation [1] used in this model.

* The Lower Convective Zone:

$$q_2 + q_3 = q_u + q_b + q_s + q_{ext} \quad (2.3)$$

The thermal efficiency η of solar ponds was derived [9] into the following expression:

$$\eta = (\alpha \bar{\tau})_{eff} - U_{Lg} (\Delta T / H) \quad (2.4)$$

Where:

ΔH : The solar heat flux absorbed in the UCZ.

H : Average solar insolation at the top surface.

q_o : The rate of heat loss due to convection and radiation from the top surface of the pond.

q_e : The rate of heat loss due to evaporation from the top surface of the pond.

q_1 : Rate of heat conducted from UCZ boundary to NCZ.

q_2 : Solar heat flux absorbed in LCZ.

q_3 : Solar heat flux reflected from the bottom and absorbed in the

LCZ.

q_u : The rate of upward heat conduction loss.

q_b : The rate of bottom heat losses.

q_s : The rate of side heat losses.

q_{ext} : Rate of heat extraction from the LCZ.

ΔT : Difference in temperature between LCZ and ambient.

U_{Lg} : Heat loss factor including ground heat losses.

$(\alpha\tau)_{eff}$: Effective absorptivity-transmittivity product.

From the above equations, it is obvious that the thermal performance of the solar pond depends on the amount of incident solar radiation collected, the amount of heat lost to the ground, the amount of heat lost through the gradient zone, the total storage capacity, and the effectiveness of the heat extraction system. Therefore, in order to maximize the extracted heat, the heat losses should be minimized.

2.4 Stability Analysis for Salt-Gradient Solar Pond

The nonconvecting solar pond concept is dependent on establishing a nonconvecting, transport liquid pool in which temperature increases with depth. To obtain such a system without use of membranes or other barriers to fluid motion, it requires that the decrease in density due to increasing temperature be offset by an increase in a salt concentration, from increased solubility at elevated temperature.

A principal advantage of the solar pond over other collector systems is its inherent capacity for long term thermal energy storage, typically on the order of monthes. A through investigation of steady state behaviour must therefore consider these systems during extended periods of solar radiation or darkness. Thus the pond must maintain an increasing density and temperature with depth [10]. This requirement can be expressed as [10]:

$$d\rho/dz = (\partial\rho/\partial T)_c \cdot \partial T/\partial z + (\partial\rho/\partial C)_t \cdot \partial C/\partial z > 0 \quad (2.5)$$

where ρ, T, z and C are density, temperature, depth and salt concentration respectively.

Thus, the required salt concentration gradient at any point of the pond should satisfy the equation:

$$\partial C/\partial z > -\alpha/\beta (\partial T/\partial z) \quad (2.6)$$

Where:

$\alpha = 1/\rho (\partial\rho/\partial T)$ is the thermal expansion coefficient.

$\beta = 1/\rho (\partial\rho/\partial C)$ is the salt expansion coefficient.

Equation (2.6) can be expressed as:

$$\Delta C_{\min} = \alpha/\beta \cdot \Delta T \quad (2.7)$$

This equation is referred to the simple " Static Stability " criterion.

Weinberger[5] states that to prevent an oscillatory disturbance that is initiated by some external perturbation and increased by time, the previous condition is not sufficient, and the following condition must be satisfied for " Dynamic Stability " criterion:

$$\partial C/\partial Z > - \left(\left[\frac{\nu + K_T}{\nu + K_c} \right] \partial \rho/\partial T \cdot \partial T/\partial Z \right) / (\partial \rho/\partial C) \quad (2.8)$$

Where:

ν : Kinematic viscosity in cm^2/sec .

K_c : Coefficient of salt diffusivity in cm^2/sec .

K_T : Coefficient of thermal diffusivity in cm^2/sec .

The concentration difference can be maintained in the pond by adding salt to the bottom layer and washing the top of the pond with clear water.

This static and dynamic criterion should be satisfied in order to maintain stability of the gradient zone and thus the solar pond. In SGSP the concentration increases with depth. This gradient causes salt diffusion in the opposite direction from the bottom to the top. The amount of diffusion depends on [11]:

1. The molecular diffusivity of the salt.

2. The salt concentration gradient.

3. The induced mass eddy diffusivity caused by surface waves on other perturbations.

2.5 General Design Considerations

Solar ponds are in principle very simple and inexpensive systems for the collection and storage of solar energy. In this section, the generally accepted requirements for successful solar pond application will be discussed. These requirements are site requirements, pond pond sizing and construction, pond filling methods and heat extraction accomplished [12].

2.5.1. Site Requirements:

For a particular location to be appropriate for a solar pond there are several essential requirements that must be satisfied, which are [12]:

- a. Use for the heat or power produced.
- b. Access to water.
- c. Access to salt.
- d. Disposal method for surface brine removal.

In addition to these requirements, there are desirable characteristics for solar pond sites such as:

- * High insolation.
- * Moving water table not too close.
- * Low wind speed.
- * Absence of wind-borne debris.
- * Relatively flat site.

- * Soil with good cohesion for walls.

2.5.2 Pond Sizing and Construction:

The size of salt-gradient solar pond should depend on the utilization of energy stored by the pond. Many factors must be considered when sizing of a solar pond designed like [13]:

- a. Average insolation, and ambient temperature.
- b. Maximum design pond temperature.
- c. Soil thermal conductivity.
- d. Pond configuration.

Construction of a solar pond is similar to that of other containment systems and water reservoirs. The usual way to construct a solar pond is to create some combination of excavation and wall embankment that produces the required depth and area [1]. The most important factors in deciding the best earth excavation strategies to be chosen are [14]:

- a. The shape and slope of walls and bottom to avoid the need for wall support.
- b. Insulation configuration, to lower thermal losses from the bottom and walls of the pond.
- c. Lining of the walls and bottom to prevent leakage.

2.5.3. Filling the Pond:

The pond is normally filled in two steps: first the containment volume is filled to the appropriate level with homogeneous concentrated brine, and then the upper portion of this brine is progressively diluted with fresh or low-salinity water so as to create the gradient and the homogeneous surface zone.

There are few methods known so far to establish the salt-gradient solar pond. From these methods:

1. Superposition of Progressive Less Dense Brine:

This method consists of initially filling the pond with a high concentrated brine up to a level of the lower convective zone, then the pond is filled in layered sections one after another, each layer have a slightly different salt concentration, until fresh water is added at the top [15].

This method is time consuming, and expensive for commercial application because it requires an external mixing tank and frequent adjustments until the large layer is stacked.

2. Zangrando's Injection Technique (Redistribution):

This conventional method consists of initially filling the pond with concentrated brine to a depth equal to the depth of lower zone

plus about half the depth of the gradient zone, then injecting fresh water into the brine at successively higher levels, usually the injection begins at the bottom of the gradient zone through a diffuser that is raised at constant rate, so as to dilute the initial filling, thus creating the gradient, and finally, adding a layer of fresh water to make the surface zone.

This technique developed by Zangrando [16] is simple to carry out and has been used for filling most of ponds now operating.

3. Brine Injection:

An opposite technique of Zangrano's method has been used in Australia [17] is to float the entire required quantity of fresh water on top of brine without mixing and then to create the gradient by injecting appropriate quantities of brine into the fresh water at successively higher levels.

4. Modified Redistribution Method:

Another method is by initially filling the pond with fresh water up to half the depth of the gradient zone. All salt is then dissolved in this water and the solution mixed to make a homogeneous brine, fresh water is then floated onto the surface of the brine, so that the pond is filled to the full operational level. This fresh water is subsequently pumped from the surface of the pond into a brine diffuser and injected into the high density brine solution. While the injection process is proceeding, the diffuser is raised from its position within the brine solution to the surface of the pond.

5. The New Passive Method:

Akberzadeh et al.[18] introduced a passive method for establishing an arbitrary density profile in a container of an arbitrary shape. Liquid is withdrawn using gravity from the bottoms of two tanks, one containing lower density liquid and the other containing higher density liquid. The liquids withdrawn from the two tanks are then mixed through a pipe which feeds the product gently to the bottom of a third tank in which a pre-specified density profile is required. The cross section of one of the filling containers is assumed to be uniform. The second filling container must be shaped in such a way that allows the desired profile in the third container to form.

2.5.4. Heat Extraction:

The extraction of the thermal energy trapped in the storage zone can be accomplished by two different schemes; The first scheme [19] consists of a heat exchanger that is submerged into the lower convective zone, and the cold fluid may be pumped through the piping array to collect the heat stored. The main disadvantages of this approach are [15]:

- Corrosion or pitting the heat exchanger pipes.
- Low heat transfer coefficient between the brine in the bottom and the heat exchanger.
- The heat exchanger must be removed from the bottom, when maintenance or repairs are required.
- Large heat exchanger area is required.

2.6 Problems Encountered During Operation of Solar Pond

Experimental solar ponds have not always yielded the results desired, and it may be useful to discuss some of the problems encountered. Many of these problems have arisen from misconceptions and inappropriate operating procedures, and there are also a few problems without good solution with the present state of knowledge. Some of the problems occurred during the operation of a solar pond are [1]:

a. Gradient Problems:

Surface zone enlargement by wind and thermal convection erodes the gradient. Some wind barriers may limit the action of wind but there is no way known to limit the gradient erosion from thermal convection in the surface zone except by increasing the gradient at the boundary, and this increase can only be realized at the expense of an increased rate of salt transport into the surface zone.

b. Flow Problems:

Pumped flow is a normal aspect of pond operation in adding or removing liquid from the surface zone, in salinity maintenance and heat extraction from the lower zone, and for special operations within the gradient zone, such as injection or removal of fluid for addition of chemicals or for gradient modification. All of these operations can be carried out so as to produce the desired results. Unfortunately, there have been many cases in which the desired flow without damage has not

2.7 Applications

Many applications of the solar pond are reported in the literature. The well known application will be presented in this section.

2.7.1 Heating and Cooling

Solar ponds provide a unique technique for collecting and storing the solar radiation including the possibilities of seasonal storage. This ability of storage from summer to winter encourages the use of solar ponds for solar heating of buildings.

Rabl and Nielsen [6] suggested that the ponds could be used for single houses, where the pond area would be about the house floor area. Bryant and Colbeck [21] suggested that the space heating of buildings with solar pond is practical, even in the climatic conditions of London.

The space heating seems to be feasible and competitive with the traditional heating using fossil fuels [1]

The availability of absorption coolers which are capable of working at temperatures of about 90°C makes it possible for solar ponds to be used in hot climate areas [15].

2.7.2 Agricultural Systems Applications

Solar energy for crop drying has been used in many parts of the world. The requirement of temperature and other factors for drying of various crops have been discussed by Sodha et al. [22]. The solar pond could provide heat for grain drying because its maximum temperature typically occurs in late summer and a properly designed pond can still retain most of its stored energy at the beginning of the grain-drying season. The University of Illinois SGSP demonstrated that solar ponds for low grade heating applications such as space heating and grain drying can be designed in a simple manner that requires minimal maintenance duties [23].

Efforts to extend the growing season using greenhouse structures, which may need external heating during period of cold weather. Solar ponds have been constructed for greenhouse heating in Ohio [24] and Portugal [25]. For this application the depth of the pond should be sufficient for the pond to supply heat throughout the winter season. A lack of sufficient heat could result in an expensive loss of a crop. Often it is most important to heat the soil of the greenhouse rather than the air.

2.7.3 Electrical Power Generation

Low-temperature solar heat usually compares most favorably with heat from other energy sources when used directly as heat. The low efficiency of thermodynamic conversion to produce shaft work or electricity excludes solar thermal power except in very favorable sites where solar pond heat is unusually low cost or other energy sources are unusually high cost, such as Dead Sea.

The solar ponds of 250,000 m² total area at Beith Ha'Arava, at the Dead Sea are in a very favorable site and are designed to operate 5 MW peaking power plant using low-temperature Organic Rankine-Cycle (ORC) [26], even though the overall efficiency is less than 2%.

2.7.4. Desalination

The development of multistage flash desalination (MSF) and multieffect distillation (MEF) technology that operates at temperature around 70°C has opened the possibility of using solar ponds as a heat source for such units in locations where fresh water is lacking but sea water or brackish water is available. The solar pond could also be used in desalination applications by producing electricity to run a reverse osmosis (RO) desalination plant or other electricity using method. Many researchers [27,28,29] have carried out several investigations for utilizing solar ponds for desalination.

2.7.5. Salt Production

Solar ponds can also be used to produce salt from sea-water, with more efficient concentration mechanism than open-pan salt evaporation pans. Matz [30] have described this method in detail.

Lesino et al.[31] described the production of industrial grade sodium sulfate from a mineral consisting in a mixture of sulfate decahydrate, sodium chloride and clay using solar ponds.

CHAPTER 3

LITERATURE SURVEY

3.1 Introduction

The researchers considered the solar ponds as a method of trapping solar energy and have proposed some means for utilizing it. Therefore, many investigations were carried out to analyze the mechanism, the thermal behaviour and stability of solar ponds theoretically and experimentally.

3.2 Theoretical Studies

Analytical and numerical studies were performed to solve the general thermal performance equations, heat balance equations and stability criteria.

Tybout [32] proposed that all time and depth variables in the general equation should be treated as discrete elements and he recommended to use finite difference method in an iterative computer model for the thermal behaviour of a solar pond, Hull [33] was the first researcher who implemented Tybout suggestion. He used time incremental numerical technique to predict the thermal behaviour of a solar pond as well as to investigate some of the assumptions employed by Weinberger [5]. He concluded that the long-term averaging functions e.g. the yearly periodic sinusoidal functions of ambient temperature and total insolation, are adequate for modeling a solar pond thermal behaviour.

Several numerical models have been designed for simulating the salt gradient solar pond:

Cha et al. [34] who developed a one-dimensional numerical model to predict the diurnal variations of vertical temperature and concentration profiles in SGSPs.

Wang and Akberzadeh [35] used finite difference formulation and found that the existence and the thickness of UCZ has a profound negative effect on the yield of solar pond.

Panahi et al. [36] described a one-dimensional model to simulate the dynamic performance of stratified solar brine ponds. They presented a study of overall pond efficiency, an optimization study of non-convective zone thickness and an investigation of the heat storage efficiency.

Kaushika et al. [37] used Wang et al. model [35] for temperature calculations and thermal storage. Duyar and Bober [38], and Hull [39] considered in detail the bottom heat loss of a solar pond in the presence of moving water table. Beniwal et al. [8] estimated the ground heat losses from the SGSPs working under natural conditions. They developed an expression for the soil thermal conductivity. Zhang and Wang [40] adopted a computer simulation method to study the ground heat loss and the heat recovery rate under varied parameters, where, Duyer et al. [38] based their analysis on the steady two-dimensional energy equation for a simplified solar pond model using finite difference direct method. Hull [39] presented both steady-state analytical and time-dependent solutions for this case.

Other numerical simulation and analytical solutions have been developed to study the steady state thermal performance and monthly performance of solar ponds [41], the time-temperature variations [42], the heat losses and thermal efficiency [9].

Atkinson [43] examined analytically the possible influence stratification on the vertical transport salt and heat in a mixed-layer simulation model for a salt gradient solar pond. He showed that when a mechanical stirring is presented in the mixed layer, double-diffusive instabilities will not be allowed to grow.

3.3 Experimental Studies

3.3.1 Introduction

Many experimental works have been conducted to get better information of constructing, operating and studying solar ponds. One of these works is by Lewis et al. [44] who simulated the mixing layer development in laboratory experiments involving salt stratified solutions heated from below, cooled from above and/or irradiated from above. An interferometer was used to visualize mixing layer development and to infer salt concentration and mass density distribution in stable regions of the solution but without allowing evaporation to occur during the experiment. This was the first step in using interferometry to study mixed layer development in a salt stratified solution.

Beniwal et al. [45] used small salt gradient laboratory solar pond made of concrete-cement. The density distributions were measured

several times at intervals of ten days in various heating loads. Temperature distributions were also measured at each operating temperature. The operation and results were discussed, and profiles were viewed.

Munoz et al. [46] performed experiments in a large tank to determine the effects of combined mixing, due to bottom heating and a horizontal recirculation, on the entrainment of salt stratified fluid.

Banat [15] conducted a small laboratory solar pond tank, (size 2m x 1m x 1m) which was the first attempt in Jordan. He used carnalite salt and observed the temperature and salinity profiles. He recommended to perform the experiment in larger tanks and to study factors affecting the stability of the pond such as the wind effect on the solar pond in Jordan climate.

Many other experiments conducted on the topic of salt gradient solar ponds. But most of them treat specific phenomenon or problem occurred in the ponds or the operation and maintenance techniques followed. These topics will be presented in details in the following sections.

3.3.2 Stability Experiments

Solar pond stability is the most crucial subject in the operation of SGSP, and once the stability is lost, the zones of solar pond will be mixed and the pond will effectively and quickly be deteriorated.

Leshuk et al. [10] executed experiments to study the solar pond stability. They reported a maximum bottom

temperature of 76°C and stable temperature gradients ranging from 150-300°C/m. They concluded that the slow top and bottom mixing layer growth occurred from diffusion was the only failure mode noted despite attempts to introduce instabilities at intermediate levels.

Wang and Akberzadeh [47] introduced one method for avoiding the diffusion effect, which is " Falling Pond ". The basic idea of this method is that extracting brine from the bottom on NCZ, a downward velocity is given to the water in the pond, when this downward velocity just offset the upward salt diffusion, the net flux becomes zero.

$$v_c - K_c (\partial c / \partial y) = 0 \quad (3.1)$$

Where K_c : Coefficient of salt diffusion cm^2/s

As a result, no make up salt is needed, and fresh water has to be separated from the extracted hot brine and returned to the top of the pond, and the resulted concentrated brine should be injected back to the bottom of the pond.

Cha et al.[48] compared the experimental results to the theoretical stability criteria of a SGSP. They reported the effect of heat extraction on the stability. Cha et al also reported on the cellular motion in the nonconvective zone may be the cause of instability. This cellular motion is known by convective cells or layers which are generated by the side wall opposite to the solar radiation.

Akberzadeh et al. [49] reported the results of a series of demonstrative laboratory experiments simulating the possible instabilities in density-gradient solar pond that can be induced by absorption of sunlight on the sun-facing wall. They have observed that under the simulated solar pond conditions, convective layers with thickness between 10 and 20 mm can be generated. The fronts of these layers advance with a speed of 0.2 to 0.3 m/h.

More recently, Akberzadeh [52] reported a series of field and experimental observations on the convective layers generation and advancement. He also simulated this situation in a laboratory tank.

3.3.3 Wind Effect

The existence of the top convective layer in solar ponds can be considered as one of the most important factors limiting the efficiency of these solar ponds. More than a third of the solar radiation falling on the surface of the pond is usually absorbed in this layer and then subsequently lost to the atmosphere. A reduction in the thickness of this layer can result in a substantial increase in the overall efficiency of solar ponds.

The formation of the top convective zone is mainly caused by the following two factors:

a. The absorption of solar radiation in the first few centimeters depth of water causes a large temperature gradient, which results in the development of a convective currents, and forming very high temperature gradient as high as $500^{\circ}\text{C}/\text{m}$ [53] which exceed the the stability limit in ordinary salt gradient solar ponds.

b. Wind effects cause mixing in the top region of solar ponds. Wind effects can be separated into two effects (i) surface waves and (ii) wind-driven currents. Waves cause turbulence and include eddy diffusivity which in turn reduces the salt concentration gradient and this may result in complete convection in this region. Wind shear effect also generates some current at the surface, which creates circulation in the vertical plane and results in layer mixing and erosion of the top surface of the density gradient layer.

Schladow [54] studied the physical processes that occur at the surface of a SGSP using a numerical model. Results indicate that the

influences of wind stirring and evaporative effects are the causes of the deepening of UCZ. He suggested a method of enhanced surface washing to control surface layer deepening and to substitute water evaporated.

Akberzadeh et al. [53] investigated the phenomenon of mixing in the top region of solar ponds and the effects of winds in creating UCZ. They reported that both the wave characteristics and the effect of surface current are fetch length dependent. The velocity v and the amplitude h of waves in terms of wind velocity and fetch length are:

$$v/h = 1.37 [1 - (1 + 0.008 X^{0.333})^{-5}] \quad (3.2)$$

$$gh/U^2 = 0.3 [1 - (1 + 0.004 X^{0.5})^{-2}] \quad (3.3)$$

Where:

U: The wind velocity.

g: The acceleration due to gravity.

X: Nondimensional length defined as:

$$X = x g / U^2 \quad (3.4)$$

Where x is the fetch length.

Therefore, the wave length λ can be given in terms of v as follows:

$$\lambda = 2 \pi v^2 / g \quad (3.5)$$

Wind shear effect on the surface of solar ponds creates surface currents. The magnitude of the surface velocity U_s in terms of wind speed U is given by Keulegan [44] as:

$$U_s / U = 0.033 \quad (3.6)$$

This equation is conditional on the Reynolds number Re greater than 100,000, where Reynolds number is:

$$Re = U_s \nu / Z > 100,000 \quad (3.7)$$

Where:

Z : The depth

ν : The kinematic viscosity of water.

Akberzadeh [53] also presented the the idea of using floating rings, which are made of material slightly lighter than water. The rings simply divide the surface of the pond into small regions. In this case the maximum wind fetch can be decreased to the diameter of the rings. Therefore, the wind action is limited to the surface of individual rings instead of the whole pond and as a result, wind action substantially decreased. This idea was tested experimentally and it was found that the floating ring wave suppressors can successfully decrease the depth of the top mixing layer [55,56,57,58].

Two arrangement of wind suppressors of PVC floating pipes were considered under the environment of Arabian Gulf area in an experimental small solar ponds (2m x 2m x 1m) by Tag and Hassab [59]. The first arrangement consists of four pipes equally placed in a cross pattern, and the second consists of two pipes spaced cross-wise. The salinity and temperature profiles were recorded, and the results showed that the wind suppressors of the floating piping type, can considerably slow down the movement of the upper convective-gradient

zone interface and prohibit any formation of localized convective zones.

It is obvious from the above literatures that plastic rings suppress the effect of the wind on the surface of the pond thus, the performance of the pond would be maintained. But the information of the proper size of the rings i.e the diameter is still questionable. On the other hand, the researchers reported on the effect of the plastic suppressors, which is based on the historical behaviour of a single specific solar pond. In this experimental work, the performance of two solar ponds under the same conditions is investigated, where one of them is provided with plastic rings while the other is left as it is. This could provide better information of the effectiveness and the importance of the plastic rings suppressors. Also, the effect of the diameter of the rings will be studied by using different sizes of rings. A comparison between the behaviour of the two ponds for each case will be held in order to generalize the proper size of such suppressors.

3.3.4 Leakage

Brine leakage from solar ponds constitutes one of the major factors to be considered, because it represents both a loss of heat and salt. Heat loss must also be taken into consideration, so that it is essential that the soil below and around the pond be as dry as possible so it will provide good insulation and minimize heat loss.

Any seepage of brine out of the pond into the soil beneath the pond will increase the heat transfer coefficient of the soil, and increase heat losses. Such losses can seriously reduce the efficiency of the solar pond and will also pollute the local under-ground water. Therefore liners will be needed to prevent this seepage.

Synthetic plastic membrane liners have been used to ensure impermeabilities to hot brine is well established. The most successful plastic films so far are XR-5 and Hypalon, in terms of reliability and ease of installation. The main disadvantage of these materials is the high cost, which could reach 26% of the total initial cost[60]. For developing countries, it is highly desirable to use cheaper and locally available materials i.e. polyethylene, clays.

Almanza et al. [61] use compacted kaolinite (inorganic clay of high plasticity) clay which as an impermeable material to reduce leakage. They evaluate experimentally the clay's mechanical and thermal properties in terms of the plastic limit, liquid limit, plasticity index, moisture content, vertical permeability and thermal diffusivity.

The liquid limit (LL) is defined as the moisture content at which the soil stops acting as a liquid and starts behaving as a plastic

EXPERIMENTAL SET-UPS AND PROCEDURES
-----4.1 Introduction

The objectives of the experimental work are the followings:

1. Studying the properties of different local clays as liners for solar ponds.
2. Considering different parameters on the stability and performance of solar ponds.

Therefore, two experimental setups are required to achieve these objectives. A full description of the experimental set-ups, the salt used, meteorological data required, measuring instruments and procedures will be discussed below.

4.2 Liner Experimental Set-up and Procedure

The investigations of the permeability of local clays to be used as lining material for solar ponds consist of two stages, which are the followings:

Stage 1:

In this stage, similar techniques to that used by Alamanza [61] have been employed to classify the local clays.

Results for liquid limit, plastic limit were obtained to calculate the plasticity index which is used to classify the clays. The liquid limit has been measured using proctor standard method where the depth a hammer can penetrate at specific water content is measured. The liquid limit is taken as the water content at depth of 20 mm from the graph of the penetration depth against the water moisture according to Lambe et al.[63]. The plastic limit for the clay is obtained by drying the clay specimens using shearing method. This is done by determining the water content of the clay when the threads of the clay 3.2 mm in diameter starts crumbling.

This technique is used to test clays from five locations in Jordan, which are; Amman, Irbid, Karak,

Tafilah and the Dead Sea. Once the best clay among these is determined in terms of low permeability, then it will be used for the second stage of investigations.

Stage 2:

This stage consists of investigations to select the best lining scheme for solar ponds in Jordan. The schematic diagram of the test rig that has been used in the investigations is shown in figure 4.1. It consists of galvanized mild steel cylinder of 0.8 m diameter and 1.25 m height with a drain in its base. A strip of plexi-glass of 5 cm was fixed along the upper 60 cm of the cylinder to permit the monitoring of the level of water. The lining scheme was formed by stacking different layers of clays and local cheap lining material as following:

- The first scheme consists (from the bottom to the top) of 10 cm of gravel, 10 cm of sand, 20 cm of the local clay and another 10 cm of sand.
- The second scheme consists (from the bottom to the top) of 10 cm of gravel, 10 cm of sand, 20 cm of the same local clay but sandwiched with low density poly ethylene layer and 10 cm of sand. This scheme will be repeated but with a punctured low density polyethylene.

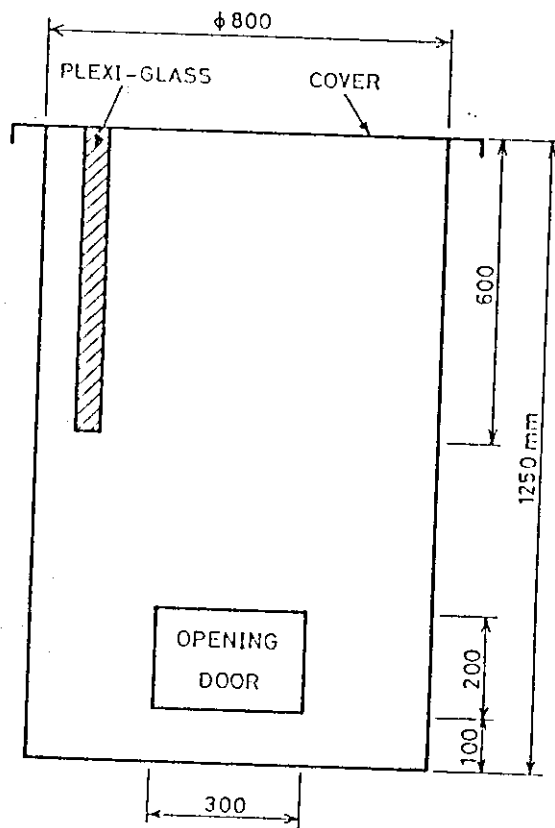


Fig. 4.1: Laboratory Apparatus For Testing Permeability

4.3 Solar Ponds Experimental Set-up and Procedure

Two identical prototype solar ponds each of 5 m^2 and 1 m depth were built. A schematic diagram for the prototype is shown in figure ^{3.1}4.2.

Each solar pond with a size of 2.5m x 2m x 1m was made of 3mm galvanized mild steel sheets and insulated with rockwool sheets. Two plexi-glass windows each of 6 mm thickness, 50 cm width and 1 m long were constructed as shown in figure 4.2 to permit the monitoring the solar ponds from inside.

The ponds were filled using redistribution technique described by Zangrando [16]. By considering the LCZ is of a depth L, concentration C and surface area A, and the NCZ of a depth H. The pond is originally filled to a depth ($L + H/2$) with a brine at the maximum concentration C. The residual of the pond with a volume of ($1/2 \times H \times A$) should be filled with fresh water by the diffuser.

The diffuser shown in figure ^{3.2}4.3 is a device that accepts water from a pipe and discharge it in a low velocity in the horizontal plane in all directions. It consists of two circular plates held apart by spacers. In this experiment the diffuser used was 30 cm diameter and 3 mm diffuser space.

Fresh water was added to the pond through the diffuser at the top of the LCZ (at 40 cm from the pond bottom) and fixed in this position until the pond surface was risen 2.5 cm. Then the diffuser was moved up 5 cm, refixed in its new position until the surface of the water was risen another 2.5 cm. This process was repeated until the diffuser reached the pond surface (at height 80 cm in this experiment).

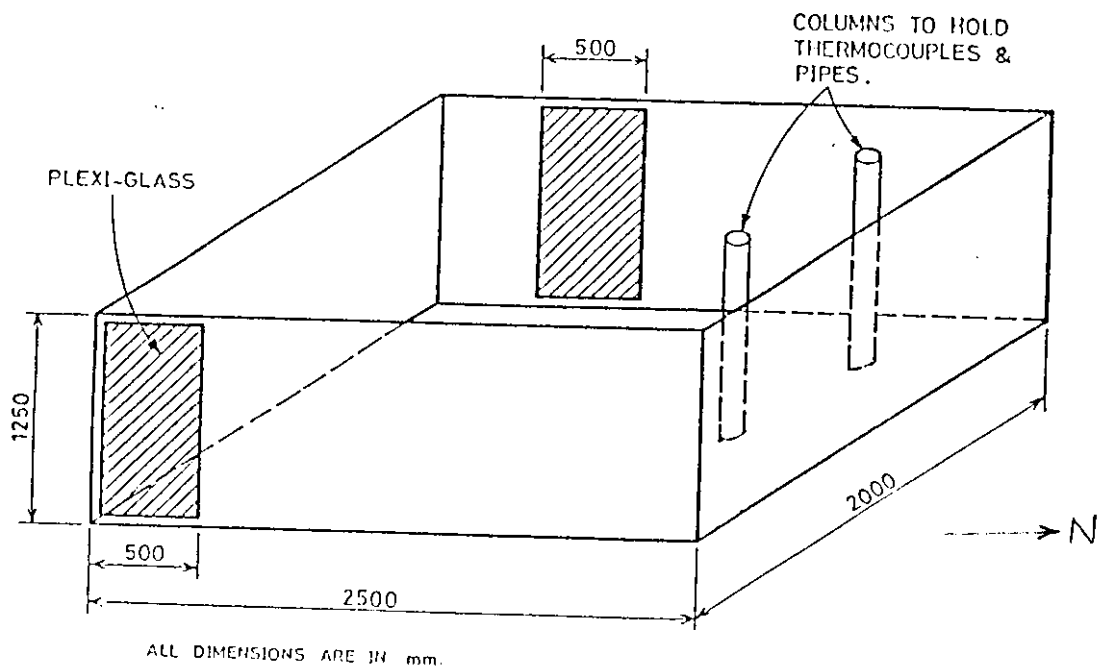


Fig 4.2: Prototype Solar Pond Tank

Diffuser size	0.3 m diam.
Diffuser space	3 mm

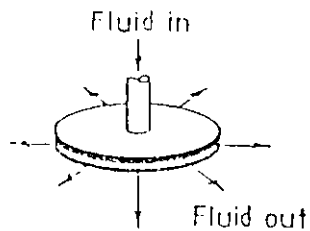


Fig.43 View of solar pond brine diffuser

4.4 Salt Quantities

The salt which is used in the present work is Carnalite salt ($\text{KCl.MgCl}_2.6\text{H}_2\text{O}$), which is harvested from the Dead Sea using the evaporations ponds of the Arab Potash Company. This salt is available in commercial quantities from the Dead Sea, and the cost of using such a salt in Jordan is minimal relatively to other salts.

It is necessary to calculate the quantity of salt required to establish solar ponds. The lower convective zone is supposed to have the maximum concentration, and the salt concentration of the non-convective zone should be reduced gradually from the bottom to the top of the solar ponds. Therefore, the volume of water in the LCZ is added to half the volume of the water in the NCZ.

In the present work, both the LCZ and NCZ have nearly the same depth of 40 cm for the two ponds. Since the dimensions of each pond are: 2.5 m length, 2 m width and 0.8 m height, therefore the volume required to calculate the salt needed is 3 m^3 ($0.6 \text{ m} \times 2.5 \text{ m} \times 2.0 \text{ m}$).

Accordingly, the mass of water required is 3000 kg.

The concentration of the saline water used in the experiments is 20%. Therefore, the salt requirement will be 750 kg.

But the salt contains 32% of its composition as water ($6 \text{ H}_2\text{O}$), thus the actual amount of salt needed is 1103 kg.

From the previous calculations, each pond needed 1103 Kg of

Carnalite salt in order to establish a solar pond with a maximum concentration of 20%.

The salt required for the liner test rig set-up for 20% concentration is 0.36 Kg of salt / Kg of water.

4.5 Meteorological Data

The meteorological data is important for analyzing the effectiveness of the solar ponds. The data needed in our research are the solar radiation, ambient temperature, relative humidity and wind speed. These data have been collected from the meteorological department for the period of 25 September to 3 November / 1993.

4.6 Measurements

4.6.1 Temperature Profile

The temperature profile has been monitored four to five times a day and three times a week by installing a set of 10 copper constantan (type T) thermocouples inside the pond. The thermocouples were fixed at equally spaced distances of 10 cm apart starting from 5 cm above the bottom, on a 1 m long rod which is 50 cm away from the North facing wall.

The temperature readings were taken directly by connecting these thermocouples to a 10 channel microprocessor thermometer (Cormak

Electronics Company, Type 6200).

The ambient temperature was measured whenever the temperature profile was monitored i.e four to five times a day three days a week using copper constantan thermocouples and the same microprocessor. But because it is necessary to measure the ambient temperature continuously, the ambient temperature data was also collected from the meteorological department.

4.6.2 Salinity Profile

The salinity profile of the pond was determined by withdrawing samples from a fixed ports located at equally spaced distances of 10 cm a part starting from 5 cm above the bottom, on 1 m rod. The samples were withdrawn using manual pumps that are connected to a pipe which is extended to the specific depth. The samples then is left to be cooled down to 20°C, and then to be weighted using 50 ml specific gravity bottles. The measurement of the specific gravity of the samples is an alternative method of measuring the salinity.

The salinity profile was measured at least once every week.

4.7 Accuracy of Measurements

4.7.1 Introduction

Errors that may cause inaccuracy in the measurements are included in Appendix A. The accuracy of temperature profile and specific gravity profile obtained for solar ponds and permeability results of different clays were estimated to be in the acceptable range.

4.7.2 Reproducibility of Measurements

Specific gravity profiles measurement of the solar pond as well as the liquid limit, plastic limit, optimum water content and permeability of the different clays were repeated different times under the same conditions and found to be within ~ 2 %.

RESULTS AND DISCUSSION

5.1 Introduction

The present work consists of two stages. In the first stage, local clays from different places in Jordan were examined to establish their potential as lining material for solar ponds. While in the second stage, two small prototype solar ponds were studied under the same conditions. The temperature and salinity behaviour of these ponds were recorded. After a period of time, plastic rings were introduced to one of these two ponds in order to study the wind effect on the behaviour of the ponds. In a later stage, a comparison between different sizes of rings were held by introducing rings with two different diameters in both ponds.

In the following sections, the results of the two stages will be presented and discussed.

5.2 Lining Material Experiment

This section reports the initial experimental results of the first stage. This stage consists of two parts. In the first part the characteristics of the various location clays have been scanned and reviewed to determine a proper clay. The second part consists of examining the permeability of a scheme that contains the proper clay selected from the first part using a clay test rig.

The characteristics of the various location clays that are examined contains; liquid limit, plastic limit, optimum moisture content, plasticity index and permeability.

5.2.1 Liquid Limit

The liquid limit (LL) for the different clays was determined using Casagrande Test [63] by plotting the water content of the caly against the depth of the hammer penetration of a special device called "Proctor".

The liquid limit was taken as the water content at depth of 20 mm. The liquid limits for Amman, Irbid, Dead Sea, Karak and Tafilah clays are shown in figures 5.1, 5.2, 5.3, 5.4 and 5.5, respectively.

5.2.2 Plastic Limit

The plastic limit was obtained for various clays using the shearing technique to crumble a sample of a clay of 0.0032 m in diameter [63]. The water content of the clay at this ponit represents the plastic limit.

5.2.3 Plastic Index

Once the plastic limit (PL) has been found, then, the plastic index (I_p) is found from following equation:

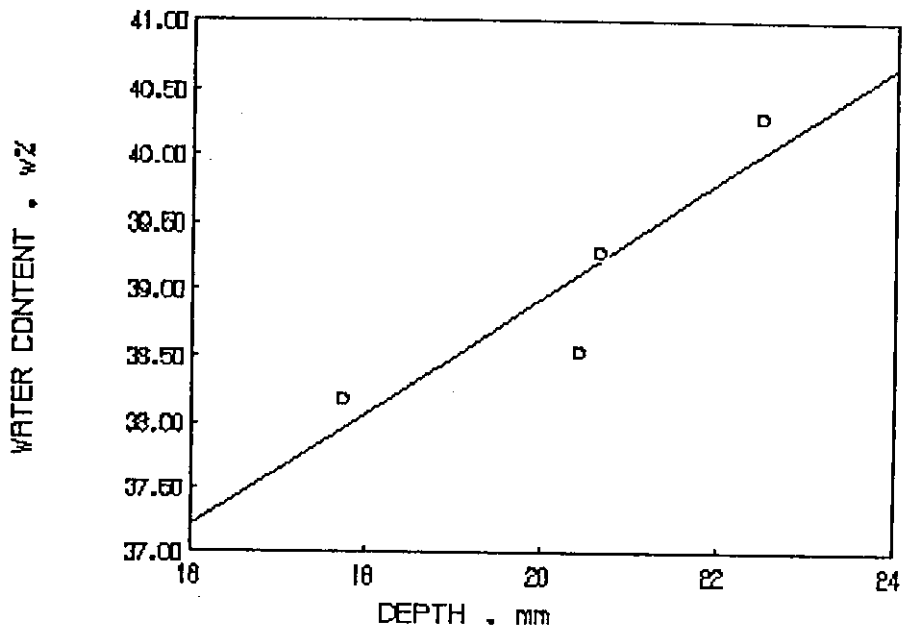


Fig. 5.1: Liquid limit for Amman clay

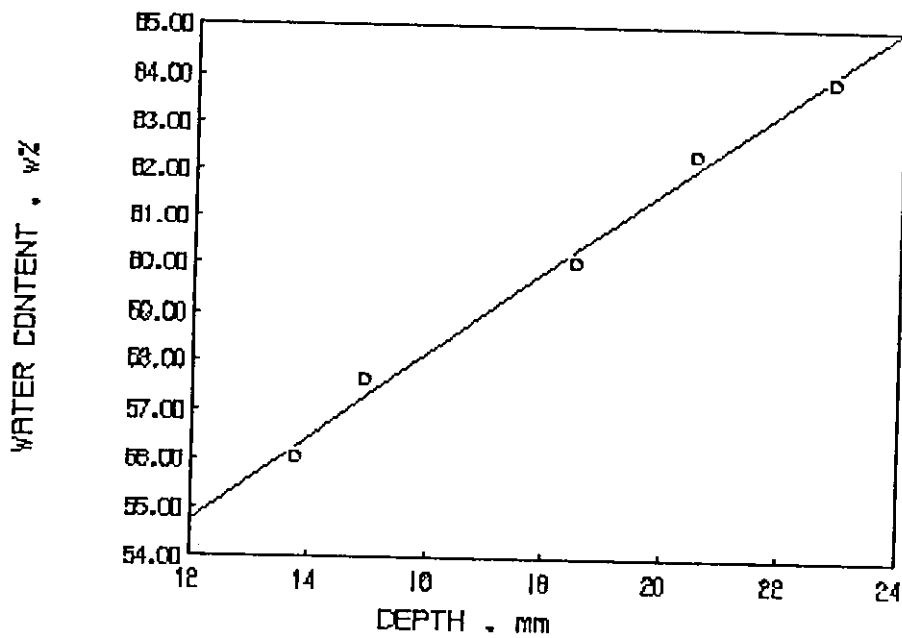


Fig. 5.2: Liquid limit for Irbid clay

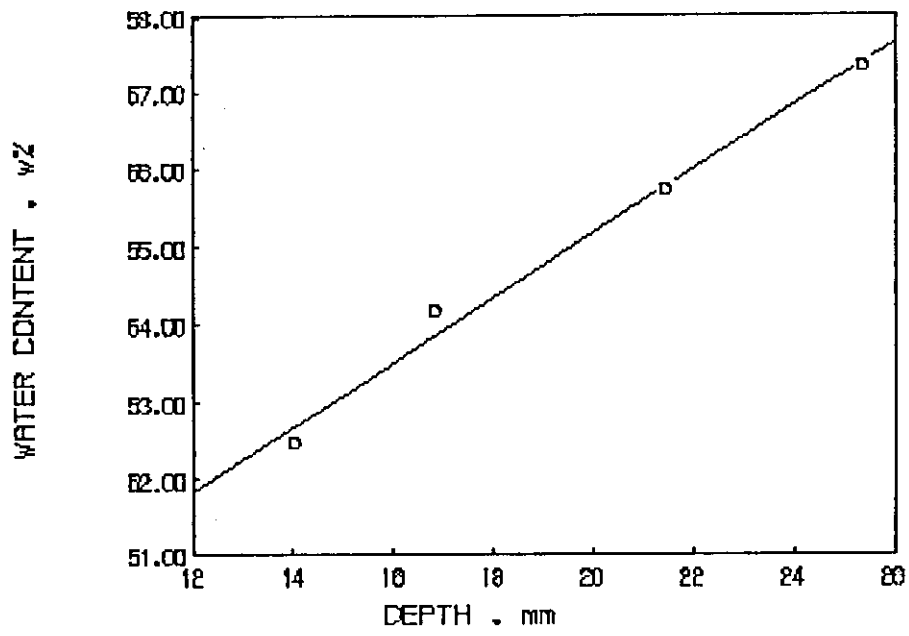


Fig. 5.3: Liquid Limit for Dead Sea clay

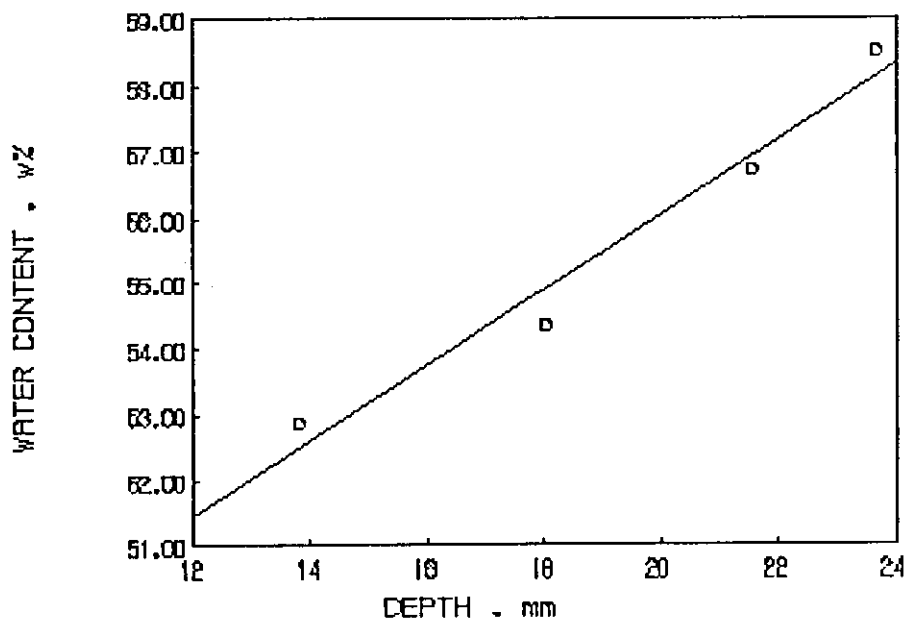


Fig. 5.4: Liquid Limit for Karak clay

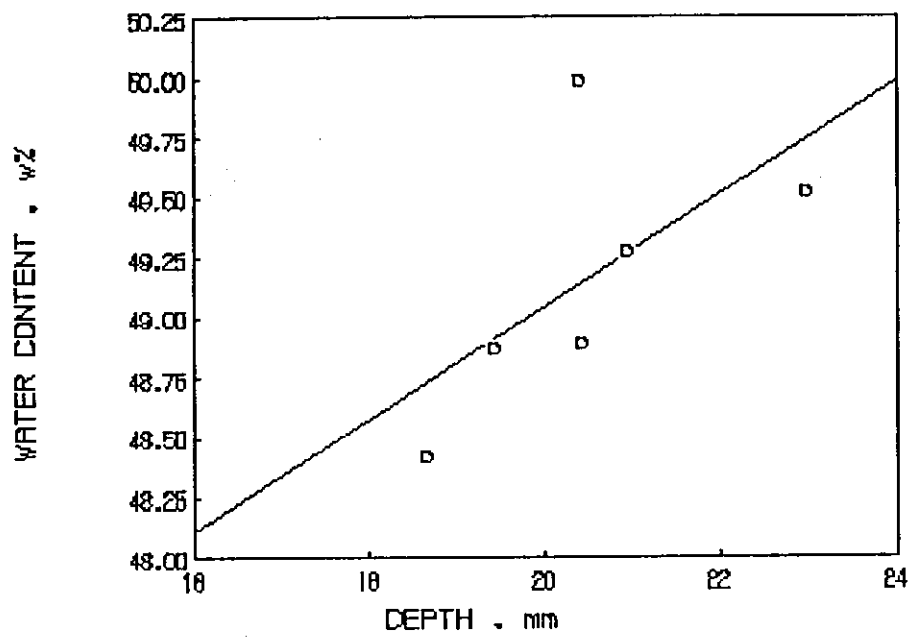


Fig. 5.5: Liquid Limit for Taflich clay

$$I_p = LL - PL \quad (3.18)$$

The plastic indices obtained for the various clays are used in conjunction with the plasticity chart, Figure 5.6, to determine the types of the clays investigated. In figure 5.6, the A line is an empirical boundary that represents the boundary between inorganic clays, CL (low to medium plasticity) to CH (high plasticity) and organic silts and clays, OL (low plasticity) to OH (medium to high plasticity), which lie below it. The location of B line shows that the clay is an inorganic with extremely high plasticity.

The clays classification for the various locations are given in Table 5.1.

Table 5.1 Clays Classifications in Jordan

Location	Plastic Index	Clay Classification
Amman	19.971	Inorganic Medium Plasticity
Irbid	35.674	Inorganic High Plasticity
Dead Sea	18.177	Organic Medium Plasticity
Karak	28.311	Inorganic High Plasticity
Tafilah	25.1332	Inorganic Medium Plasticity

5.2.4 Optimum Moisture Content

The optimum moisture content for the various clays was found by weighing the samples of the clays before and after drying them in the

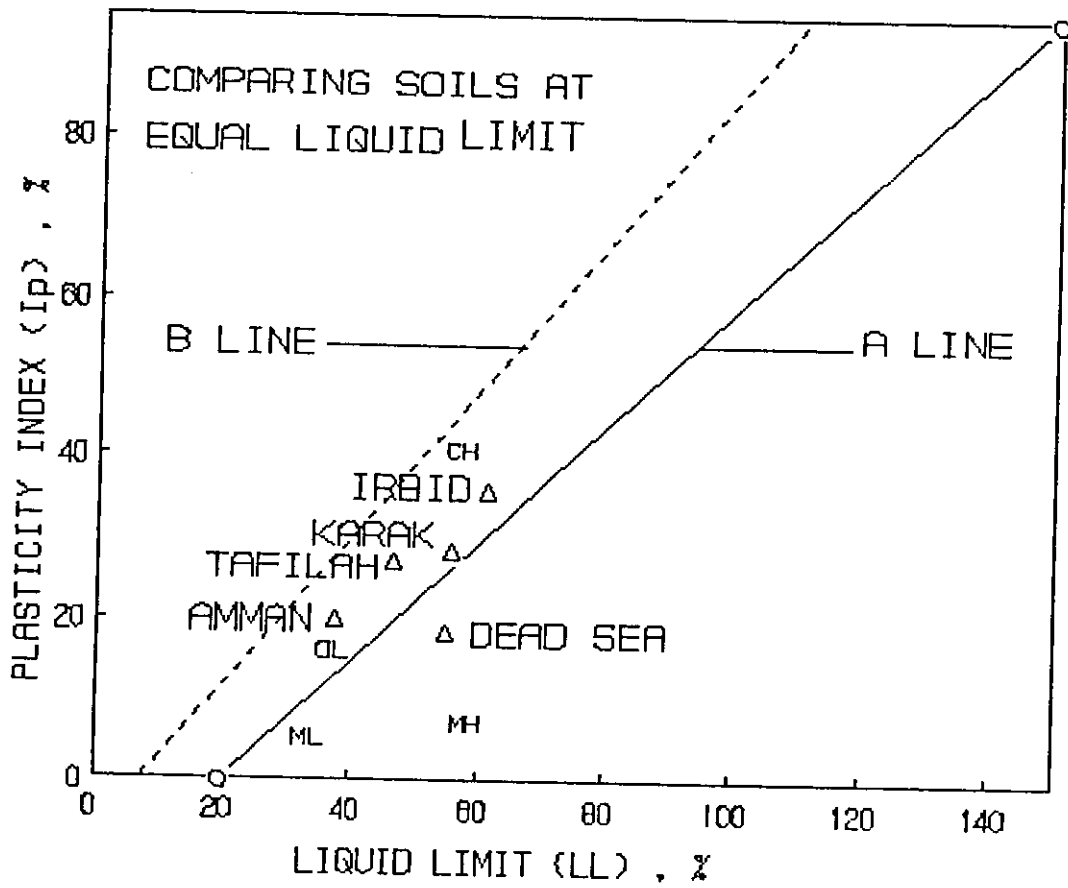


Fig. 5.6: Plasticity chart for clay classification in Jordan

oven. The difference between the weights represents the weight of the water content in the clay. The water content percent (w %) was found using the following formula [64]:

$$w \% = \text{Weight of Water} / \text{Weight of Dry Soil} \quad (5.1)$$

The optimum moisture content of the various location clays were obtained by plotting the different water content of one clay versus the dry density of the clay at this point. The dry density of the clay is determined from the following equation [64]:

$$\text{Dry Density} = \text{Wet Density} / (1 + \text{Water Content}) \quad (5.2)$$

Where the wet density is the mass of the clay before drying per unit volume.

The optimum water moisture content of Amman, Irbid, Dead Sea, Karak and Tafilah clays are shown in figures 5.7, 5.8, 5.9, 5.10 and 5.11, respectively.

5.2.5 Permeability

The permeability of the different clays has been scanned by using special molds connected to a water pipe, and by observing the level of the water over a period of time ranging from 3 days to 14 days for each sample. The permeability of the clays can be reduced by compacting the clay that contains the moisture necessary for maximum impermeability, i.e. the optimum moisture content that has been determined for each

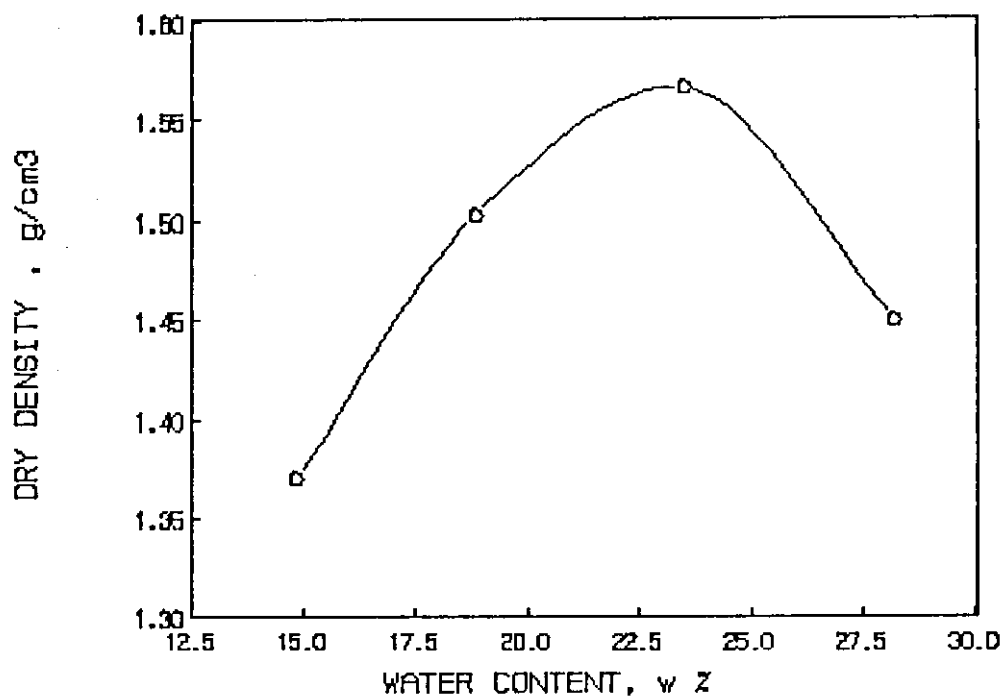


Fig. 5.7: Optimum moisture for Amman clay

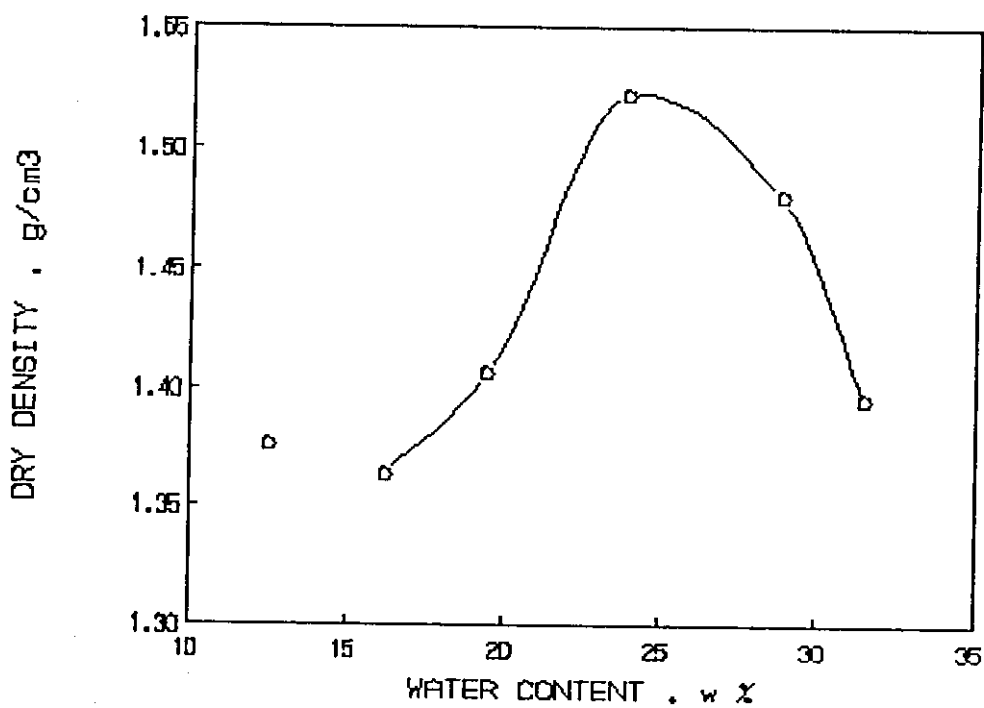


Fig. 5.8: Optimum moisture for Irbid clay

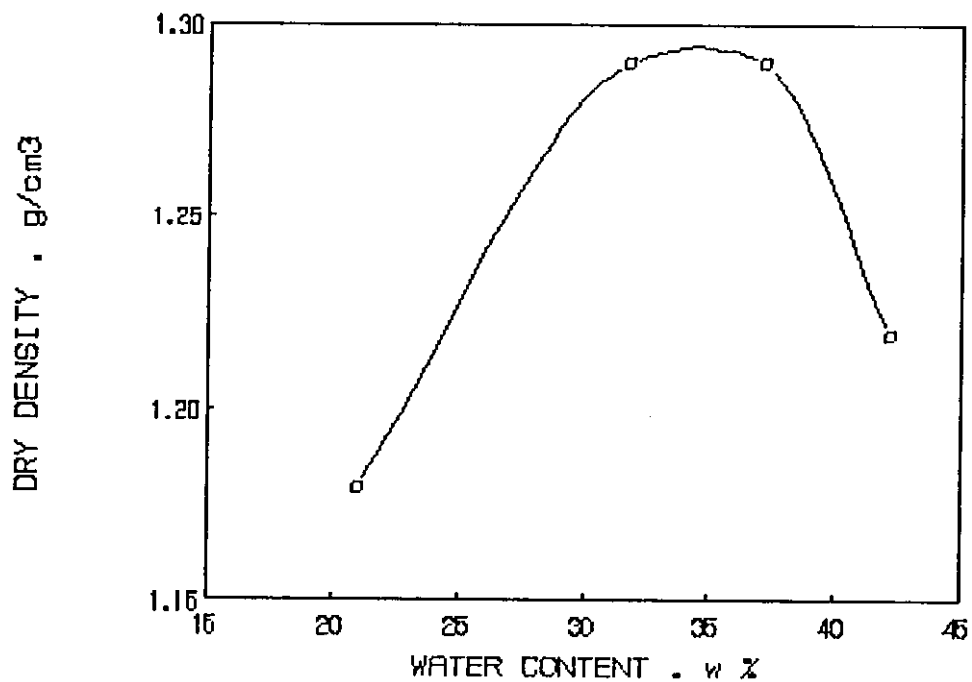


Fig. 5.9: Optimum moisture for Dead Sea clay

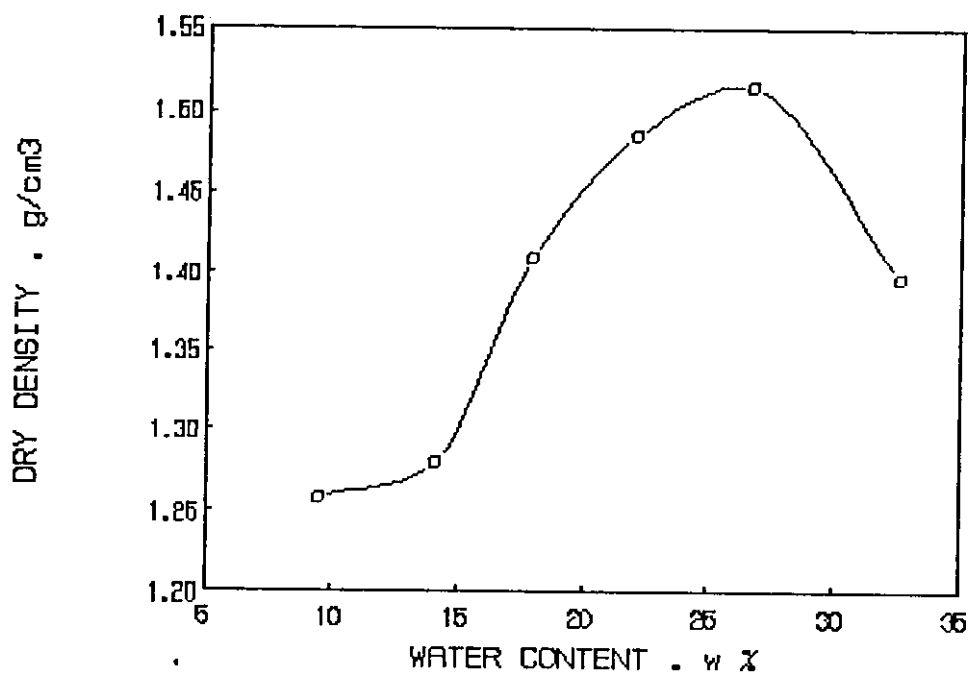


Fig. 5.10: Optimum moisture for Karak clay

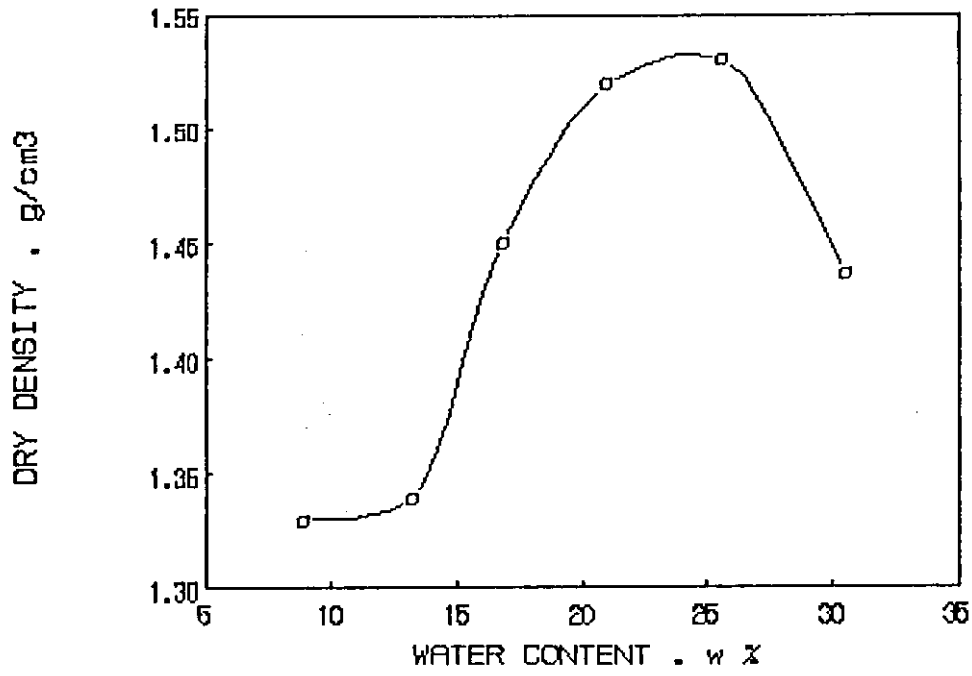


Fig. 5.11: Optimum moisture for Tafilah clay

sample in the previous step. The vertical permeability of each sample was calculated by:

$$Q = K_p \times i \times A \quad (3.9)$$

All previous tests were repeated few times, and the results obtained were found to be within 5%. A summary of the results are shown in Table 5.2.

Table 5.2 Summary of Clays Scanning Results

Location	LL	PL	I _p	Opt.w%	Permeability (cm / sec)
Amman	38.94	18.97	19.97	22.50	4.76 x 10 ⁻⁸
Irbid	61.63	25.96	35.67	24.75	1.7 x 10 ⁻⁷
Dead Sea	55.18	37.00	18.18	34.50	1.58 x 10 ⁻⁶
Karak	56.06	27.75	28.31	26.75	4.45 x 10 ⁻⁸
Tafilah	49.05	23.92	25.13	24.00	2.6 x 10 ⁻⁸

It can be shown from the previous figures that the Dead Sea clay has the lowest potential as a lining material, because it tends to have very high permeability value as well as it is an organic clay, which could introduce some problems such as insects and bushes. The results show that Irbid clay has a high permeability value, which makes it unfavourable candidate for use with the lining schemes.

On the other hand, Amman, Karak and Tafilah clays are inorganic clays and tend to have the lowest values of permeability, which makes them candidate for clay lining schemes investigations (part 2).

Karak clay is classified as high plastic clay which tends to be fractured more than the low and the medium clays such as Amman and Tafilah clays. Therefore, In the next lining schemes investigations, Amman clay will be studied as an inorganic medium plasticity low permeability local clay.

5.3 Results of Liner Test Rig

The liner test rig shown in figure 4.1 is designed to determine the permeability of different schemes in order to get the optimum scheme that can be used as a local lining system in solar ponds in Jordan.

The schemes tested in this stage consists primarily from various thicknesses of the following layers;

Gravel layer with a thickness of 10 cm.

Sand layer with a thickness of 20 cm.

Clay with a thickness of 20 cm.

Sand with a thickness of 20 cm.

All the above materials are local materials, where the sand used was Swieleh sand and the clay used is a compacted Amman clay with its optimum moisture content ($w = 22.5\%$). The water used in this experiment is the Dead Sea water.

This scheme was examined few times and was repeated with two modifications. The first modification was done by inserting a Low Density Polyethylene (LDPE) film inside the local clay to ensure impermeability. The second modification was done by inserting a punctured LDPE inside the clay layers.

5.3.1 Results of the Scheme without LDPE Film

This test was carried out by pouring the gravel layer, then the

sand layer in the rig. Then, the clay was prepared by adding water to it in order to have the optimum moisture content, then the prepared clay was poured in the rig and compacted using a plastic sheet and a compaction hammer. The second sand layer was poured on the compacted clay. Finally, the Dead Sea Water was added to a level of 40 cm.

The seepage rate was recorded for one month. The average daily seepage rate about 311 ml in the 24 hours. Therefore, the permeability can be calculated using Darcy's law [61] (equation 3.9):

$$Q = K_p \times i \times A \quad (3.9)$$

$$\begin{aligned} \text{Where, } Q &= 3.5995 \times 10^{-9} \text{ m/s} \\ A &= 0.50265 \text{ m}^2 \\ i &= 3 \end{aligned}$$

Therefore the vertical permeability of this scheme (K_p) is found to be $= 2.387 \times 10^{-7}$ cm/sec.

5.3.2 Results of the Scheme with LDPE film

The scheme described above was modified and retested. Where a Low Density Polyethylene (LDPE) of a thickness of 0.05 mm was sandwiched between the two compacted Amman clay layers, each of 10 cm thickness.

The scheme has been left for three weeks, and it was noticed that there is no seepage at all. The level of water has also been observed from the plexi-glass fixed on the rig, and it can be concluded that no

serious drop of the water level has been recognized. Therefore, it can be said that this scheme is impermeable and can be used as a good local inexpensive lining material.

The scheme described above could be deteriorated i.e. the LDPE film may be punctured due to bushes grow in the site, or to high rates of heat and pressure that the film would face. Therefore, it is necessarily to test the same scheme with a punctured LDPE film.

5.3.3 Results of the Scheme with a punctured LDPE film

This scheme has been prepared by making two cracks each of 30 cm length and 0.5 mm width in the LDPE film using a knife. The total area of the crack would thus be about 3 cm^2 which is equivalent to having a hole of 2 cm diameter. The area of the hole is only 0.06% of the bottom area, but it could be significant for solar pond application.

After cutting the LDPE film, it has been sandwiched between two compacted Amman clay layers, each of a thickness of 10 cm, and the previous scheme is reconstructed and retested again.

The scheme was observed for one month, and the seepage rate was very little. It was very difficult to determine the permeability of the scheme from the seepage flow due to the evaporation of the water commulated from the seepage. It was found that measuring the drop of the water level in the rig is more accurate than measuring the seepage rate itself..

The water level in the rig was maintained at 34 cm, and it was found that the average drop of water level in the rig for this scheme was about 0.75 mm daily. The average permeability can be calculated using equation (3.9) and found to be 3.2152×10^{-10} cm/s.

This scheme is retested again by using thicker compacted Amman clay of a thickness of 30 cm, where the LDPE was sandwiched above 20 cm thick clay, and another 10 cm thick clay. The drop of the water level was reduced to 0.55 mm per day on the average. The permeability of this scheme was determined to be 2.7×10^{-12} m/s. Therefore, it can be said that the thickness of the clay used does not have any effect on the permeability of the scheme, but it effects on the seepage rate.

The result of the different schemes experiments in the liner test rig can be summerized in Table 5.3

Table 5.3 Summary of Permeability Results of Different Schemes

Scheme	Average Permeability (cm / sec)
- Scheme contains Amman Clay without LDPE film	2.387×10^{-7}
- Scheme contains Amman Clay with LDPE film	impermeable
- Scheme contains Amman Clay with punctured LDPE film	3.215×10^{-10}

It can be concluded from Table 3 that using a thin layer of low density polyethylene would effectively reduce the permeability of the schemes which contain a low permeable clay and this suggests that such a scheme would be an optimum one for use for salt gradient solar ponds in Jordan

5.4 Results of Prototype Solar Ponds

5.4.1 Introduction

The two small solar ponds were filled on 26/9/1993, and left for ten days to show stability. After that, three different sizes of plastic rings were introduced to one pond (each size was introduced for one week), while the other pond was left as it is, in order to study the effect of introducing those rings on the performance of the solar ponds.

The results of the above experiments will be shown and discussed in the following sections.

5.4.2 Results of SGSPs Behaviour After Filling

After three days from the construction of the solar ponds, we started measuring the temperature and salinity profiles of the two ponds namely; pond A and pond B. Figures 5.12-5.17 show the temperature profiles of the ponds on September 29 and October 4. Figure 5.18 shows the salinity profile on October 2.

From the temperature profiles of the ponds on September 29, the regions of the three zones are clear, where the UCZ thickness is around 5 cm, the the depth of the LCZ is almost 50 cm, where the the NCZ region is limited to 35 cm thick and is consisted of a uniform high temperature gradient of 43,C/m in the morning and 35,C/m in the evening. On October 4, the upper convective zone extended to about 7

cm, while the LCZ was reduced to 30 cm. The NCZ was the greatest zone of the solar ponds and showed uniform gradient again of $60\text{ }^{\circ}\text{C/m}$ on the top of the NCZ and $30\text{ }^{\circ}\text{C/m}$ gradient at the bottom of the $23\text{ }^{\circ}\text{C/m}$.

Although some scattering of the temperatures in the beginning of the LCZ are shown on October 4, it can be said that the general temperature profiles of both ponds in this period of time are smoothly distributed and indicate good stability of the two ponds after less than 3 days of their construction.

The salinity profile on October 2 of the two ponds (figure 5.18) also shows the three different zones but with some instabilities in the beginning of the storage zone.

By comparing the temperature and salinity profiles of the two ponds, it can be said that they show very similar thermal and concentration behaviours.

The maximum storage zone temperatures and the meteorological data on September 29 and October 4 are shown in figures 5.19-5.22. It can be said that these days were normal sunny days in the Autumn, where the global radiation was high and reached 309 J/cm^2 and 288 J/cm^2 at noon on September 9 and October 4 respectively. The maximum ambient temperatures for these two days were $28.7\text{ }^{\circ}\text{C}$ and $27.5\text{ }^{\circ}\text{C}$, and the wind was in relatively low speed in these days.

The storage zone temperature increased about $5\text{--}8\text{ }^{\circ}\text{C}$ from the morning to the evening, and it reached $38\text{ }^{\circ}\text{C}$. It is obvious that the ponds show very good behaviour after less than 10 days of their filling.

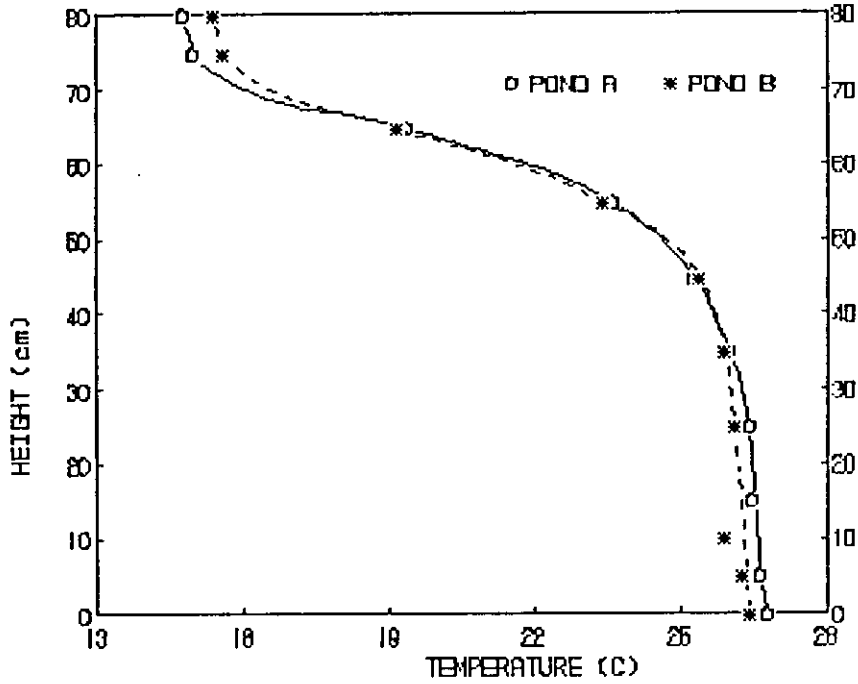


Fig. 5.12: Temperature profiles on 29/9/1993 at time 9:30, $T_a = 20.8$ C.

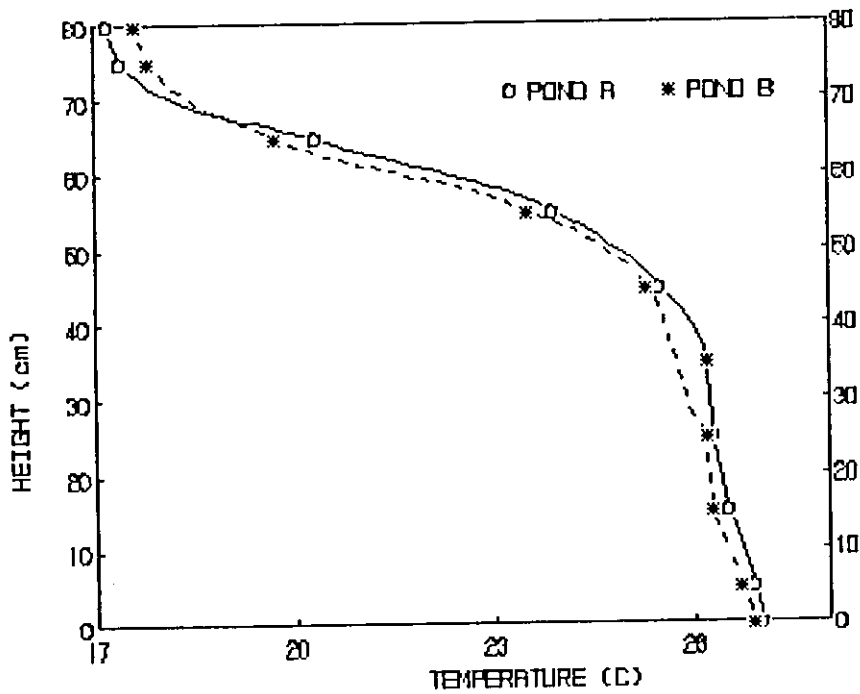


Fig. 5.13: Temperature profiles on 29/9/1993 at time 11:30, $T_a = 25.5$ C.

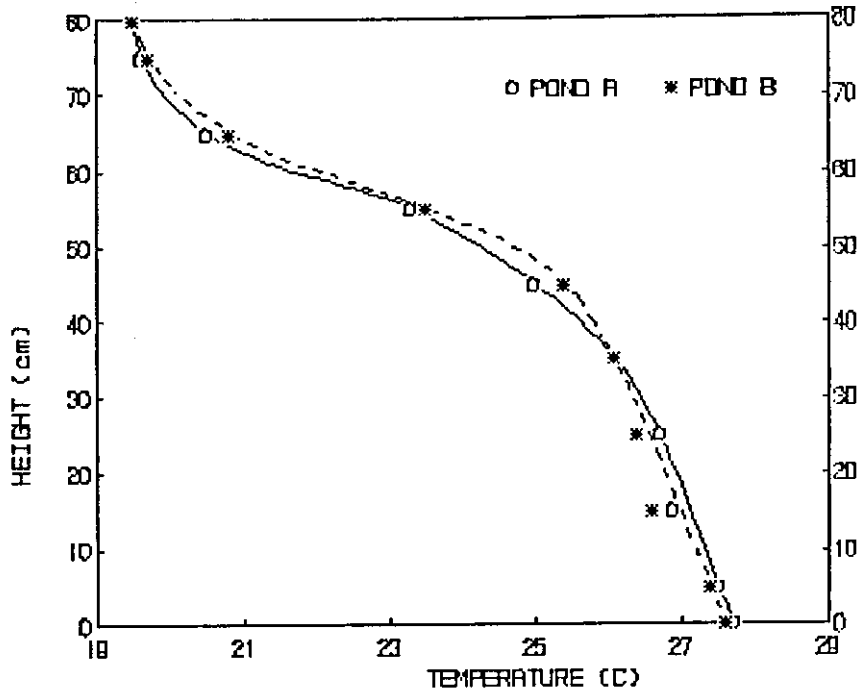


Fig. 5.14: Temperature profiles on 29/9/1993 at time 13:00, $T_a = 25.6$ C.

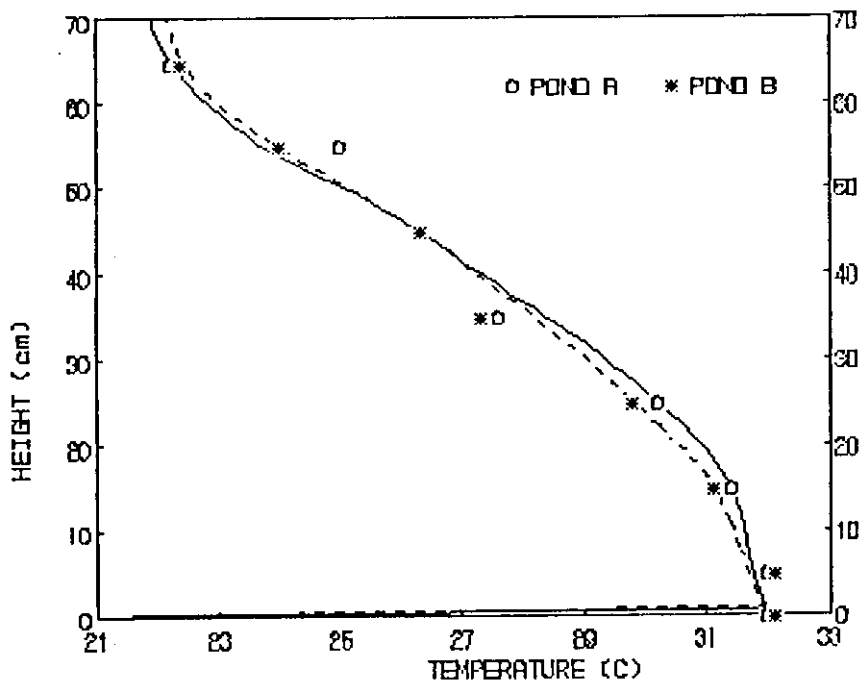


Fig. 5.15: Temperature profiles on 29/9/1993 at time 15:00, $T_a = 30.3$ C.

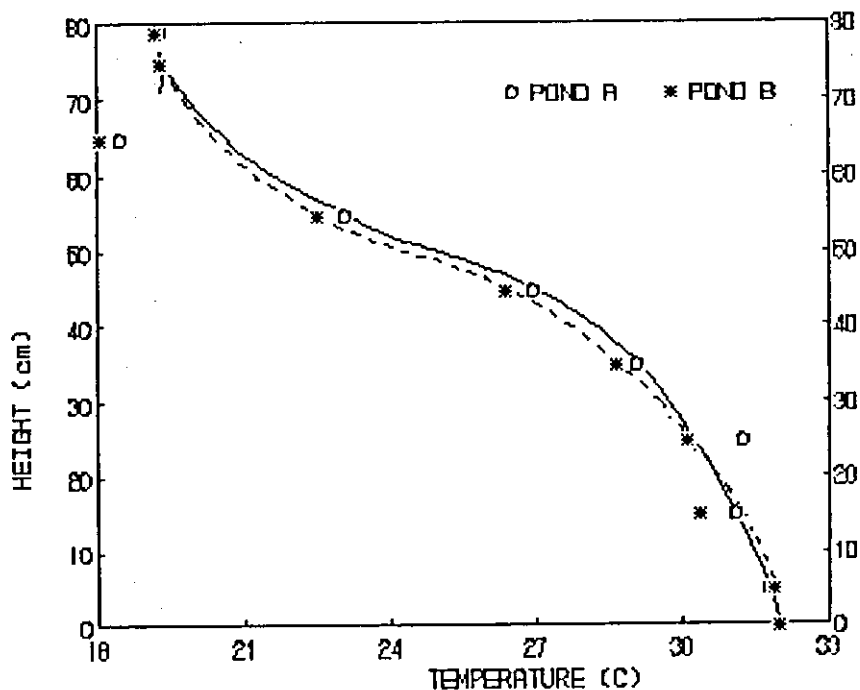


Fig. 5.16: Temperature profiles on 4/10/1993 at time 11:00, $T_a = 24.2$ C.

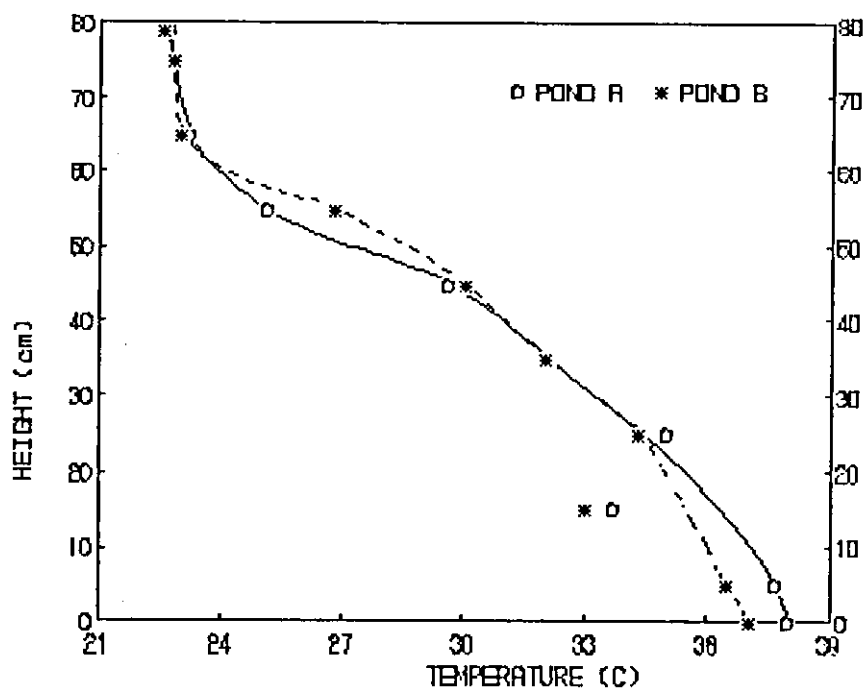


Fig. 5.17: Temperature profiles on 4/10/1993 at time 15:00, $T_a = 25.6$ C.

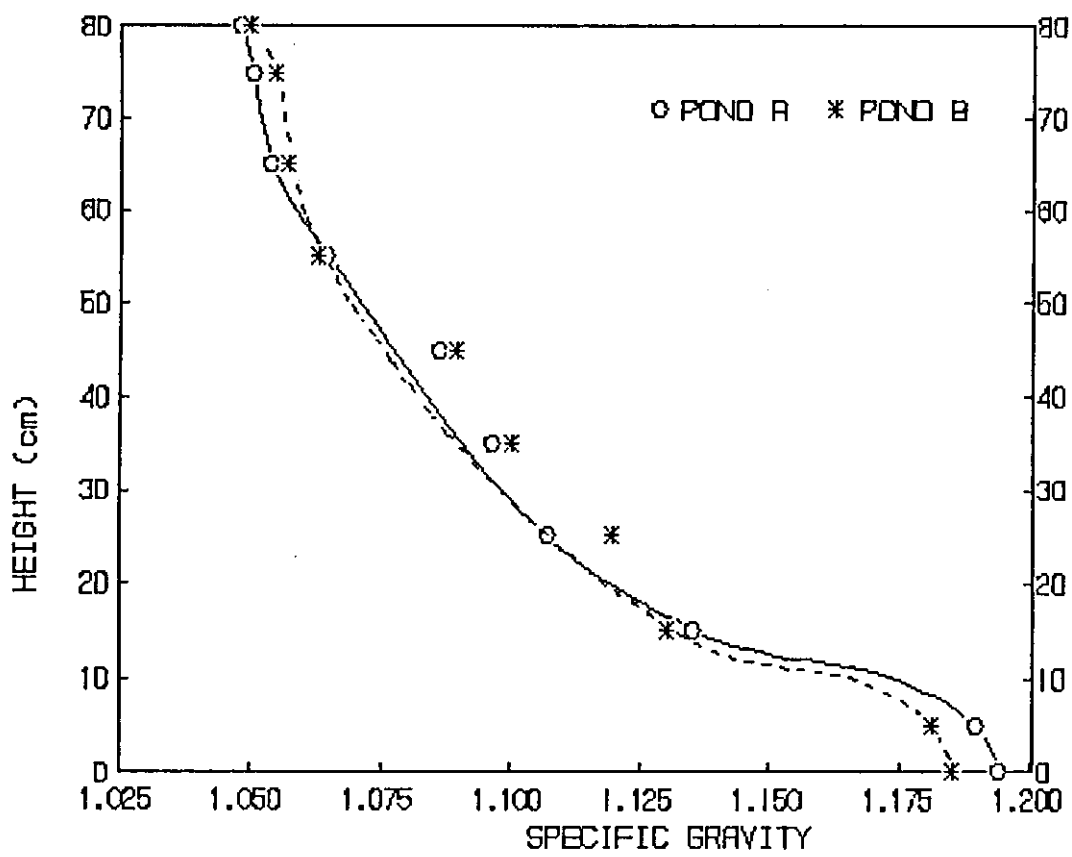


Fig. 5.18: Salinity Profiles on 2/10/1993

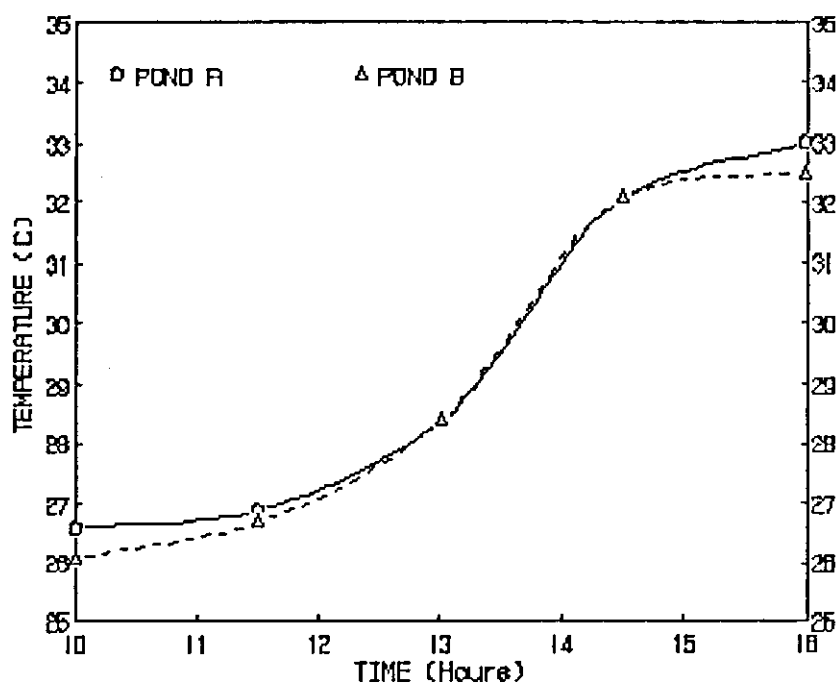


Fig.5.19: Storage zone temperature history on 29/8/1993.

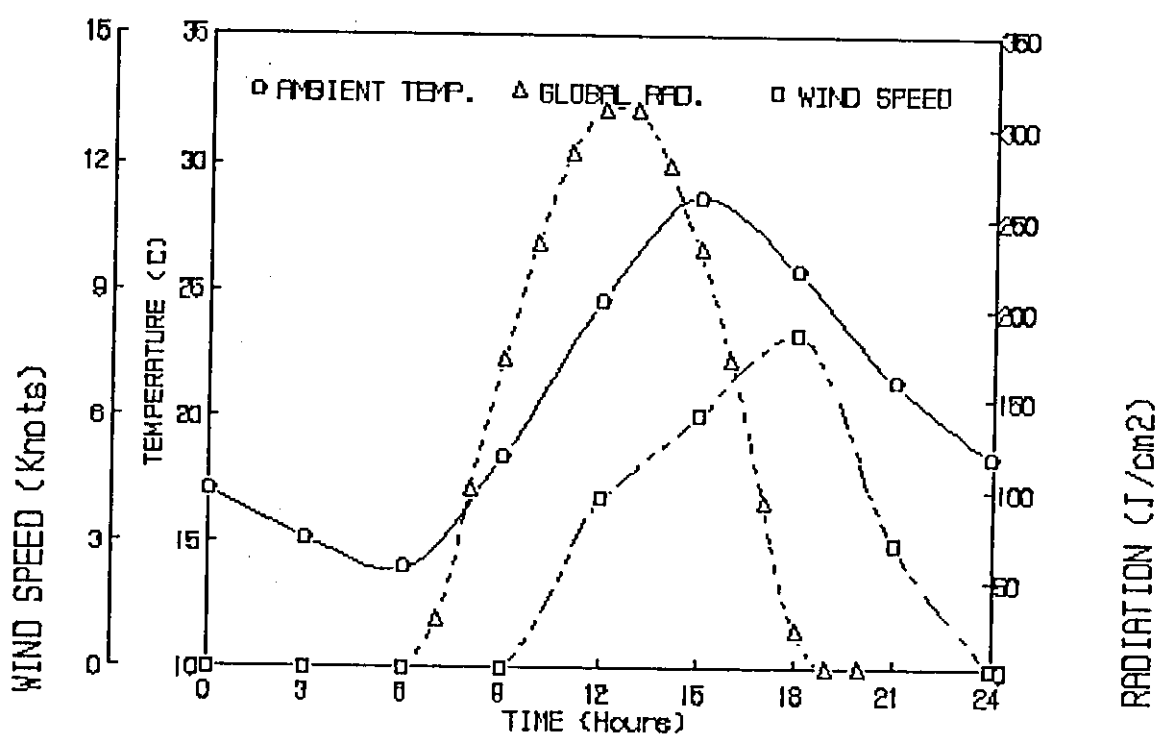


Fig.5.20: Meteorological Data for Amman on 29/8/1993

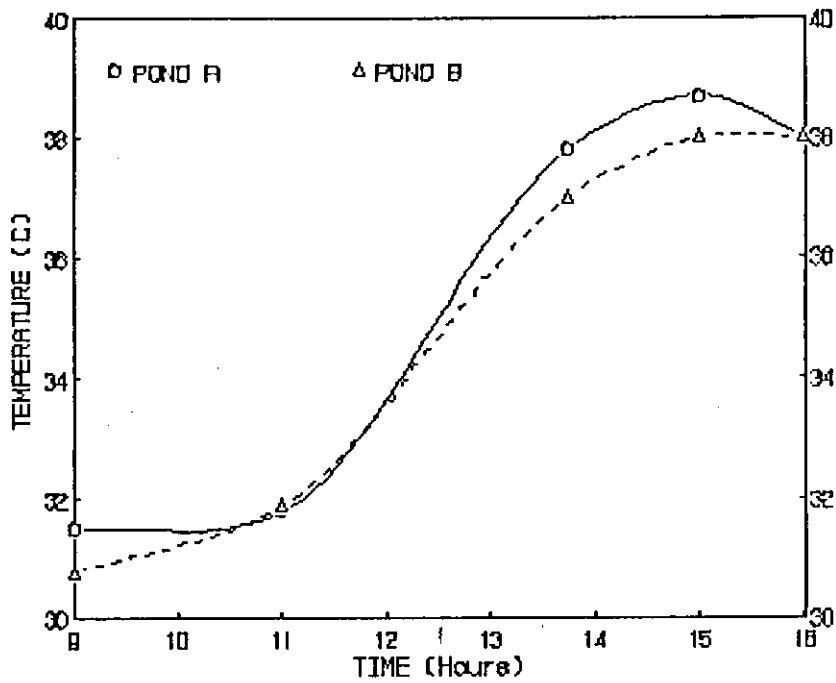


Fig.5.21: Storage zone temperature history on 4/10/1993.

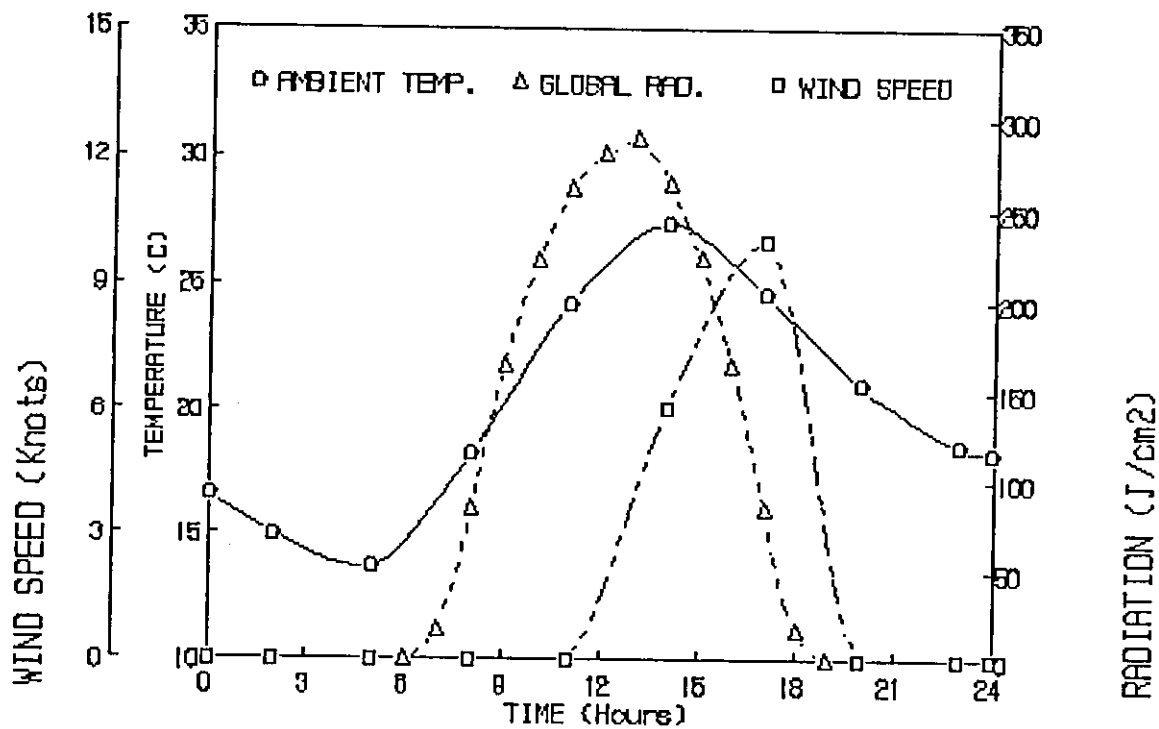


Fig.5.22: Meteorological data for Amman on 4/10/1993.

5.4.3 Results of SGSPs Behaviour After Introducing Rings

Plastic rings that were introduced to the solar ponds to test their potential as wind suppressors and to highlight their effect on the stability of the solar ponds. Therefore, three sizes of plastic rings with diameters of 30 cm, 40 cm and 50 cm were introduced to pond A in three consecutive weeks, and in fourth week, rings with diameter of 30 cm were put on pond A, where rings with diameter of 50 cm were introduced to pond B in order to find out the effect of the rings size on the stability of solar ponds.

1. Introducing of 30 cm Rings to Pond A

Rings with diameter of 30 cm were introduced to pond A from October 6-13. Temperature profiles on October 9 and 13 are presented in figures 5.23-5.26. Salinity profile on October 9 is shown in figure 5.27.

From the figures of temperature profiles, it can be shown that the gradient of NCZ of pond A is almost a straight line of 34-40°C/m at the top of NCZ and about 25-30 at the bottom of it. The gradient zone of pond A is much better than pond B, indicating that pond A has a higher degree of stability than pond B, which is very clear from the temperatures scattering shown in figures 5.23-5.27, specially in the NCZ region. This scattering indicated that the gradient of the NCZ in pond B was not smoothly distributed, where it is high in one point and low in the next point and suffered from mixing of layers due to wind driven currents. This supports Akberzadeh et al. [53] and Atkinson[57] findings regarding the effect of rings on the stability of solar ponds.

It can be also concluded from the figures that the UCZ was continued to enlarge and reached about 20 cm thick at the evening of October 13 for both ponds. The effect of the plastic rings in reducing this layer is not clear in this period of time. On the other hand the gradient zone still occupied the greater region of the ponds (about 45% of the pond size).

The scattering of the measured points in NCZ of pond B is also observed in the salinity profile (figure 5.27). This scattering of salinity profile is located in the lower part of the NCZ exactly as that shown for the temperature profile. However, the salinity and temperature profiles are very similar to each other in this period, which is an indication of the ponds stability. Also, it can be concluded that the rings improve the stability of the ponds.

Another important improvement that resulted from the introduction of rings is the increase in the temperature of the storage zone. Figures 5.28 - 5.31, which present the maximum storage zone temperature and the meteorological data on October 9 and 13 indicate that the storage zone temperature of pond A is higher than pond B throughout the day under the same climatic conditions, and the difference was maintained to be approximately 5°C in this week. Also, the storage temperature of pond A reached a maximum temperature recorded throughout the experiments which is 41°C. This rise of the storage zone temperature was supported by relatively hot weather in this week, where the ambient temperatures for the two days at noon were around 29°C and the wind was calm except in the afternoon, where it becomes about 10-15 km/h. Also, The global radiation were 268 J/cm² and 256 J/cm² at noon for October 9 and 13, respectively.

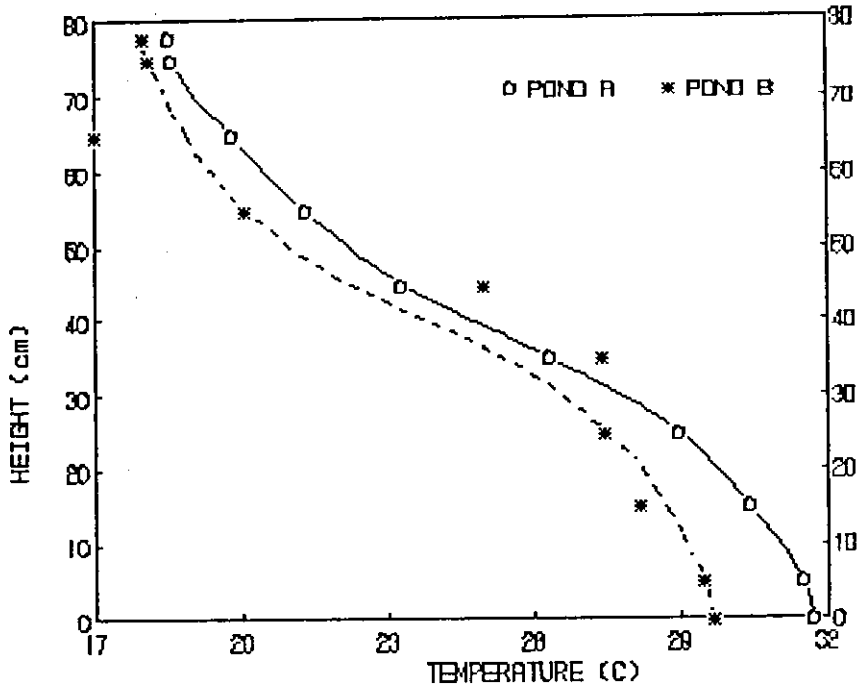


Fig. 5.23: Temperature profiles on 9/10/1993 at time 10:30, when 30 cm rings are introduced into pond A, $T_a = 25.3$ C

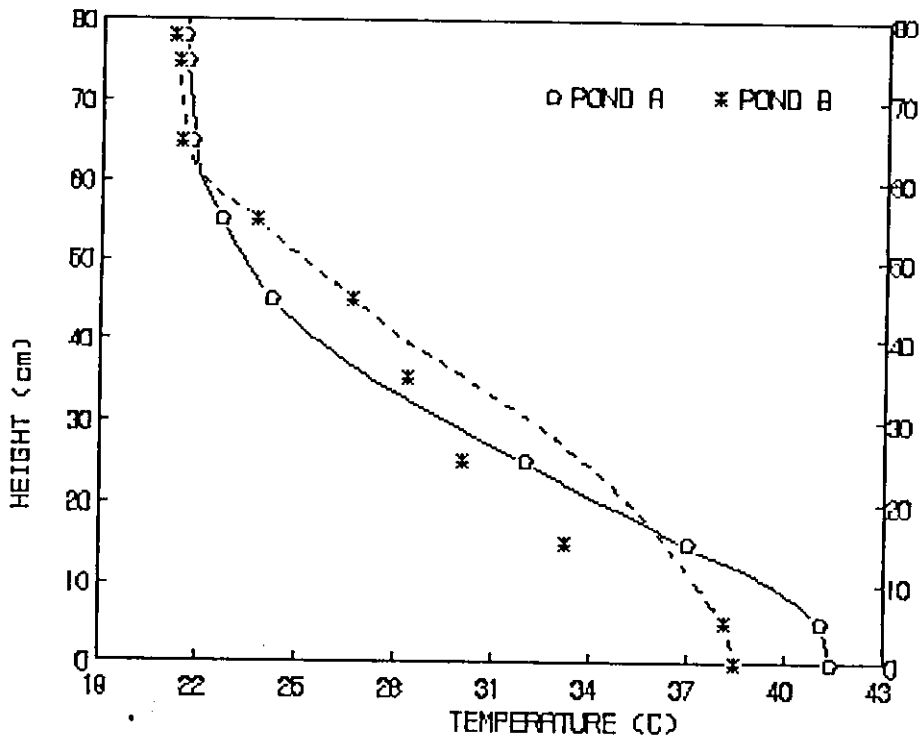


Fig. 5.24: Temperature profiles on 9/10/1993 at time 15:30, when 30 cm rings are introduced into pond A, $T_a = 25.7$ C.

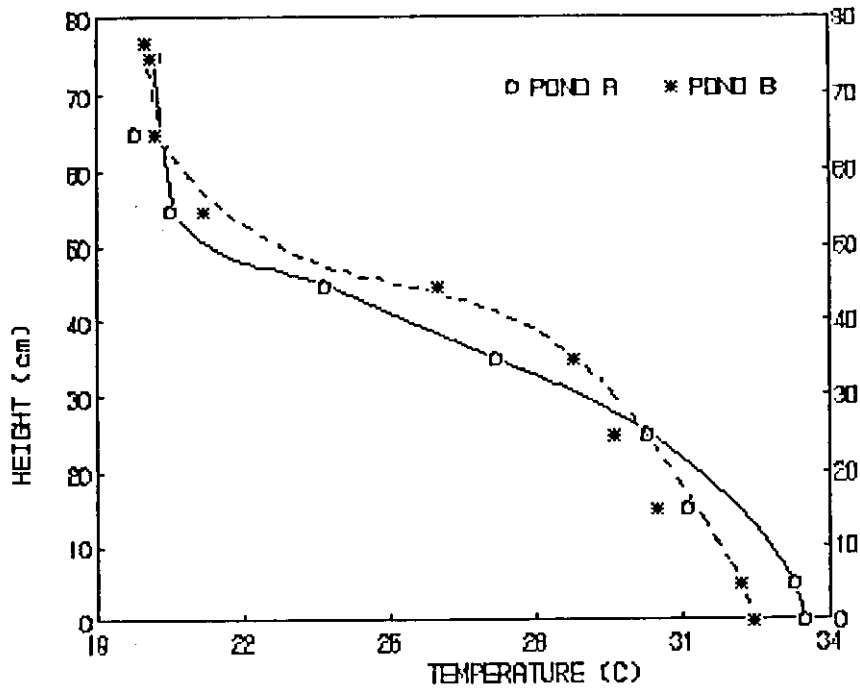


Fig.5.25: Temperature profiles on 13/10/1993 at time 11:00, when 30 cm rings are introduced into pond A. $T_a = 23.4$ C.

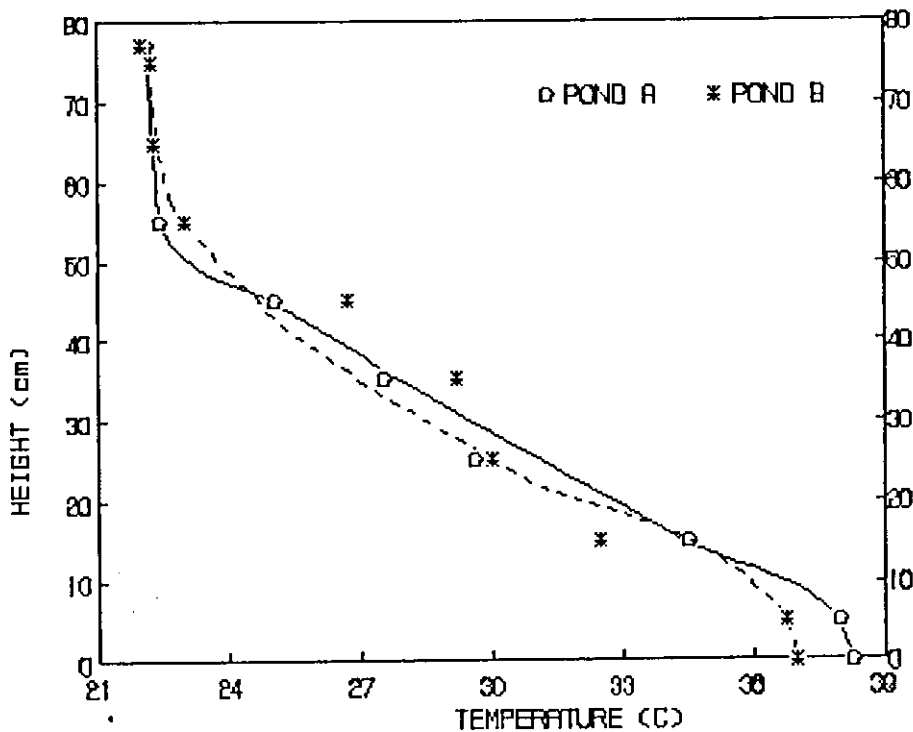


Fig.5.28: Temperature profiles on 13/10/1993 at time 15:30, when 30 cm rings are introduced into pond A. $T_a = 27.5$ C.

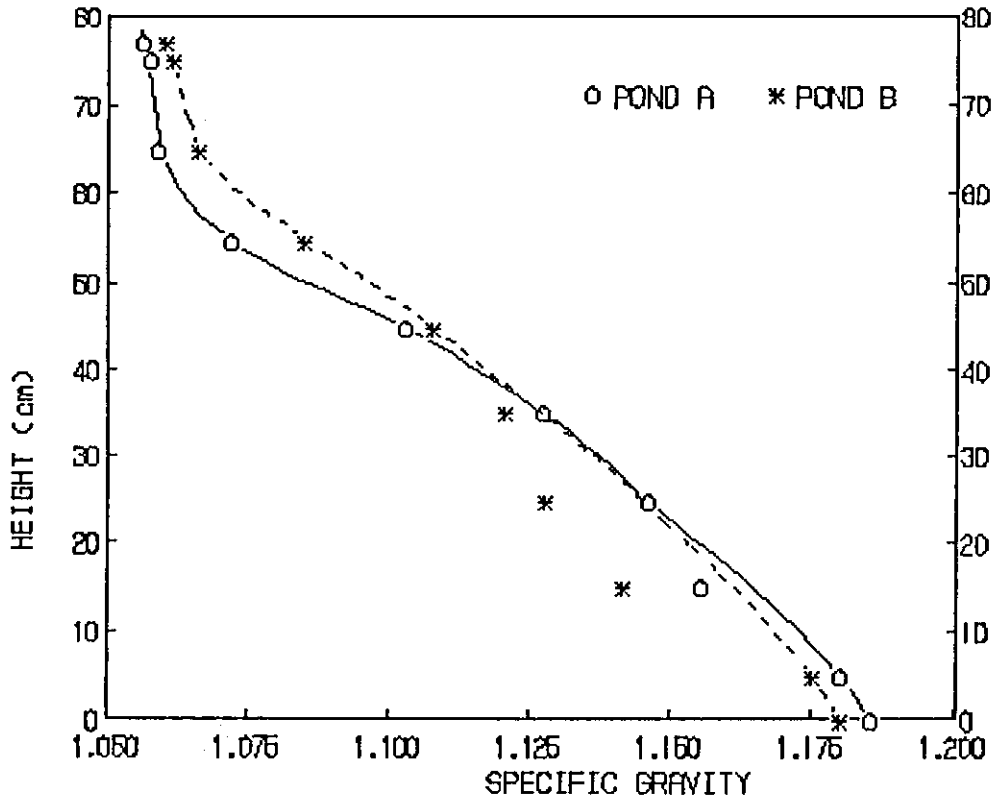


Fig.5.27: Salinity profiles on 9/10/1993, when 30 cm rings are introduced into pond A.

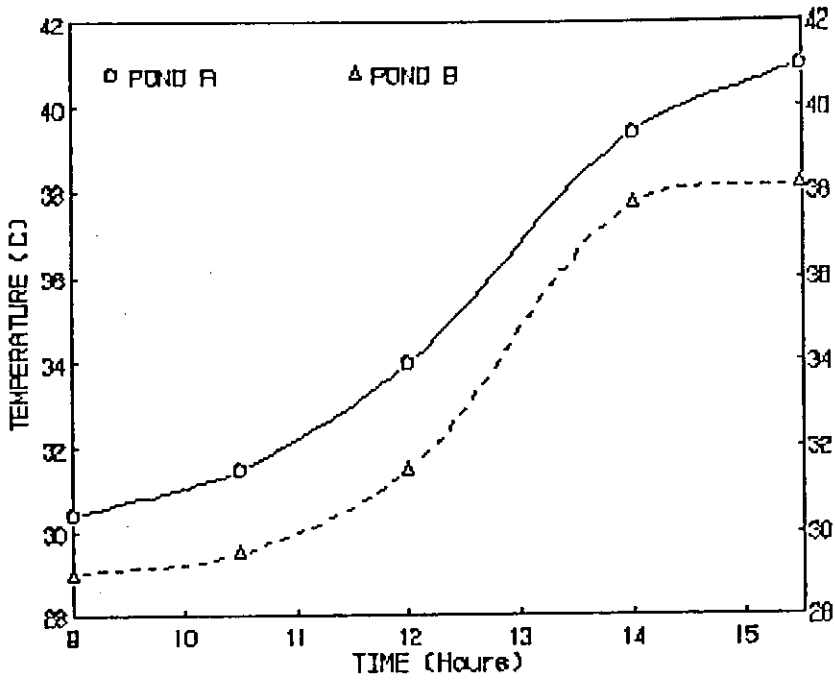


Fig.5.28: Storage zone temperature history on 9/10/1993. when 30 cm rings on pond A.

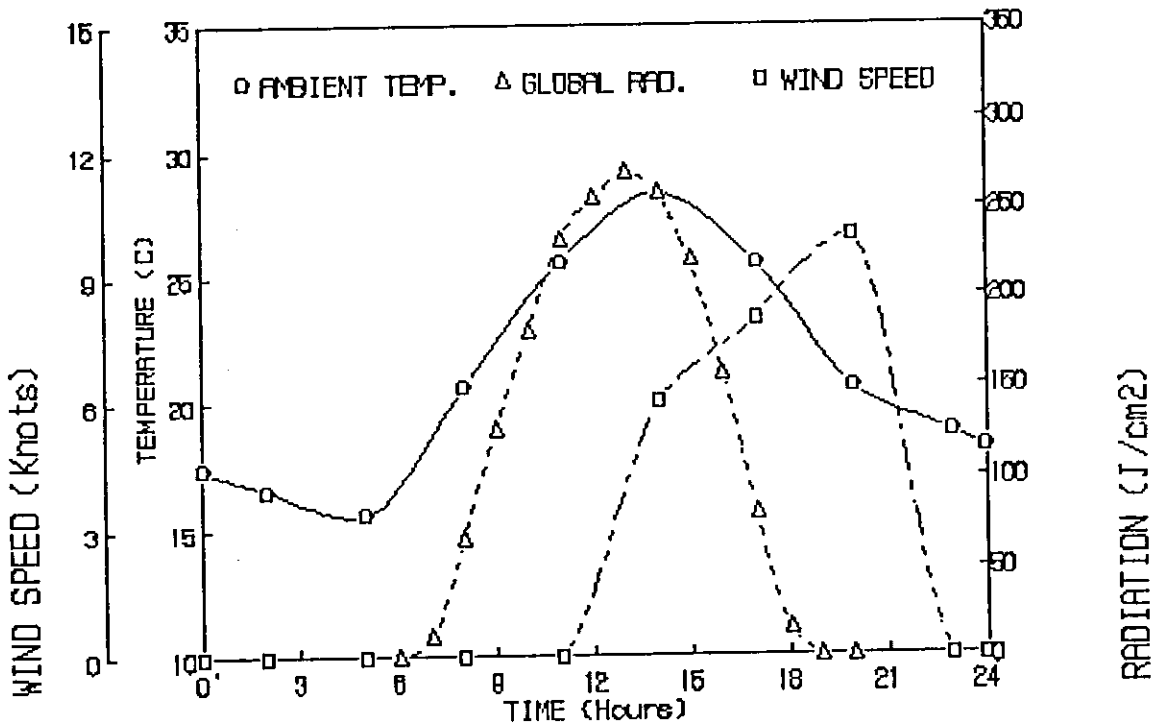


Fig.5.29: Meteorological data for Amman on 9/10/1993.

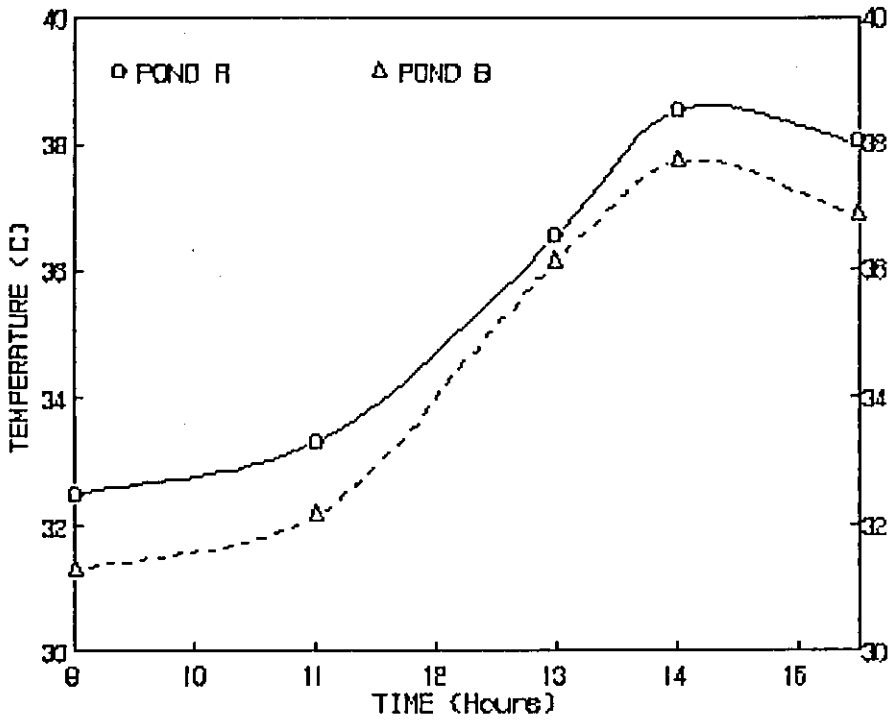


Fig.5.30: Storage zone temperature history on 13/10/1993, when 30 cm rings on pond A.

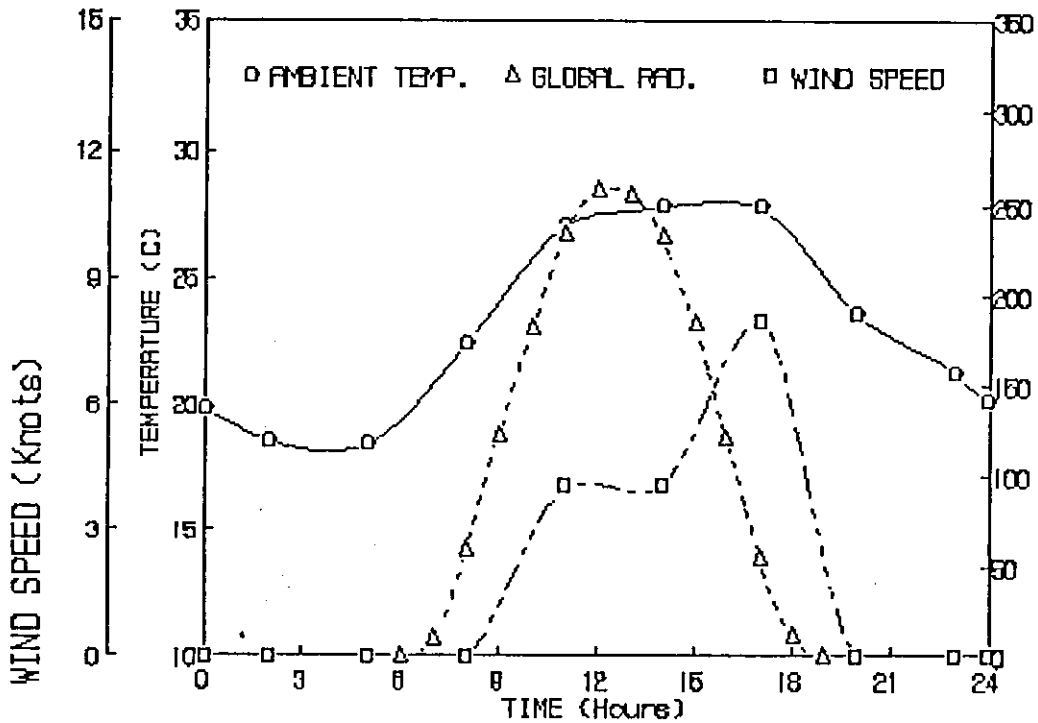


Fig.31: Meteorological data for Amman on 13/10/1993.

2. Introducing of 40 cm Rings to Pond A

The rings of 30 cm diameter were removed from pond A at hour 16:00 on October 13, when rings of 40 cm diameter were introduced to it. Figures 5.32-5.35 present the temperature profiles of the two ponds on October 16 and 20. Salinity profile on October 16 is illustrated in figure 5.36 where the maximum storage zone temperature and the meteorological data on October 16 and 20 are shown in figures 5.37 - 5.40.

The temperature profiles indicate that pond A still has better gradient in NCZ region than pond B which is still suffering from instabilities and temperatures scattering in this zone. The scattering of temperatures of pond B extended from the bottom part of NCZ in the previous week to almost the whole zone in this week as shown in figures 5.32 and 5.33.

The gradient of pond A shows a straight line when 30 cm rings were introduced, with a gradient of 40-55°C/m. Pond B tends to have similar gradient but with more scattering of the measured points. Also, It can be noted that the instability of the NCZ of pond B has been affected seriously.

The upper convective zone was increased in this week from 20 cm height in the beginning of this week to about 30 cm height in the end of this week, which is 37.5% of the size of the pond. This phenomenon affects the performance of the ponds and it lowers the temperature of the storage zone to about 3°C. This enlargement of UCZ was due to high

wind speed in this week, where it reached a maximum of 27km/h, and due to the evaporation, where, ponds lost about 5 cm height (6.25% of their sizes).

The UCZ region is also clear in the salinity profile (Figure 5.36). In this figure, it can be shown that the effect of wind on mixing of the layers of solar ponds, resulted in an increase in the specific gravity of upper surface, where it became about 1.07, which is relatively high. Also, it is clear that the salinity gradient of pond A is almost a straight line and is much better than it is in Pond B. Therefore, it is clear that the rings reduce the influence of the wind on the gradient zone.

By considering the figures of the storage zone temperatures. Once again, pond A experiences higher storage temperature throughout the week with a difference of about 3°C. Also, it can be observed from the meteorological data in this week that high wind rates existed throughout the days; October 16 and 20, which affected the stability of pond B and enlarge the UCZ in both ponds.

It is important to mention that the water lost due to evaporation made a lot of problems such as increasing the salinity of the UCZ, lowering the depth of ponds and contributing in maximizing the UCZ. Therefore, it became essential to substitute the water lost and to make a surface washing for both ponds, which is done at hour 15:00 on October 20.

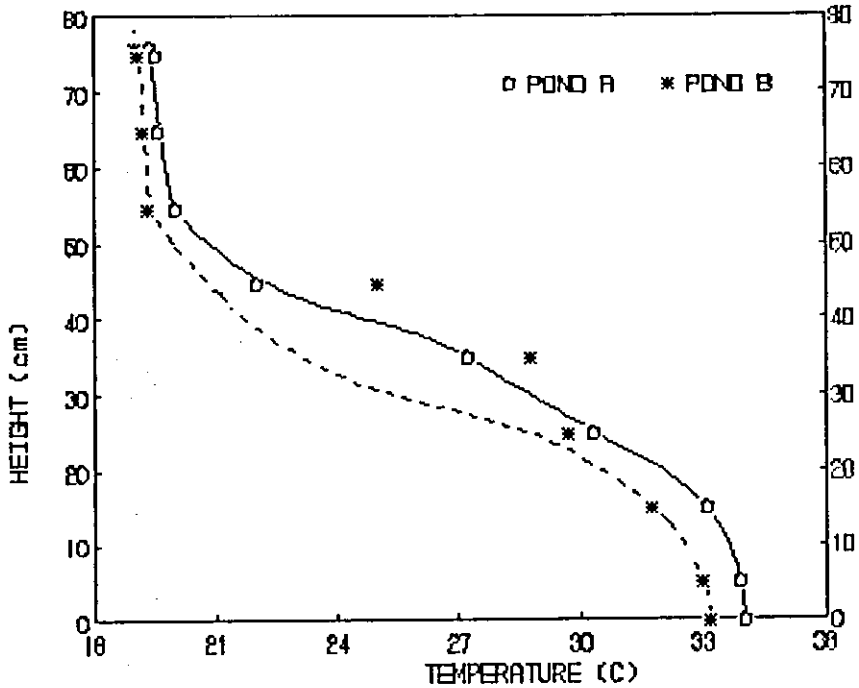


Fig.5.32: Temperature profiles on 16/10/1993 at time 11:00, when 40 cm rings are introduced into pond A. $T_a = 26.8$ C.

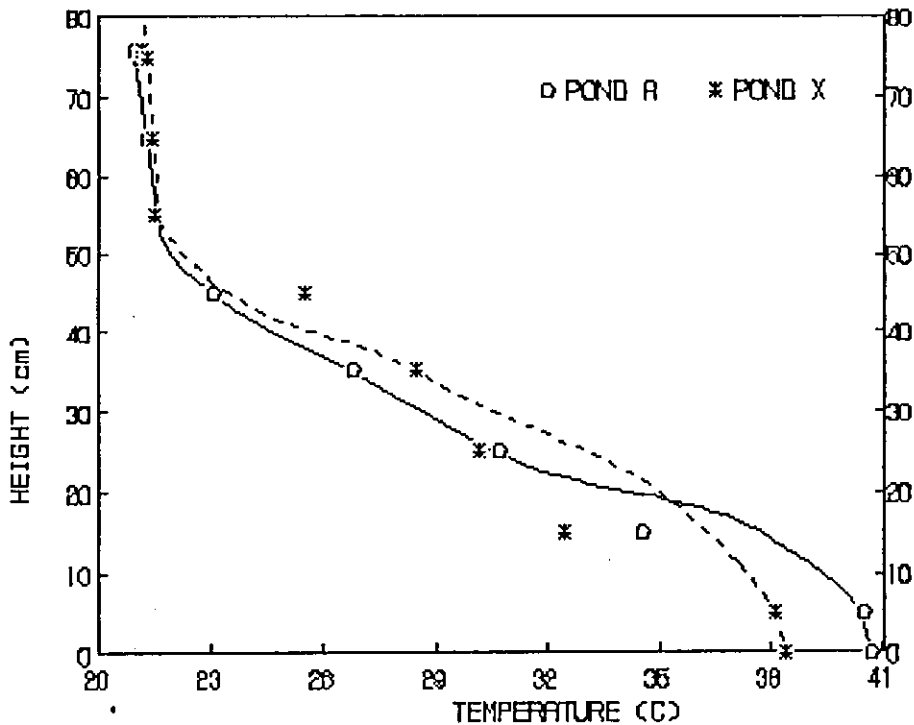


Fig.5.33: Temperature profiles on 16/10/1993 at time 15:00, when 40 cm rings are introduced into pond A. $T_a = 27.1$ C.

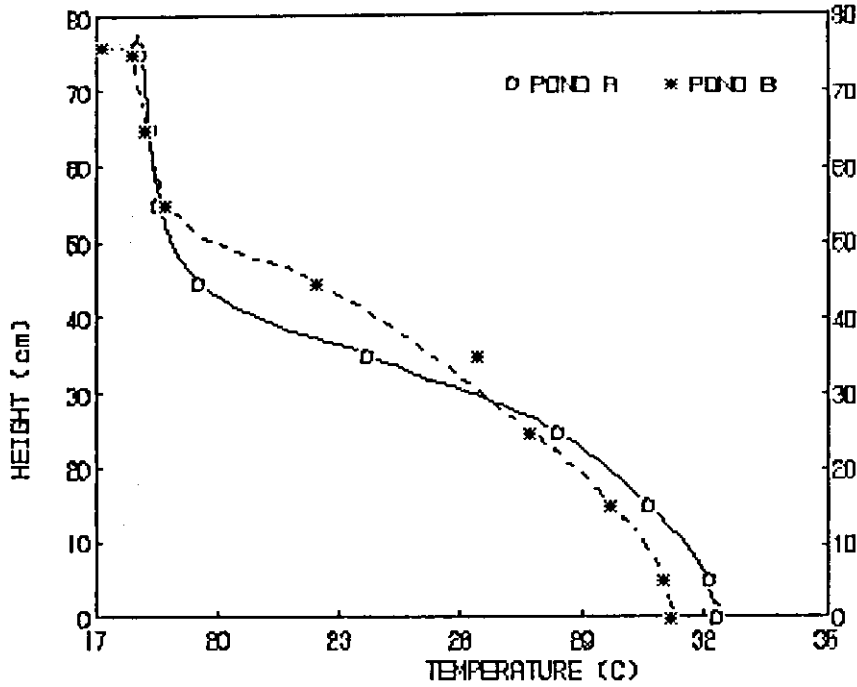


Fig.5.34: Temperature profiles on 20/10/1993 at time 11:00, when 40 cm rings are introduced into pond A, $T_a = 27.3$ C.

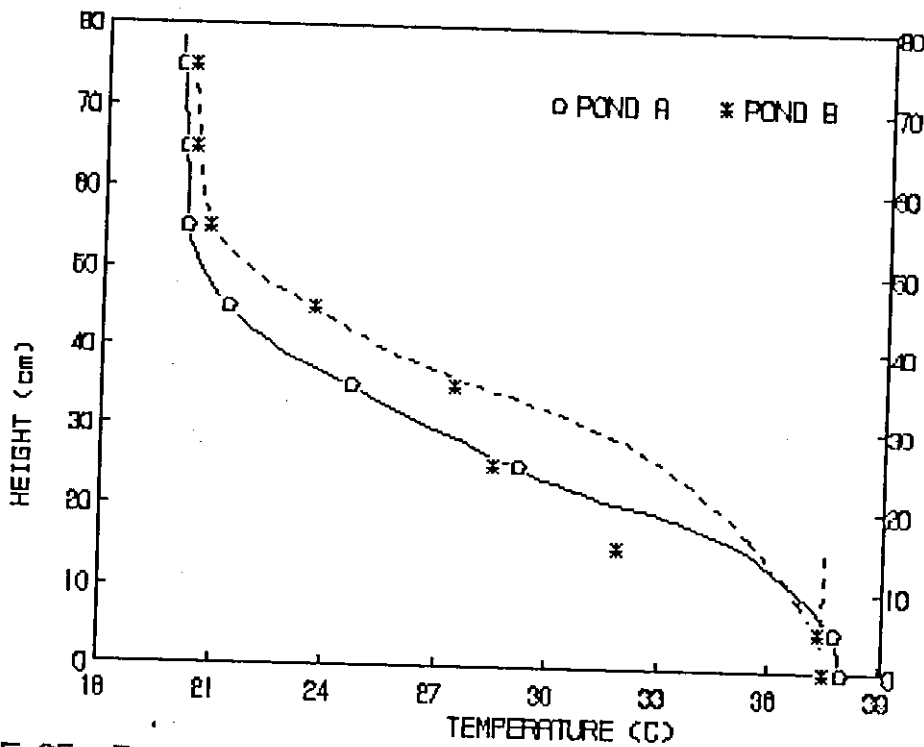


Fig.5.35: Temperature profiles on 20/10/1993 at time 15:00, when 40 cm rings are introduced into pond A, $T_a = 27.1$ C.

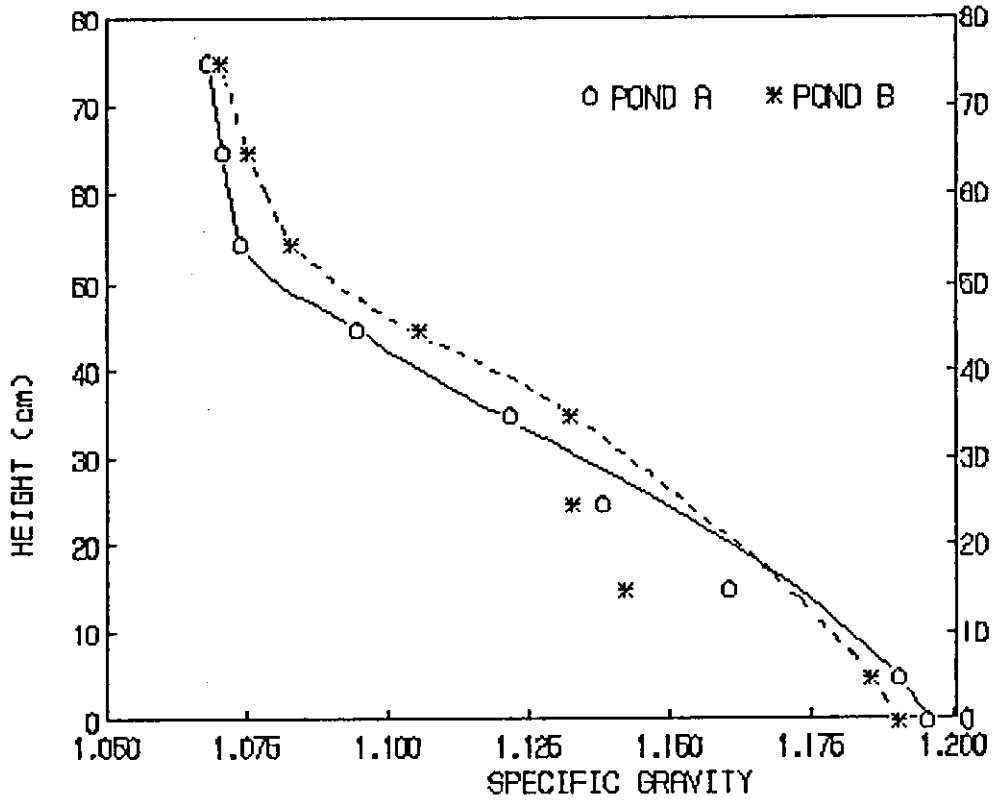


Fig.5.36: Salinity profiles on 16/10/1993, when 40 cm rings are introduced into pond A.

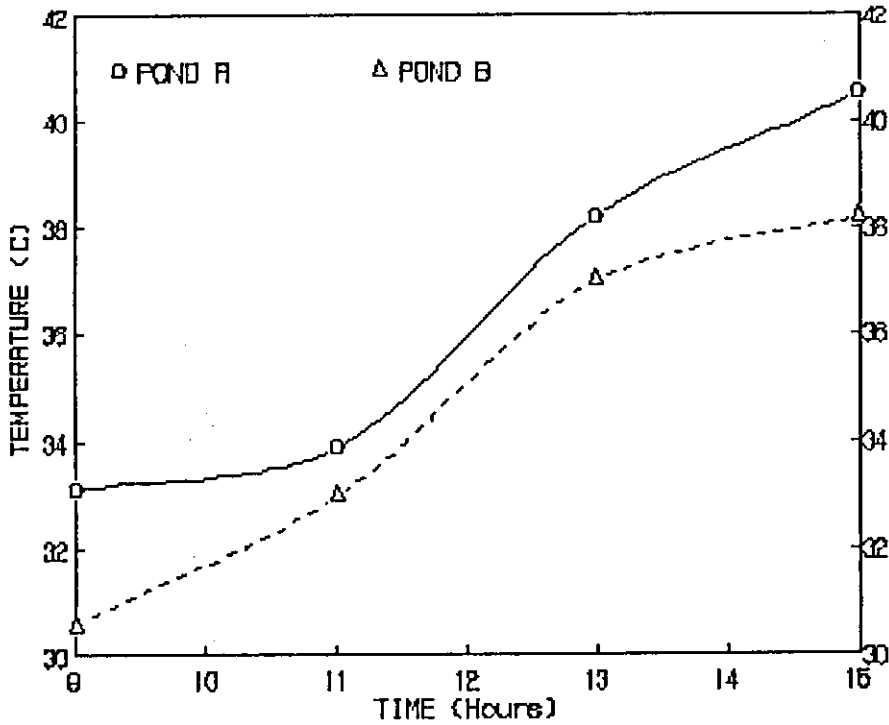


Fig.5.37: Storage zone temperature history on 16/10/1993, when 40 cm rings on pond A.

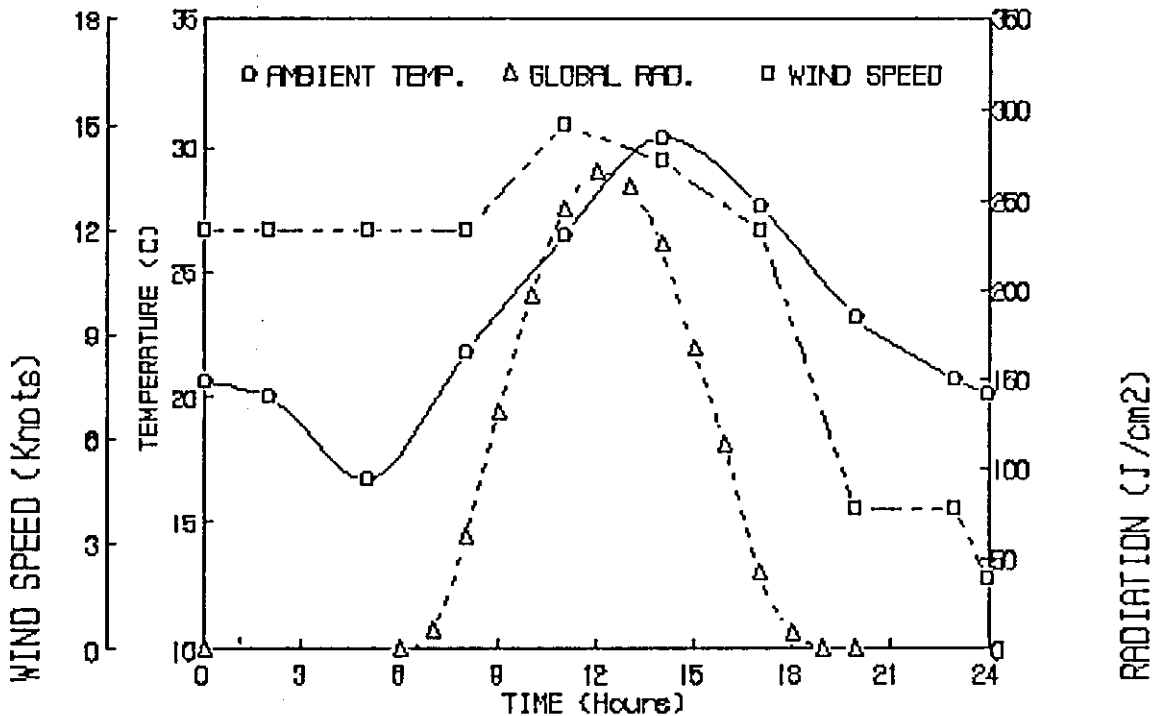


Fig.5.38: Meteorological data for Amman on 16/10/1993.

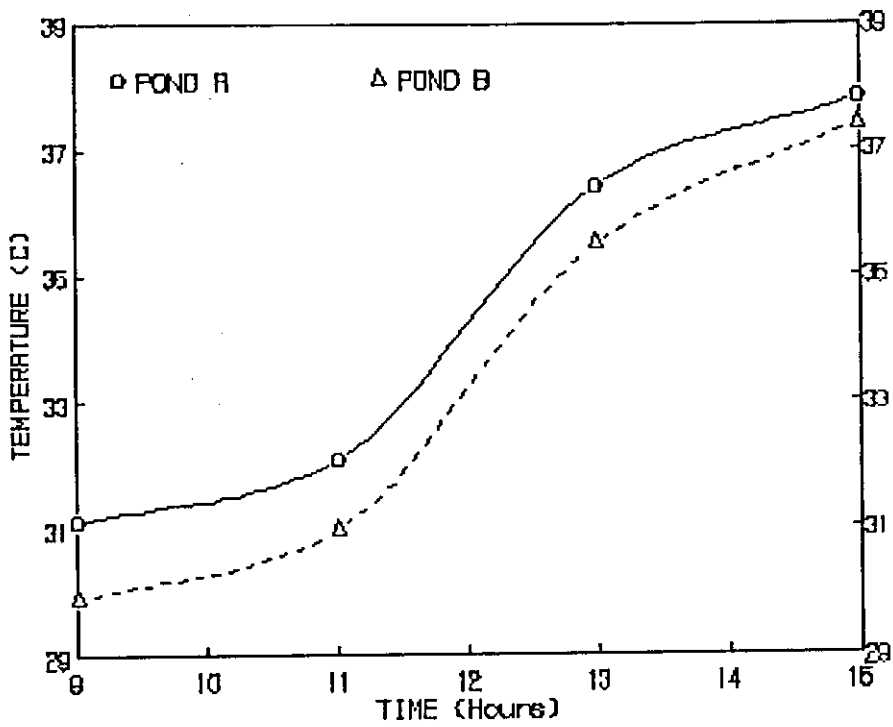


Fig.5.39: Storage zone temperature history on 20/10/1993, when 40 cm rings on pond A.

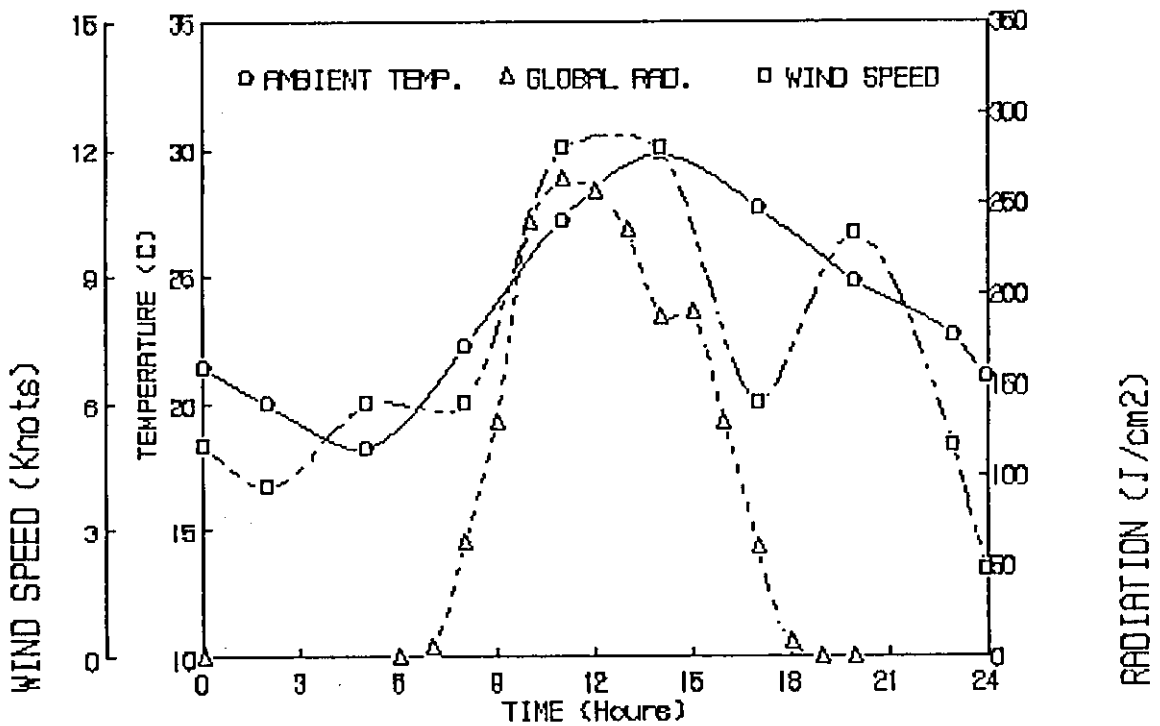


Fig.5.40: Meteorological data for Amman on 20/10/1993.

3. Introducing of 50 cm Rings to Pond A

The rings of 40 cm diameter were removed from pond A at 17:00 on October 20, and rings of 50 cm diameter were introduced to pond A for one week. The temperature profiles of the ponds on October 23 and 27 are shown in figures 5.41-5.44. The salinity profile on Oct.23 is shown in figure 5.45. Also, the maximum storage temperature and the meteorological data on Oct.23 and 27 are presented in figures 5.46-5.49.

The temperature and salinity profiles indicate that the behaviour of both ponds were getting better with the UCZ is reduced to less than 5 cm due to the surface washing done three days before.

The temperature gradient of pond A is again almost a straight line with a gradient of about 25-30°C/m at the top of NCZ and about 15-20°C/m which is less than before and is similar or a little bit greater than the gradient of pond B.

By considering the temperature and salinity profiles very thoroughly, it can be noted that some instability (points scattering) started to occur for pond A specially at the top of the NCZ and at the bottom of NCZ. On the other hand, pond A still behaves better than pond B, where the points scattering for pond A are less than pond B. This is also clear from the salinity profile, where the instabilities in NCZ zone of pond B are more critical than pond A, which indicates that salinity profile of pond B is more disturbed due to the winds.

The storage zone is affected by the addition of water on the

surface of the pond, the surface washing stopped the declination of the LCZ temperatures, which is illustrated in the storage zone temperature profiles. The storage zone temperature increased strongly from the morning of October 23 to the evening and maintained this increasing of temperature to the following days. Again, the storage temperature of pond A is much better than that of pond B, and the difference in the evening of the two days always around 4-5°C. It is obvious from the figure 5.49 of the meteorological data that continuous high rates of wind speed has been blown in this week and reached about 20 km/h. The effect of the wind is obviously greater on pond A. Also, the global radiation in this week was 253 J/cm² and 248 J/cm² at noon for October 23 and 27 respectively, and the maximum ambient temperature reached was 26°C for these days.

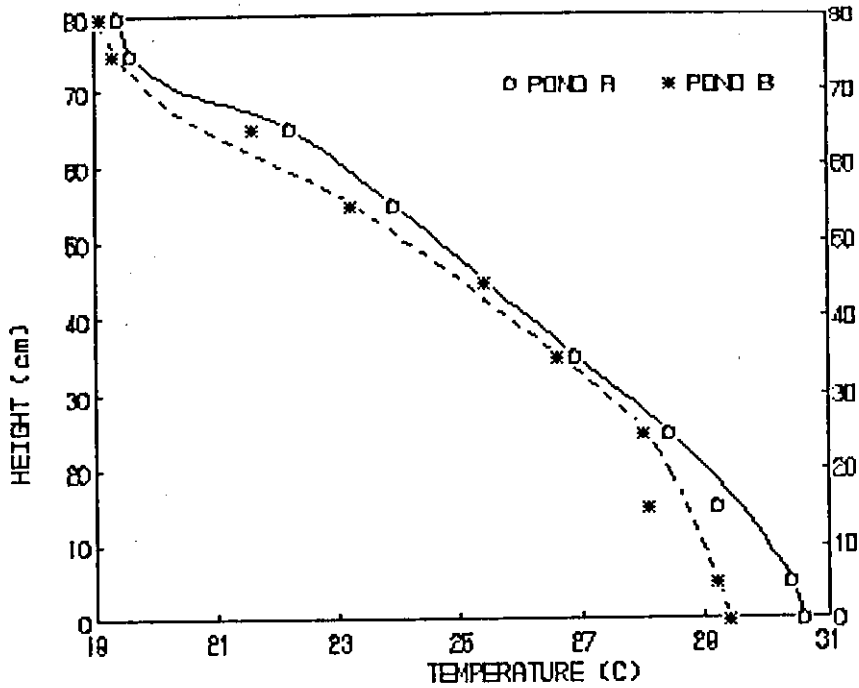


Fig.5.41: Temperature profiles on 23/10/1993 at time 11:00, when 50 cm rings are introduced into pond A. $T_a = 23.4$ C.

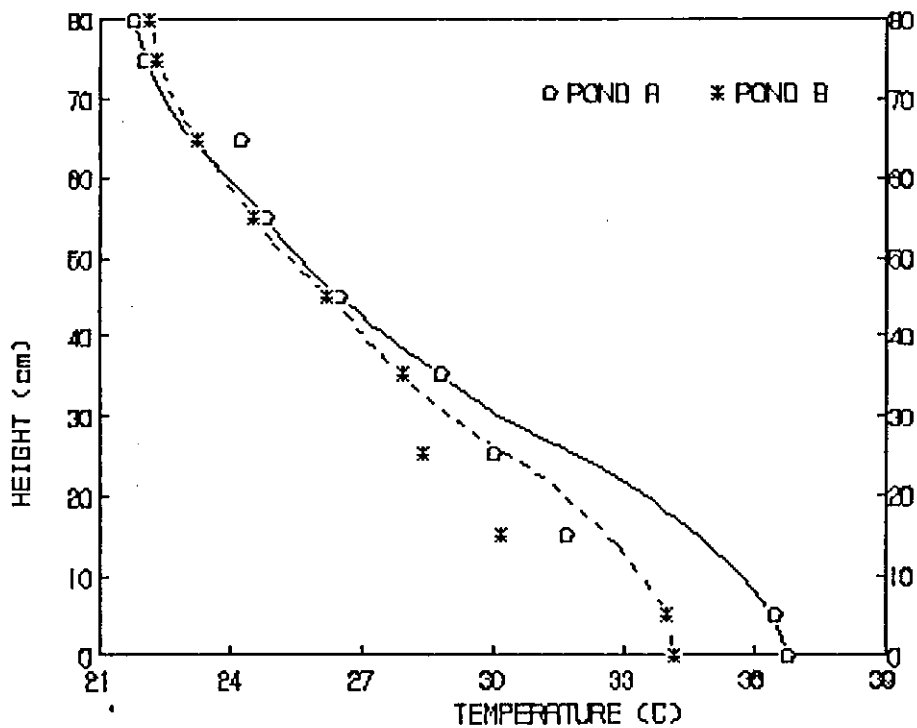


Fig.5.42: Temperature profiles on 23/10/1993 at time 15:00, when 50 cm rings are introduced into pond A. $T_a = 25.2$ C.

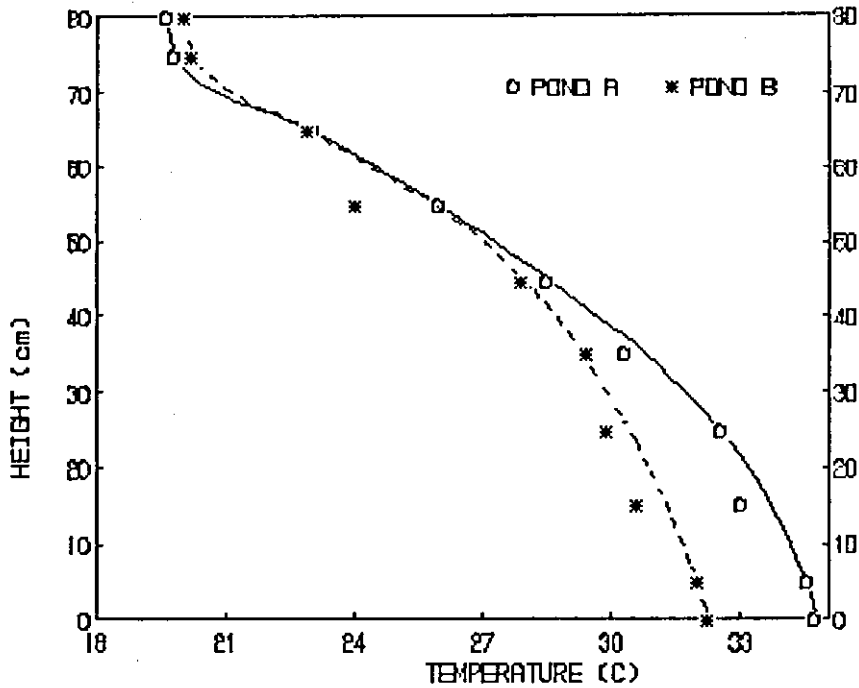


Fig.5.43: Temperature profiles on 27/10/1993 at time 11:00, when 50 cm rings are introduced into pond A, $T_a = 24.8$ C.

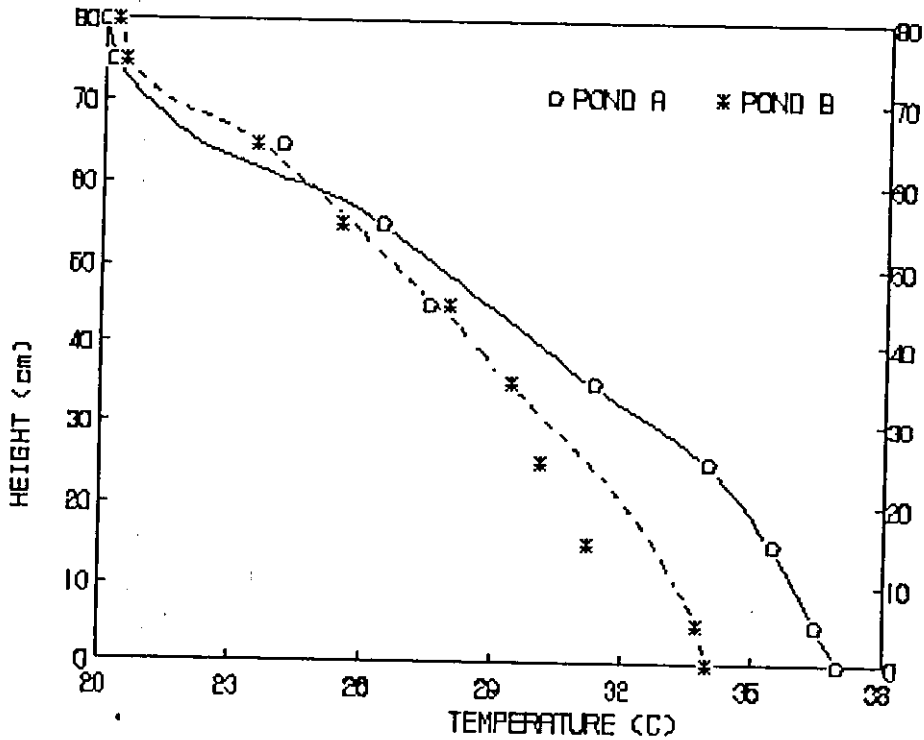


Fig.5.44: Temperature profiles on 27/10/1993 at time 15:00, when 50 cm rings are introduced into pond A, $T_a = 24.4$ C.

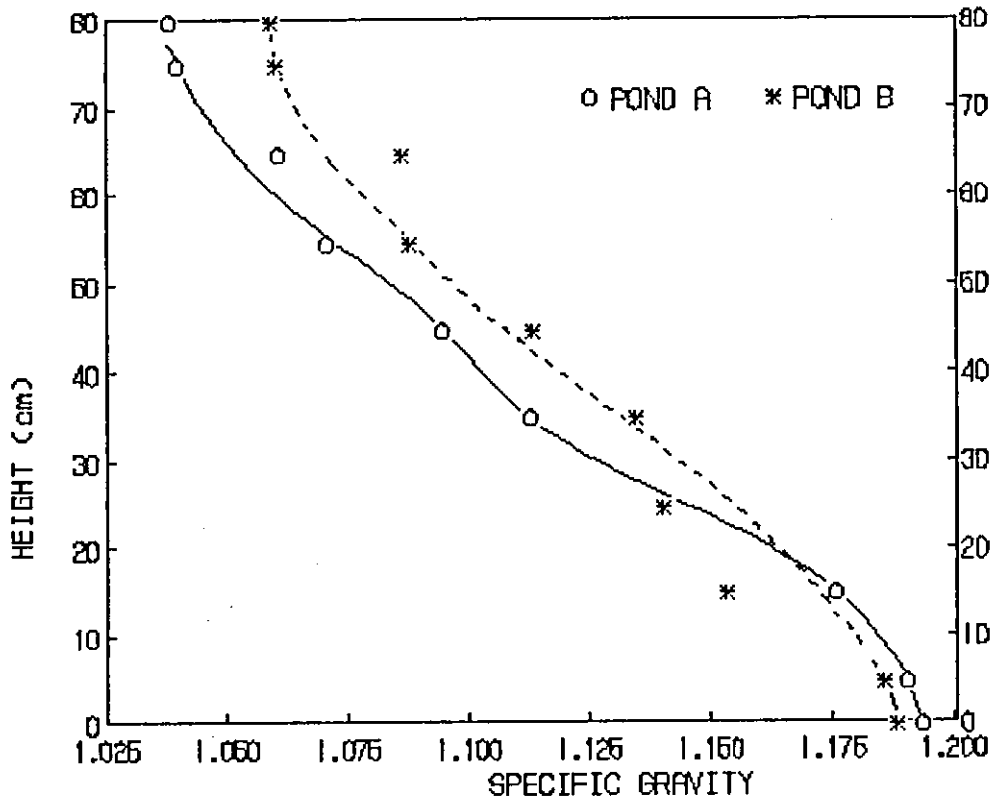


Fig.5.45: Salinity profiles on 23/10/1993, when 50 cm rings are introduced into pond A.

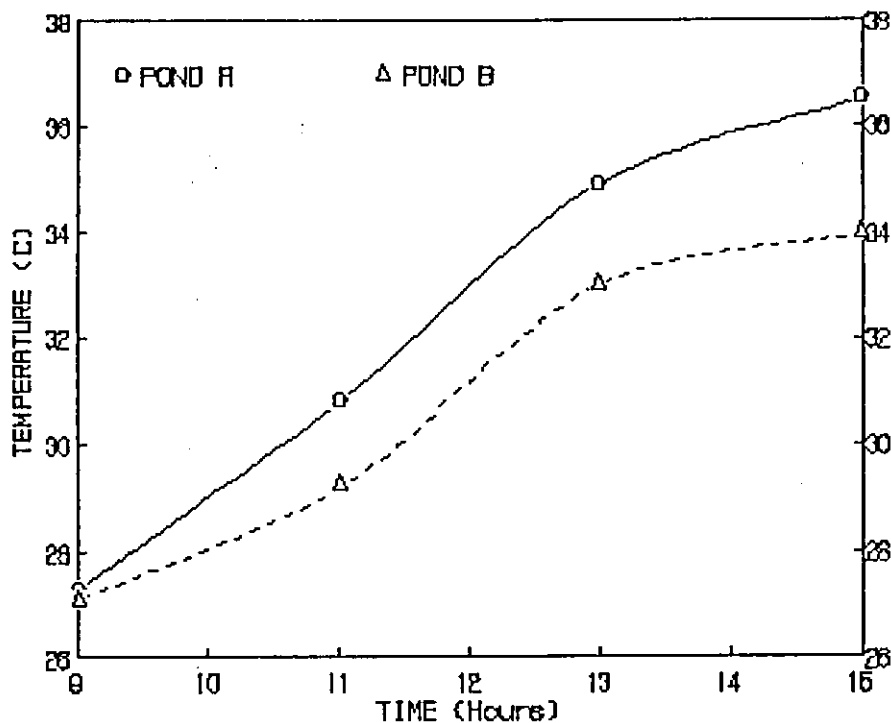


Fig.5.48: Storage zone temperature history on 23/10/1993, when 50 cm rings on pond A.

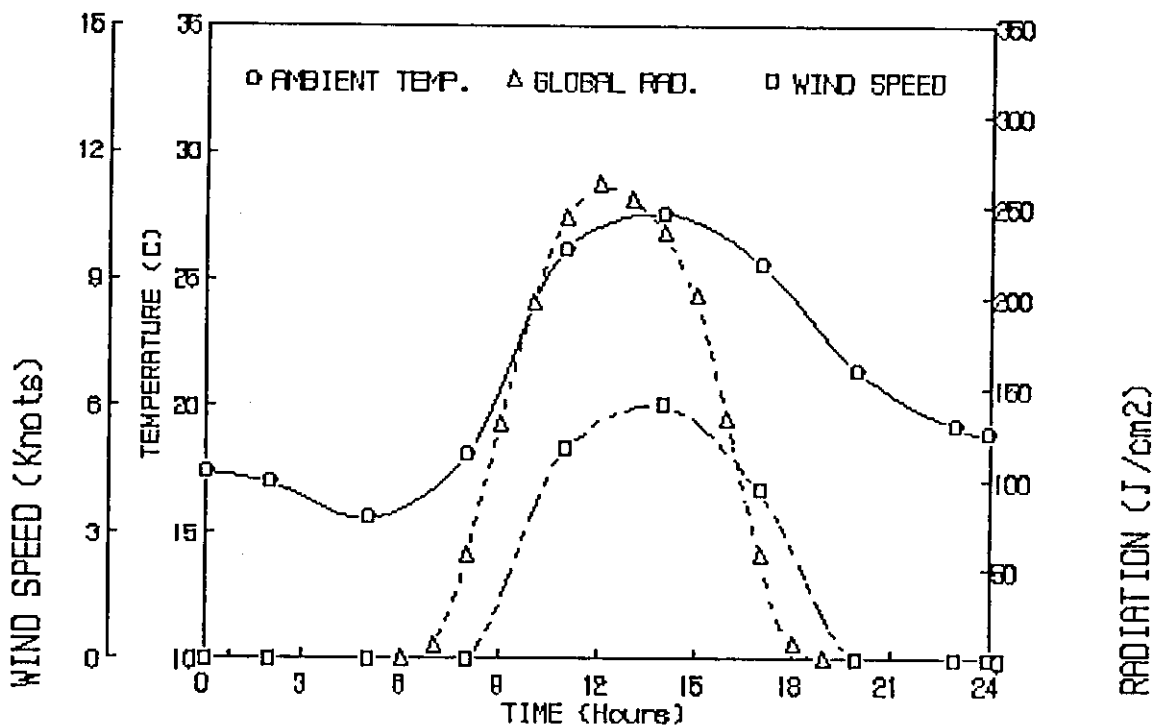


Fig.5.47: Meteorological data for Amman on 23/10/1993.

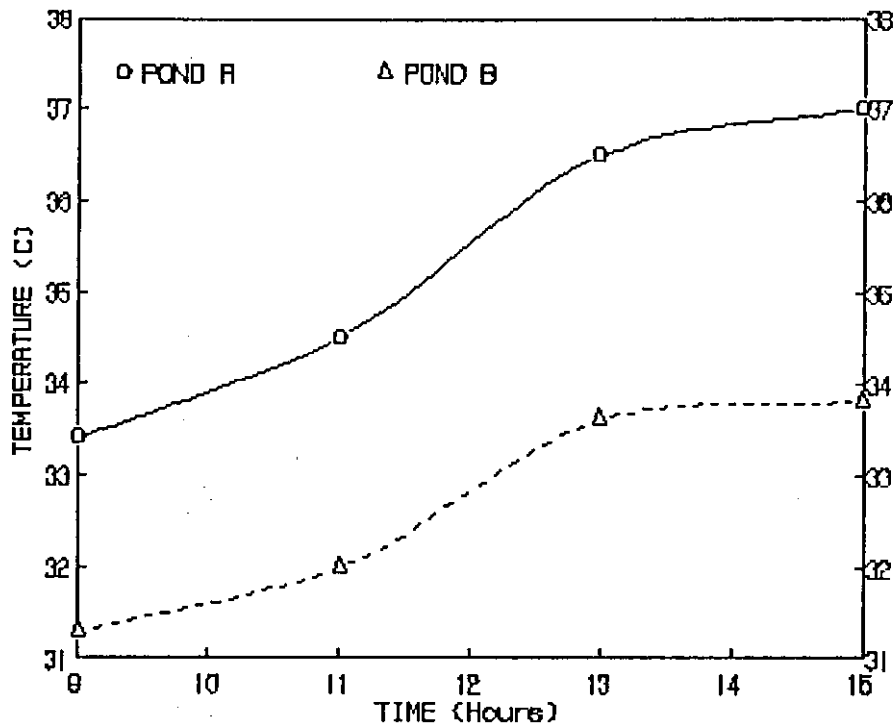


Fig.5.48: Storage zone temperature history on 27/10/1993, when 50 cm rings on pond A.

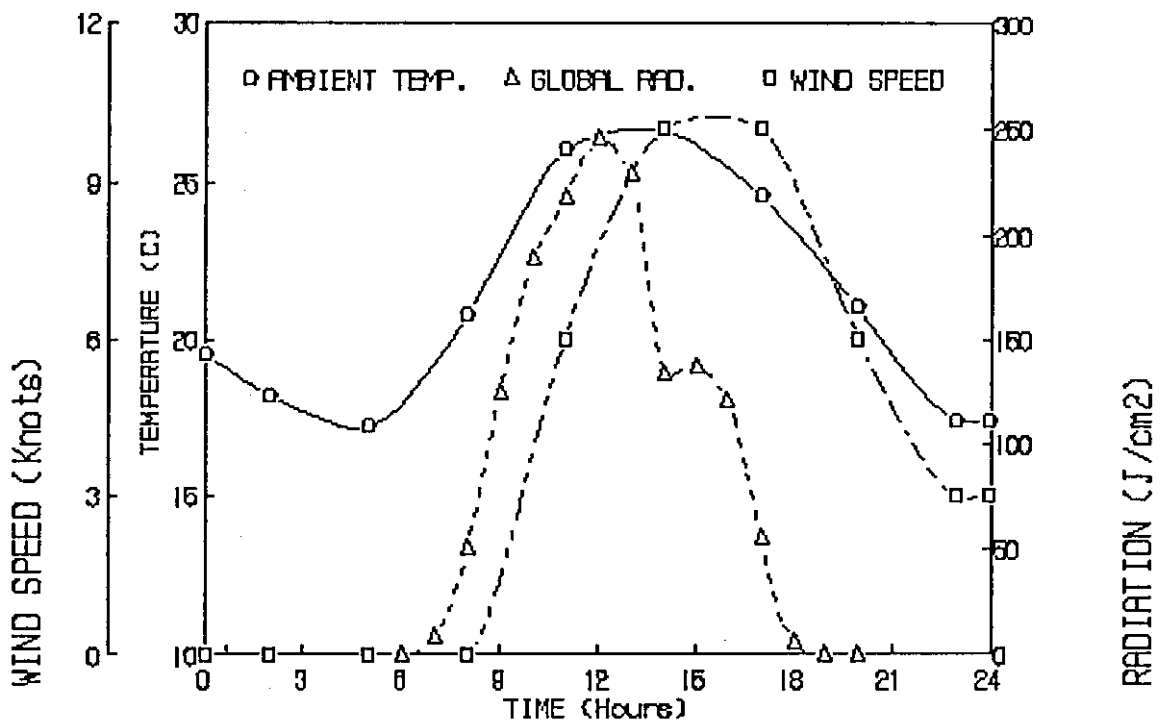


Fig.5.49: Meteorological data for Amman on 27/10/1993.

4. Introducing of 30 cm Rings to Pond A and 50 cm Rings to Pond B

Although, it was shown that the plastic rings had reduced the wind effect significantly, the effect of the ring's size was not yet established. Therefore, it was necessary to introduce two different sizes of ring to each pond and to study their effects under exactly the same conditions.

Rings of 30 cm diameter were introduced to pond A, while 50 cm diameter rings were introduced to pond B at 16:00 on October 27 for one week. The temperature profiles of the ponds on October 30, November 1 and 3 are presented in figures 5.50 - 5.55. The salinity profiles on October 30 and November 1 are given in figures 5.56-5.57. The maximum storage temperature on October 30, November 1 and 3 are shown in figures 5.58-5.63.

The temperature profiles indicate that the difference of the thermal behaviour of the two ponds has been greatly reduced, where the gradient of pond B became almost a straight line very similar to that of pond A but with slightly lower gradient values. The temperature gradient values of pond A and B range from 20-30°C/m at the top of NCZ to 10-15 at the bottom of NCZ.

It can also be noted from the temperature profiles that the temperature scattering in the NCZ of pond B have been greatly reduced and therefore the stability of pond B has been enhanced. On the other hand, Pond A still characterized by a smooth temperature gradient as

seen from the reduction in scattering of the temperature points, and hence a better stability than that of pond B.

The difference in the salinity profiles of the two ponds is also reduced as shown in figures 5.56 and 5.57. The specific gravity of the saline water for both ponds increases smoothly with the depth of the pond.

The maximum storage zone temperature and the meteorological data figures show that pond A experienced higher values of storage temperature than pond B, where it reached 36.5°C for pond A and 35.0°C for pond B on October 30. This storage temperature has been dropped greatly on November 1 and 3 because of the strong rainfall on November 1, which was accompanied by a very high wind speed of about 22 km/h in November 1. The low global radiation in November 1 (not exceeding 160 J/cm² at noon) had also contributed significantly to the reduction in the storage zone temperature. Although these meteorological factors lowered the storage zone temperature yet they did not have any effect on the stability of the solar ponds.

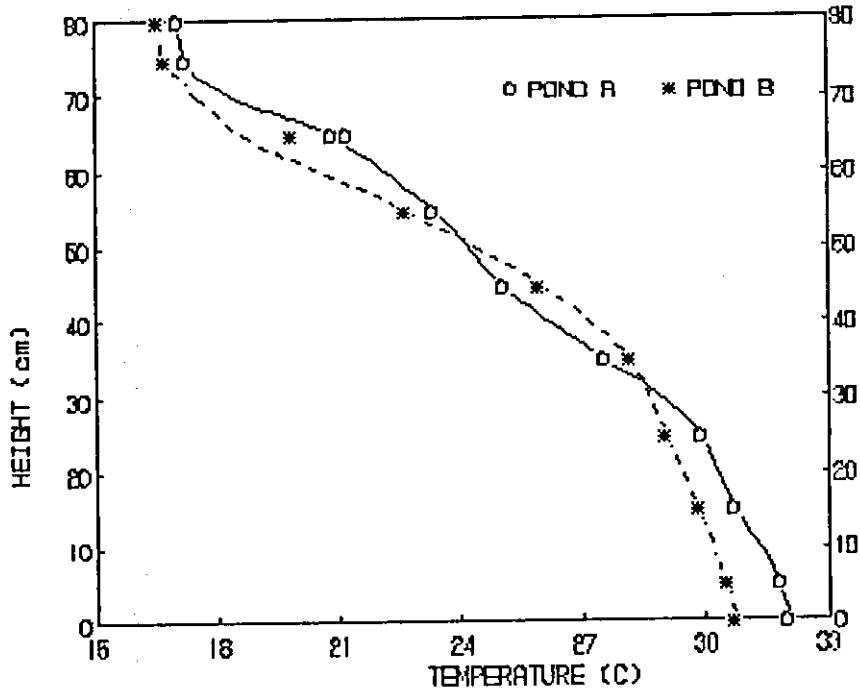


Fig.5.50: Temperature profiles on 30/10/1993 at time 11:00, when 30 cm rings are introduced into pond A and 50 cm rings are introduced into pond B. $T_a=23.6C$.

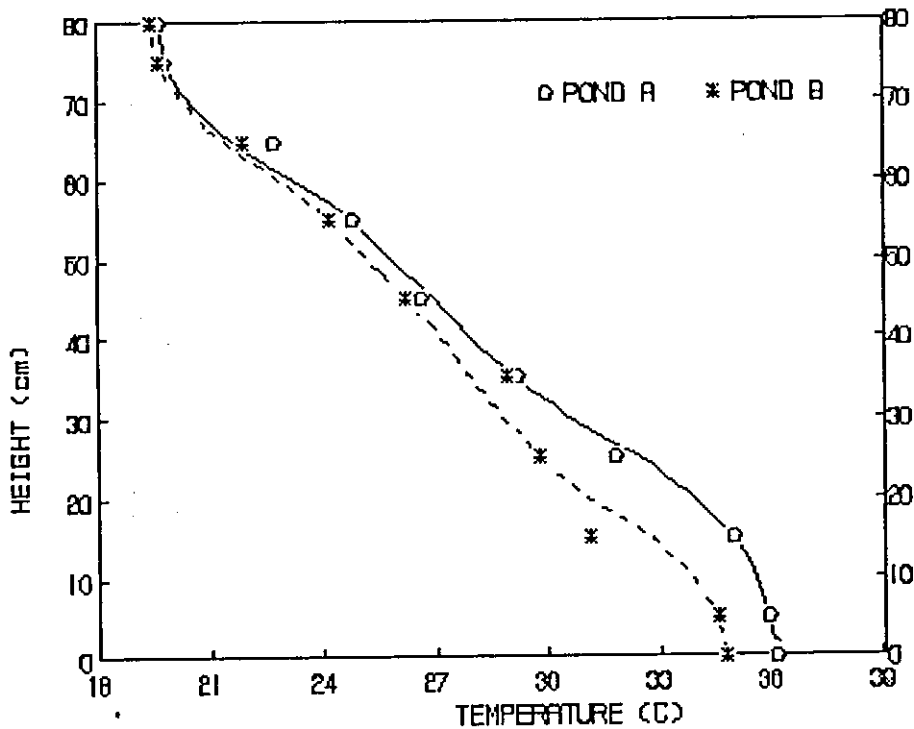


Fig.5.51: Temperature profiles on 30/10/1993 at time 15:00, when 30 cm rings are introduced into pond A and 50 cm rings are introduced into pond A. $T_a=25.5C$.

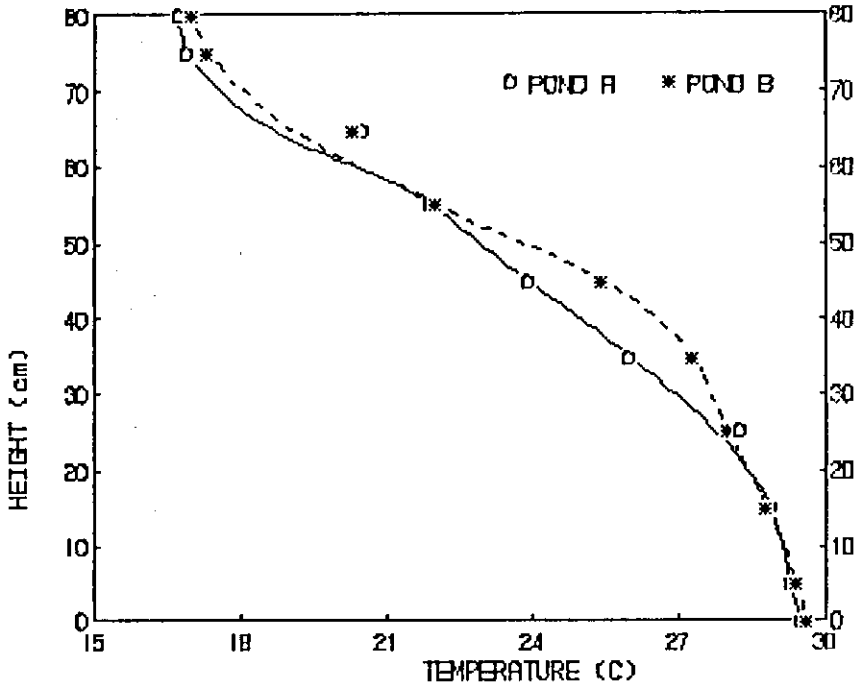


Fig.5.52: Temperature profiles on 1/11/1993 at time 11:00, when 30 cm rings are introduced into pond A and 60 cm rings are introduced into pond B. $T_a=15.6C$, rainfall = 16 ml.

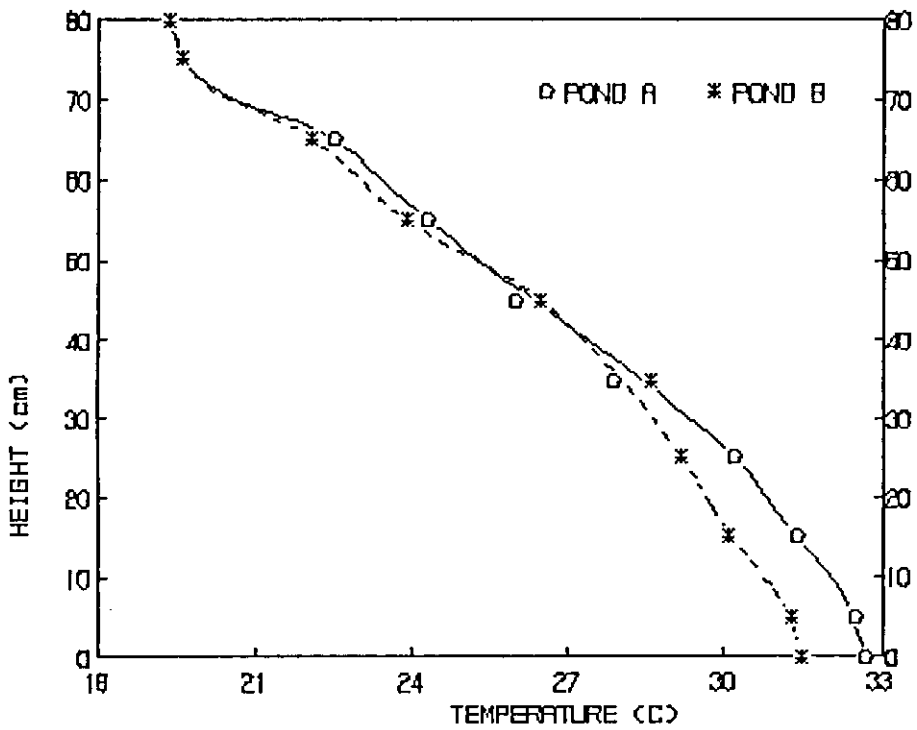


Fig.5.53: Temperature profiles on 1/11/1993 at time 15:00, when 30 cm rings are introduced into pond A and 60 cm rings are introduced into pond B. $T_a=15.7C$, rainfall = 16 ml.

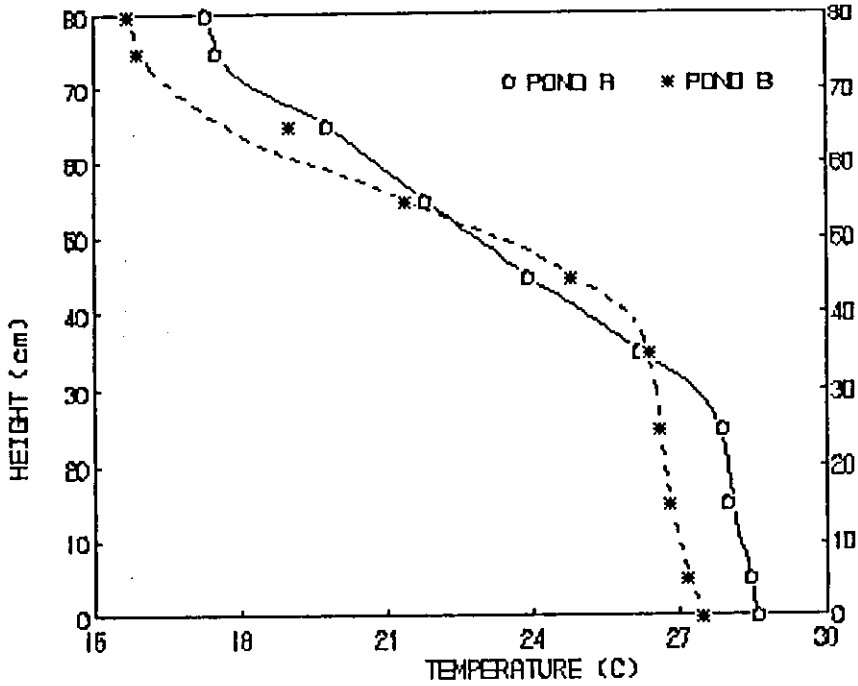


Fig.5.54: Temperature profiles on 3/11/1993 at time 11:00, when 30 cm rings are introduced into pond A and 50 cm rings are introduced into pond B. $T_a=14.5C$.

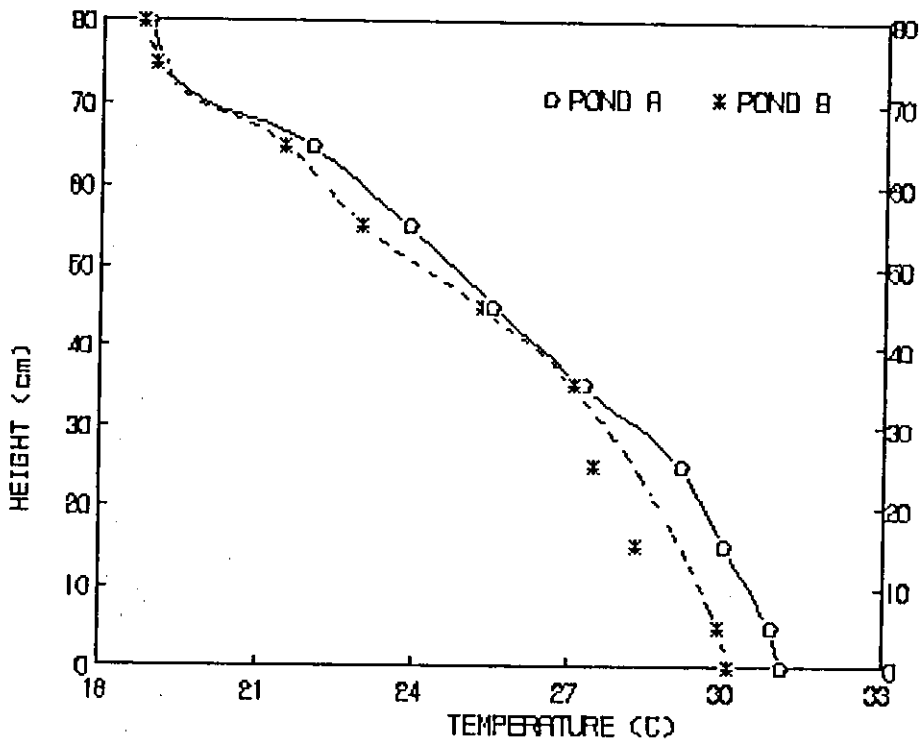


Fig.5.55: Temperature profiles on 3/11/1993 at time 13:30, when 30 cm rings are introduced into pond A and 50 cm rings are introduced into pond B. $T_a=15.7C$.

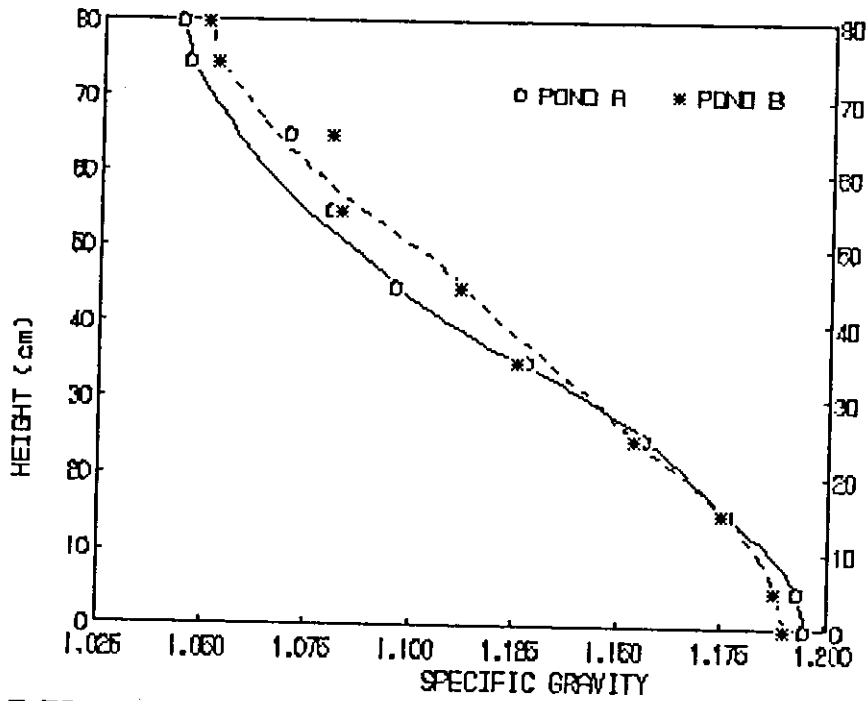


Fig.5.56: Salinity profiles on 30/10/1993, when 30 cm rings are introduced into pond A and 50 cm rings are introduced into pond B.

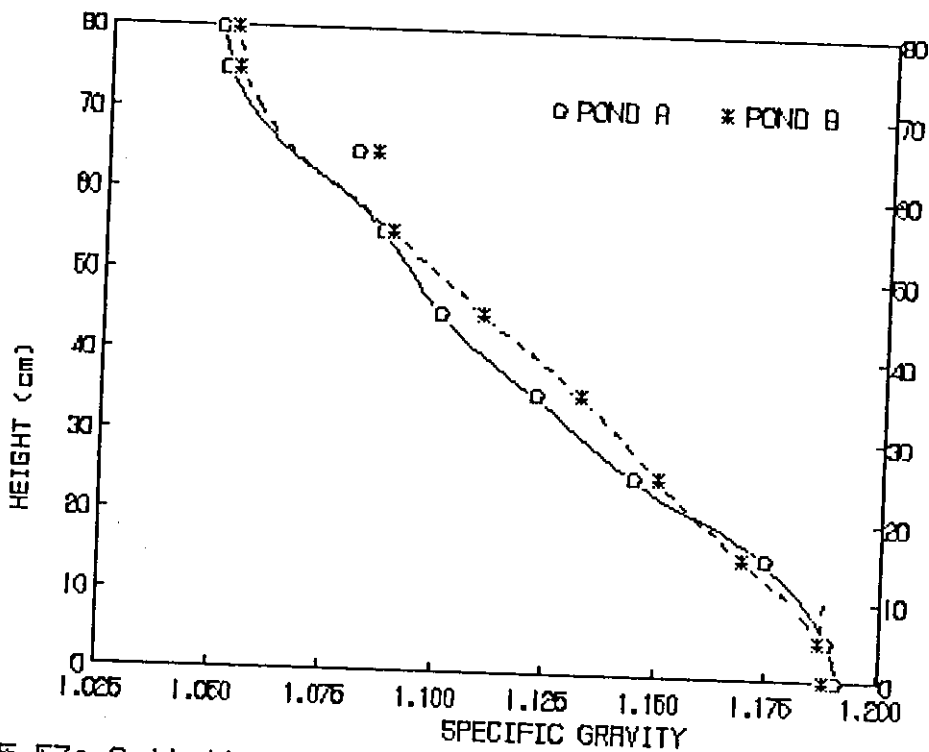


Fig.5.57: Salinity profiles on 1/11/1993, when 30 cm rings are introduced into pond A and 50 cm rings are introduced into pond B.

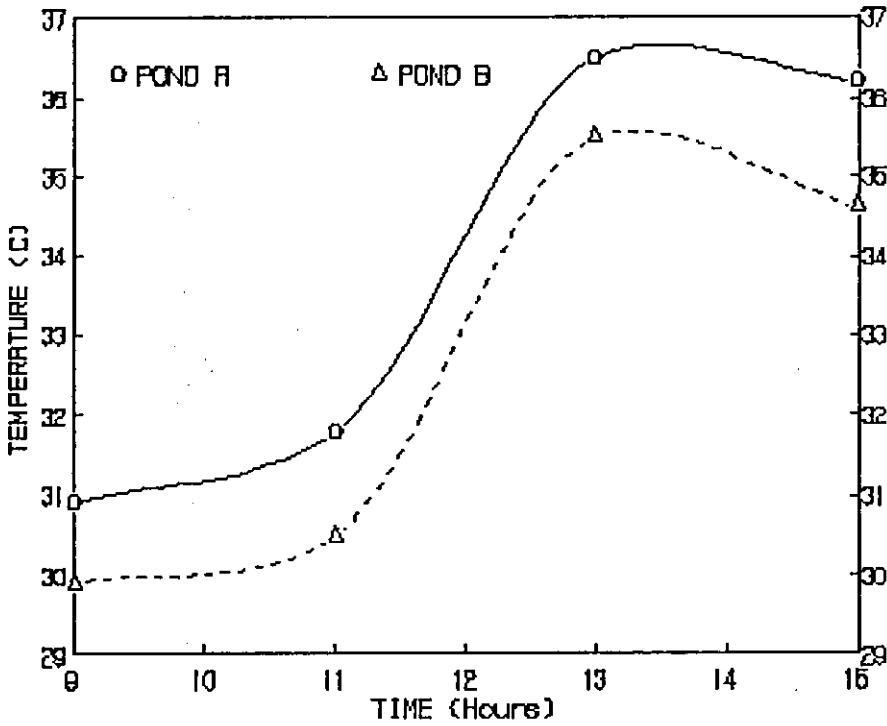


Fig.5.58: Storage zone temperature history on 30/10/1993, when 30 cm rings on pond A and 50 cm rings on pond B.

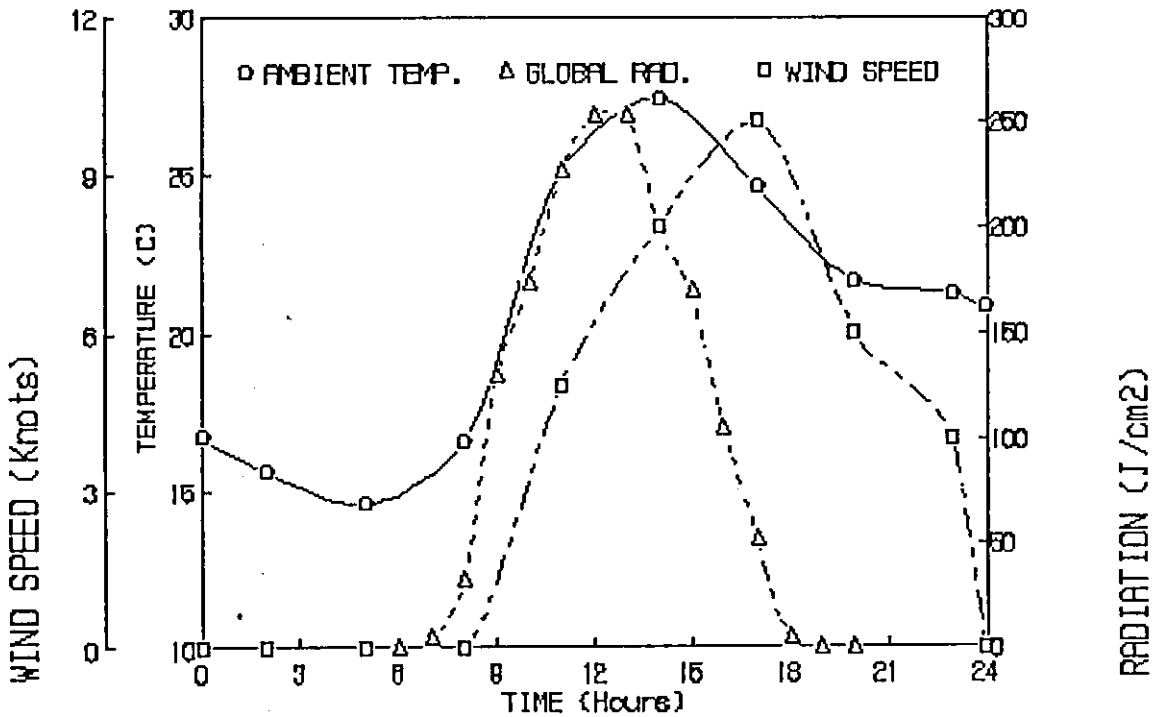


Fig.5.59: Meteorological data for Amman on 30/10/1993.

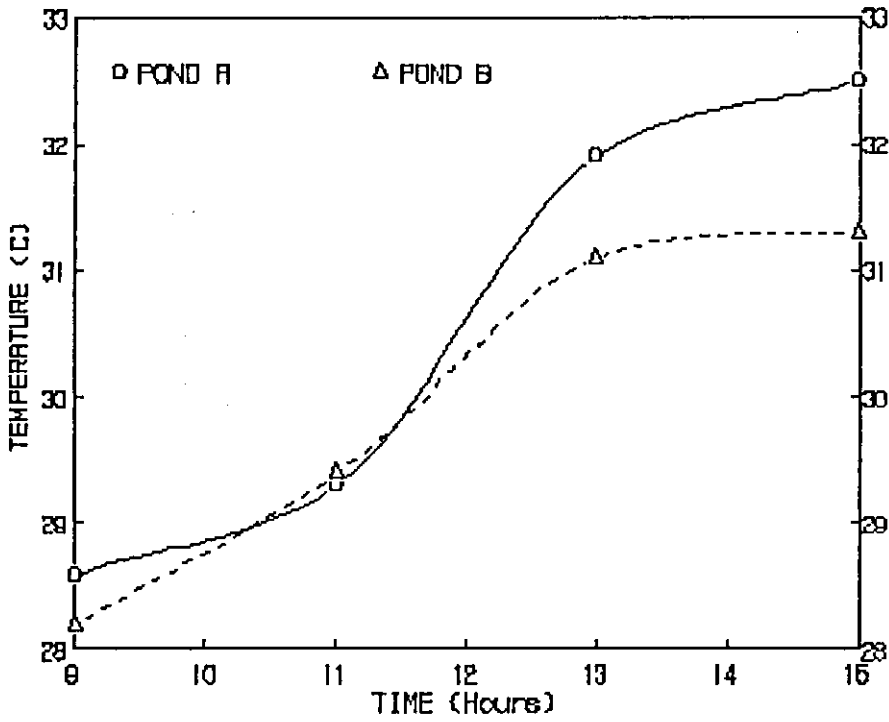


Fig.5.80: Storage zone temperature history on 1/11/1993 when 30 cm rings on pond A and 50 cm rings on pond B.

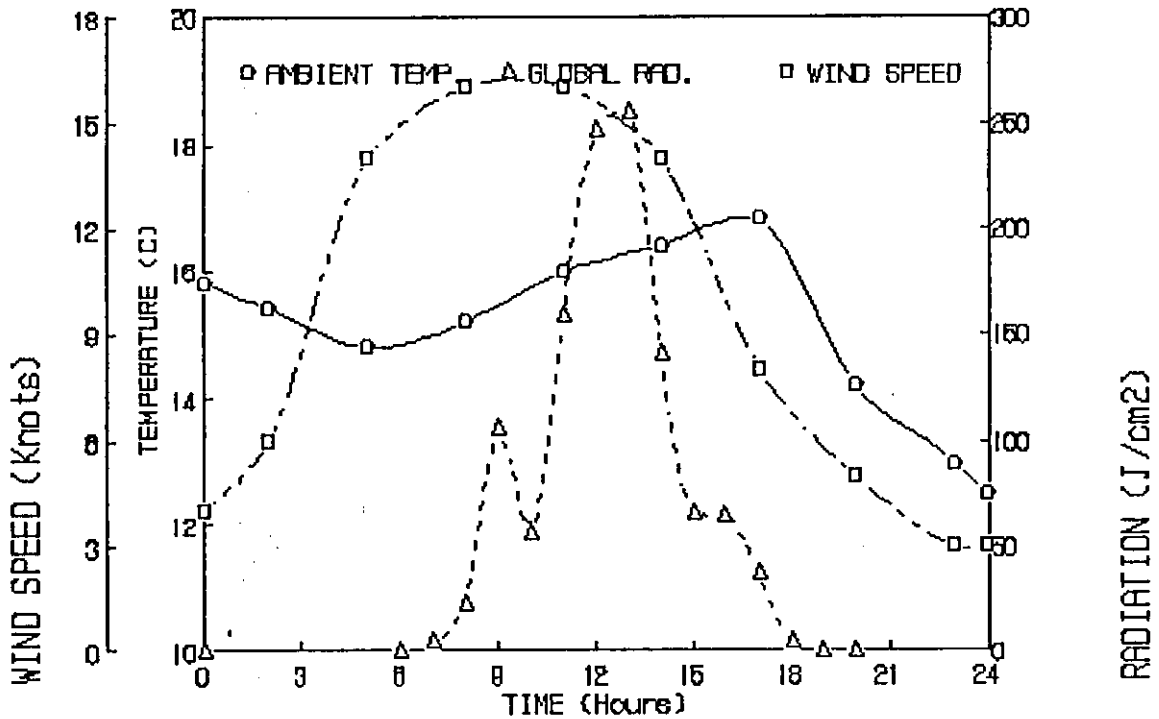


Fig.5.81: Meteorological data for Amman on 1/11/1993, when rainfall = 16 ml.

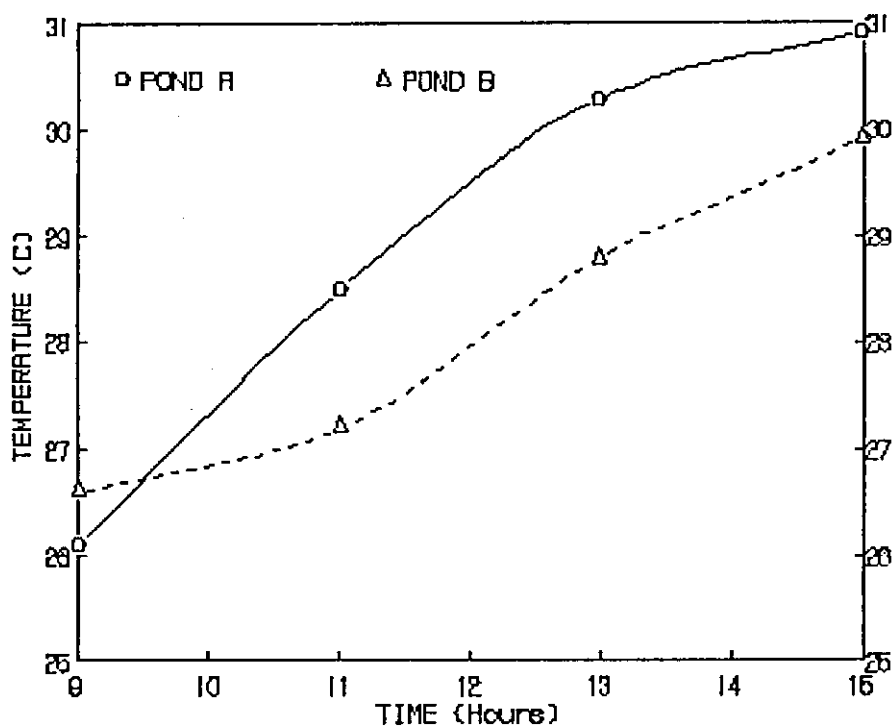


Fig.5.62: Storage zone temperature history on 3/11/1993, when 30 cm rings on pond A and 50 cm rings on pond B.

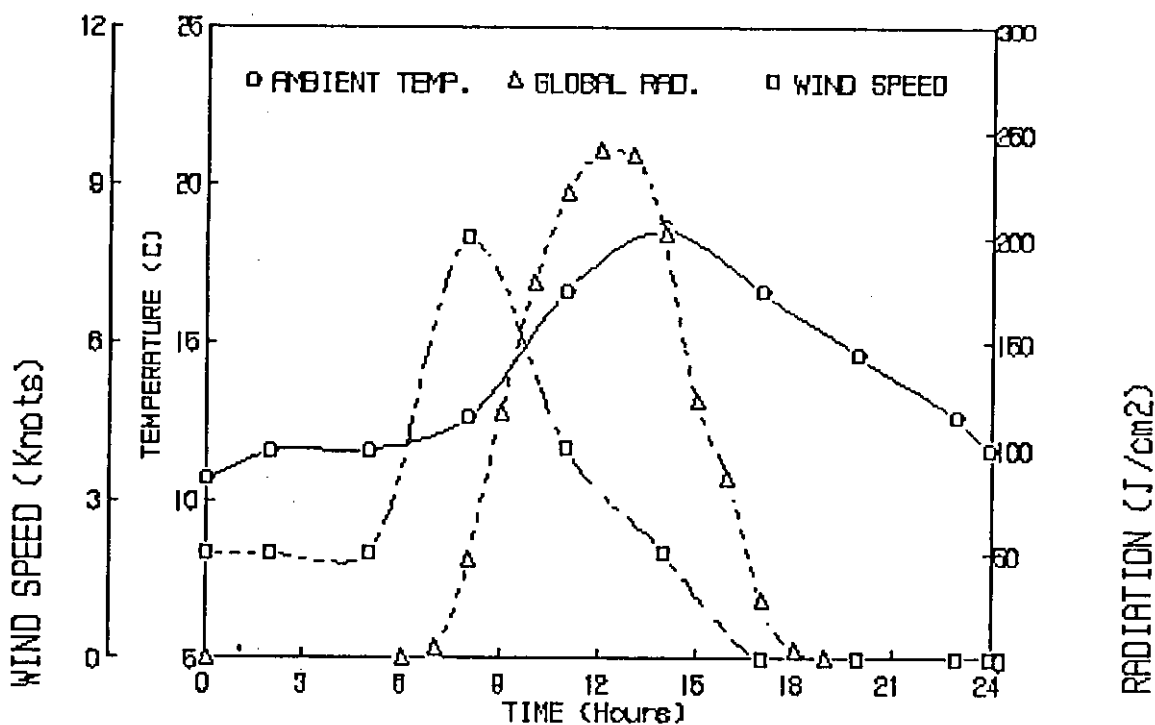


Fig.5.63: Meteorological data for Amman on 3/11/1993.

CHAPTER 6

CONCLUSIONS AND RECOMMENDATIONS

6.1 Introduction

This study has been conducted to study the performance of solar ponds under Jordanian climate as well as testing various types of local clays to be used as liners for future construction of solar ponds in Jordan. This work also paved the way toward the construction of a prototype solar pond in Jordan.

6.2 Conclusions

Based on the experimental results presented in the previous chapter, the following conclusions can be drawn:

1. Some local Jordanian clays such as Amman clay and Tafilah clay have low permeability values and medium plasticity index, and this makes them good candidates as a lining materials for the solar ponds.
2. The optimum low cost lining scheme that can be used for solar pond in Jordan consists of low density polyethelene film sandwiched between two compacted local low permeable clay layers.
3. The wind speed tends to have an adverse effect on the stability of the solar pond, the gradient zone, the formation of the upper

convective zone and the temperature of the storage zone.

4. The plastic rings reduce the fetch size of the pond, and can be considered as wind suppressors. A solar pond that is supplied with rings experiences a more smooth temperature and salinity profiles and higher storage temperature than a solar pond without rings.
5. A solar pond with 30 cm diameter rings has a thermal performance better than a pond with 50 cm diameter rings, which means that it is better to use rings with smaller diameters.
6. The influence of rains on the gradient and the stability of solar ponds is negligible for the conditions tested.
7. The variations in the temperature and salinity profiles in the non-convective zone are significant. Therefore, it is needed to increase the number of the temperature and salinity sensors in this region in order to increase the resolution of the results.

6.3 Recommendations and Future Works

1. Although this study contributes to the know how associated with solar pond technology. It is still important to demonstrate the salt gradient solar pond technology in Jordan with a large scale pond in order to study the associated problems in a more realistic scale.

2. Investigations and detail studies of the process of heat extraction from the pond, the effect of hot brine removal on the stability of the gradient zone, the rates of brine withdrawing at different seasons of the year.
3. The effect of the climatic conditions on a large scale salt gradient solar ponds.
4. Comprehensive study of heat losses from the walls, the underground soil and the surrounding environment of a large scale ponds in order to minimize the heat losses from the storage zone.
5. Investigations on the convective cells generated on the side walls of solar ponds and their effects on the stability of the salt gradient solar ponds, and the optimum angle of the pond's walls that reduce the convective cells generated.
6. It is recommended to design and develop a transversing mechanism that can be used to measure the temperature and salinity profiles without having any effect on the solar pond stability, but at the same time increases the resolution of the results.
7. Investigating some of the applications of solar ponds that can be used successfully in Jordan.
8. Surveying the local types of salts that can be used for solar pond in Jordan and establishing criteria needed for these salts.

9. Exploring the potential of using fertilizer salts for solar ponds, specially when these ponds are used for agricultural applications.

NOMENCLATURE

- A : The cross sectional area, (m^2).
- C : Salt concentration, (kg/m^3).
- e : The water level, (m).
- g : The acceleration due to gravity, (m/s^2).
- h : Wave amplitude, (m).
- ΔH : The solar heat flux absorbed in the UCZ., (W/m^2).
- H : Average solar insolation at the top surface, (W/m^2).
- I : The irradiance on the top surface, (W/m^2).
- I_p : Plasticity index, (%).
- i : The hydraulic gradient.
- k : The thermal conductivity of the medium, (W/m_oC).
- K_c : Coefficient of salt diffusivity, (cm^2/sec).
- K_p : The vertical permeability coefficient, (m/s).
- K_T : Coefficient of thermal diffusivity, (cm^2/sec).
- l : The thickness of near impermeable layer, (m).
- LL : Liquid limit, (%).
- PL : Plastic limit, (%).
- Q : The quantity of seepage rate, (m^3/s).
- q_b : The rate of bottom heat loss, (W/m^2).
- q_e : The rate of heat loss due to evaporation from the top surface of the pond, (W/m^2).
- q_{ext} : The rate of heat extraction from the LCZ, (W/m^2).
- q_o : The rate of heat loss due to convection and radiation from the top surface of the pond, (W/m^2).
- q_s : The rate of side heat losses, (W/m^2).
- q_u : The rate of upward heat conduction loss, (W/m^2).
- q_1 : The rate of heat conducted from UCZ boundary to NCZ, (W/m^2).

- q_2 : Solar heat flux absorbed in LCZ, (W/m^2).
 q_3 : Solar heat flux reflected from the bottom and absorbed in the LCZ, (W/m^2).
 Re : Reynolds number.
 T : Temperature, ($^{\circ}C$).
 T_a : Ambient temperature, ($^{\circ}C$).
 ΔT : Difference in temperature between LCZ and ambient, ($^{\circ}C$).
 t : Time, (sec).
 U : The wind velocity, (m/s).
 U_{Lg} : Heat loss factor including ground heat losses, ($W/m^2 \cdot ^{\circ}C$).
 U_s : Water surface velocity, (m/s).
 V : Vertical velocity measured positive downward, (m/s).
 v : Wave velocity, (m/s).
 $w\%$: The percentage of Water content in a clay, (%).
 X : Nondimensional length.
 x : Fetch length, (m).
 Y : Depth measured from the surface, (m).
 Z : The depth measured as positive downward, (m).

Greek Letters:

- α : Thermal expansion coefficient, (K^{-1}).
 β : Salt expansion coefficient, (kg/m^3).
 $(\langle\langle\tilde{\tau}\rangle\rangle)_{eff}$: Effective absorbitivity-transmisivity product
 λ : The wave length, (m).
 ν : Kinematic viscosity, (cm^2/sec).
 ρ : Density, (kg/m^3).
 $\tilde{\tau}(z)$: The fraction of the incident radiation transmitted to depth Z.

ABBREVIATIONS

GZ	: Global Radiation.
GZ	: Gradient Zone.
LCZ	: Lower Convective Zone.
NCZ	: Non-Convective Zone.
SG	: Specific Gravity.
SGSP	: Salt Gradient Solar Pond.
SP	: Solar Pond.
SZ	: Storage Zone.
UCZ	: Upper Convective Zone.

REFERENCES

1. Hull, J., Nielsen, C. and Golding, P., " Salinity Gradient Solar Ponds ", CRC Press, Inc., Boca Raton, Florida, (1987).
2. Federica Zangrando, " Observation and Analysis of a Full Scale Experimental Salt Gradient Solar Pond ", Dissertation of PHD in Physics, The University of New Mexico, Albuquerque, New Mexico, (1979).
3. Tabor, H., " Solar Collector Developments ", Solar Energy, 3, 8 (1959).
4. Tabor, H. and Martz, R., " Solar Pond Project ", Solar Energy, 9, 177 (1965).
5. Weinberger, H., " The Physics of Solar Pond ", Solar Energy, 8, 45 (1964).
6. Rabl, A. and Nielsen, C.F., " Solar Ponds for Space Heating ", Solar Energy, 17, 1 (1975).
7. Kooi, C.F., " The Steady State Salt Gradient Solar Pond ", Solar Energy, 23, 37 (1979).
8. Beniwal, R., Singh, R., Pande, R., Chaudhary and Bakore, P. " Thermal Performance of Solar Ponds Under Different Salt Soil Conditions ", Heat Recovery Systems, 7, 139-149 (1987).
9. Beniwal, R. and Singh, R., " Calculation of Thermal Efficiency of Salt Gradient Solar Ponds ", Heat Recovery Systems & CHP, 7, 497-516 (1987).
10. Leshuk, J., Zawarski, R., Styris, D. and Harling, O. " Solar Pond Stability Experiments ", Solar Energy, 21, 237-244 (1978).
11. Akberzadeh, A. and MacDonald, R.W., " Introduction of a Passive Method for Salinity Replenishment in the Operation of Solar Ponds ", Sol Energy, 29, 71-76, (1982).

12. Nielsen, C.E., " The Latest on Solar Ponds ", Proc.Am Sol. Energy Soc., Boulder, Colorado (1986).
13. Hull, J.R., Liu, K.V. and Shah, W.T., " Dependence of Ground Heat Loss Upon Solar Pond Size and Perimeter Insolation ", Solar Energy, 33, 25-33 (1984).
14. AlHomoud, AlKandari and AlMarafie, "The Philosophy of Design and Construction of the Kuwait 1700 m² Solar Pond ", Int. J. of Energy Res., 13, 217-224, (1989).
15. Banat, F., " A Study of Carnalite Salt-Gradient Solar Ponds ", M.Sc Thesis, University of Jordan (1990).
16. Zangrando, F., " A Simple Method to Establish Salt Gradient Solar Ponds ", Solar Energy, 25, 467 (1980).
17. Golding, P., " The Use of Solar Ponds for the Production of Process Heat ", Final Report to Development of Resources & Energy, Canberra, Australia (1985).
18. Akberzadeh, A. and Shayan, E., " A Passive Method for Setting Up a Density Gradient ", J. Energy, 13, 719-724, (1988).
19. Harris, M.J. and Wittenberg, L.J., " Heat Extraction from a Large SGSP ", 2nd Ann Solar Heating & Cooling Conf., Colorado Springs, Nov.(1979).
20. Tabor, H. and Martz, R., "Large Area Solar Collectors for Power Production ", Solar Energy, 7, 189 (1963).
21. Bryant, H.C. and Colbeck, I., " A Solar Pond for London ", Solar Energy, 19, 321-322 (1977).
22. Sodha, M.S., Bansal, N.K., Kumar, A., Bansal, P.K. and Malik, M.A., " Solar Crop Drying, CRC Press, Boca Raton, Florida (1987).
23. Newell, T.A, Cowie, R.G., Upper, J.M., Smith, M.K. and Cler, G.L., " Construction and Operation Activities at the University of Illinois Salt Gradient Solar Pond ", Solar Energy, 45, 231-239

- (1990).
24. Shah, S.A., Short, T.H. and Fynn, R.P., " A Solar Pond-Assisted Heat Pump for Greenhouses ", Solar Energy, 26, 491 (1981).
 25. Collares-Pereira, M. and Joyce, A., " Salt Gradient Solar Pond for a Greenhouse Heating Application ", Proc. Int Sol. Energy Soc., Montreal (1985).
 26. Tabor, H.Z. and Doron, B., " The Beith Ha'Arava 5 MW (e) Solar Pond Power Plant (SPPP) - Progress Report " , Solar Energy, 45, 247-253 (1990).
 27. Delyannis, A. and Delyannis, E., " Recent Solar Distillation Developments ", Desalination, 45 (1983).
 28. Borsh, R.A., " Trends in the Application of Solar Energy to Water Desalination ", Desalination, 40 (1982).
 29. Ophir, A. and Nadav, N., " Solar Energy as a Source of Power and Desalinated Water ", Desalination, 40 (1982).
 30. Matz, R., Fiest, E. and Bloch, M.R., " The Production of Salt by Means of a Solar Pond ", Inst. of Chemical Eng., London, Chem. Eng., pp.CE 81-87, April(1965).
 31. Lesino, G., Saravia, L. and Galli, D., " Industrial Production of Sodium Sulfate Using Solar Ponds", Solar Energy, 45, 215-219 (1990).
 32. Tybout, R.A., " A Recursive Alternative to Weinberger's Model of the Solar Pond ", Solar Energy, 11, 109 (1967).
 33. Hull, J.R., " Computer Simulation of Solar Pond Thermal Behaviour ", Solar Energy, 25, 33-40 (1980).
 34. Cha, Y.S., Sha, W.T., Schertz, W.W., " Modeling of the Surface Convective Layer of Salt Gradient Solar Ponds ", J. of Solar Energy Eng., 104, 293 (1982).
 35. Wang Y.F. and Akberzadeh, A. " A Parametric Study on Solar Ponds ", Solar Energy, 30, 666-562 (1983).
 36. Panahi, Z., Batty, J.C. and Riley, J.P., " Numerical Simulation

- of the Performance of a Salt-Gradient Solar Pond ", J.of Sol. Energy Eng., 105, 369 (1983).
37. Kaushik, N.D. and Sharma, M.S., " Numerical Model of Solar Pond ", Energy Conversion Mgmt., 25, 459-461 (1985).
 38. Duyar, A. and Bober, W., " The Bottom Heat Loss of a Solar Pond in the Presence of Moving Ground Water ", J. of Solar Energy Eng., 106, 335 (1984).
 39. Hull, J.R. " Solar Pond Ground Heat Loss to a Moving Water Table ", Solar Energy, 35, 211-217 (1985).
 40. Zhang, Z. and Wang, Y., " A Study on the Thermal Storage of the Ground Beneath Solar Ponds by Computer Simulation ", Solar Energy, 44, 243 (1990).
 41. Joshi, V. and Kishore, V. " Applicability of Steady State Equations for Solar Pond Thermal Performance Predictions ", Solar Energy, 11, 821-827 (1986).
 42. Ho-Ming Yeh, Shau-Wei Tsai and Wang-Tang Hsieh, " Time-Temperature Variations in the Storage Zone of Salt Gradient Solar Pond ", Energy, 12, 25-31 (1987).
 43. Atkinson, J., Eric Adams, E and Harleman, D. "Double Diffuse Fluxes in a Salt Gradient Solar Pond", J. of Solar Energy Eng., 110, 17 (1988).
 44. Lewis, W., Incropera, F. and Viskanta, R., " Interferometric Study of Mixing Layer Developement in a Laboratory Simulation of Solar Pond Condition ",Solar Energy, 28, 389-401 (1982).
 45. Beniwal, R., Singh, R., Saxena, N. and Bhandari, R., " Characterisation and Heat Losses from a Laboratory Salt-Gradient Solar Ponds ", Heat Recovery Systems, 6, 105-115 (1986).
 46. Munoz, D., Zangrando, F., Viskanta, R. and Incropera F., " Gradient Layer Entrainment Correlation for a Salt-Gradient Solar Pond with Storage Layer Recirculation ", Transactions of

431710

- ASME, 110, 248 (1988).
47. Wang, Y.F. and Akberzadeh, A., " A Further Study on the Theory of Falling Ponds ", Solar Energy, 29, 557-563 (1982).
 48. Cha, Y.S., Sha, W.T. and Soo, S.L., " Effect of Friction and Extraction on the Stability of Solar Pond ", Transaction of ASME, 105, 356 (1983).
 - 49 Akberzadeh, A. and Manins, P., " Convective Layers Generated by Side Walls in Solar Ponds ", Solar Energy, 41, 521-529 (1988).
 50. Chen, C.F., Briggs, D.G. and Wirtz, R.A., " Stability of Thermal Convection in a Salinity Gradient Due to Lateral Heating ", Int. J. of Heat and Mass Transfer, 14, 57-66 (1971).
 51. Chen, C.F. and Shok, M.W.K., "Cellular Convection in Salinity Gradient Along a Heated Inclined Wall ", Int. J. Heat & Mass Transfer, 17, 51-60 (1974).
 52. Akberzadeh, A., " Convective Layer Generated by Side Walls in Solar Ponds : Observations ", Solar Energy, Vol. 43, 17-23, (1989).
 53. Akberzadeh, A., MacDonald, R. and Wang, Y.F., " Reduction of Surface Mixing in Solar Ponds by Floating Rings ", Solar Energy, 31, 377-380 (1983).
 54. Schladow, S.G., " The Upper Mixed Zone of a Salt Gradient Solar Ponds : Its Dynamics Prediction and Control ", Solar Energy, 33, 417-426 (1984).
 55. Keulegan, G.H., " Wind Tides in a Small Closed Channels ", J. Res. Natl. Bur. Stand., 46, 358-381 (1951).
 56. Bye, J.A., " Wind-Driven Currents in Unstratified Lakes ", J. Marine Res., 10(3), 451-458 (1965).
 57. Atkinson, J.F. and Harleman, D.R.F., " A Wind-Mixed Layer Model for Solar Ponds ", Solar Energy, 31, 243-259 (1983).